Contract NAS 8-20229

DEPARTMENT OF ELECTRICAL ENGINEERING

FINAL REPORT

DEVELOPMENT OF A VALID MATHEMATICAL FORMULA OR GROUP OF FORMULAS TO ESTABLISH AN ACCURACY OF WITHIN 5% THE AUDIO RANGE INDUCTANCE RESULTING IN BERYLLIUM COIL ASSEMBLY

ENGINEERING AND INDUSTRIAL RESEARCH STATION

MISSISSIPPI STATE UNIVERSITY

STATE COLLEGE, MISSISSIPPI

DEVELOPMENT OF A VALID MATHEMATICAL FORMULA OR GROUP OF FORMULAS TO ESTABLISH WITHIN AN ACCURACY OF 5% THE INDUCTANCE AUDIO RANGE RESULTING IN BERYLLIUM COIL ASSEMBLIES

FINAL REPORT

by

D. D. Wier, B. J. Ball,
C. G. Catledge, and L. J. Hill

PRINCIPAL INVESTIGATOR:

D. D. Wier
Associate Professor
Department of Electrical Engineering
Mississippi State University
Box 326, State College, Mississippi 39762
Telephone: 601+323-4321, Ext. 396

APPROVED:

D. W. Colvard, President
Mississippi State University
State College, Mississippi 39762

TABLE OF CONTENTS

INTRODUCTION

The purpose of this study is to establish the net inductance of both the hammer coil and the cryogenic sealing coil now being used at the Marshall Space Flight Center at Huntsville, Alabama. Although the electrical characteristics of both coils are similar, the differences in the physical dimensions and cross-sections of the two indicate that they should be handled as separate problems.

Section A of this report is concerned entirely with the hammer coil and Section B with the cryogenic sealing coil. Both sections contain the complete derivations and results of the study for the respective coils. It is not necessary for a person interested in only one of the coils to refer to the other section.

The same method of attack was used with both coils with the exception of the determination of the electric fields. Due to the different shapes of the two coils, a different method of electric field determination was used for each. For the hammer coil, an electrolytic tank was used to obtain an electric field map. Due to the simpler cross-section of the cryogenic sealing coil, the electric field map was obtained by a geometrical solution described by A. D. Moore.

In both cases, the effects of resistance, capacitance, and inductance on the net inductance were taken into account in the final equations.

SECTION A

HAMMER COIL

INTRODUCTION

Hammer coil is the name given a device used in the fabrication and assembly of rocket and aerospace components by the George C. Marshall Space-flight Center, Huntsville, Alabama. The hammer coil, as its name implies, has the ability to hammer and form metallic material. Furthermore, the coil has the unique ability to form metal with an absolute minimum of structural fatigue and work hardening. This task is accomplished by an intense magnetic field set up between the hammer coil and the metal under its influence. The physical principle involved is that of a large current with a very high rate of change with respect to time creating an intense and rapidly changing magnetic field. Any metallic object within this field has induced within itself a large current according to Faraday's law, and a correspondingly large magnetic field is produced in direct opposition to the original magnetic field. These opposing fields cause a common repulsion between the coil and the metal which is dependent upon the time rate of change of the coil current, the geometry of the coil, the properties of the metal and its position in the field of the coil. For the purpose of predicting the performance of existing hammer coils and for improving the design of future coils, it is imperative that the impedance characteristics of the coil be known. The purpose of this section of this report is to analytically determine the unloaded characteristic impedance of the hammer coil, described graphically by drawings number MR&T sk 182 between the frequencies of 20 cps and 20,000 cps within an accuracy of 5 percent, and to provide formulaes for calculating the impedance of any similar coil whose dimensions are scaled directly from the coil described in MR&T sk 182.

As with any physical device which carries an electric current, the hammer coil may exhibit the electrical parameters of resistance, capacitance and inductance. The impedance seen at the terminals of the coil, which is pictured

in cross section in Figure A-1, is dependent upon frequency, the values of the electrical parameters and, futhermore, on the manner in which these parameters are distributed within the coil. Certainly, it would be fallacious reasoning to assume that the parameters exist as three discrete components; hence, it is necessary to develop a distributed parameter model that closely approximates the true impedance situation within the coil. Examination of Figure A-1 shows that the coil is wound spirally starting at the centrally located coil spool and terminating on the coil shell. Modified transmission line techniques, which would allow a simple impedance solution, could be used in the model except for the fact that on a per unit length basis, the inductance of the coil is not a constant. As an alternative, the coil parameters are assumed to exist on a one turn basis. That is, the resistance, capacitance, and inductance of each turn are lumped and considered to be in a series connection with lumped parameters of the adjacent turns. In addition, the resistance and inductance of the supporting and connecting members of the coil are assumed to be in series with the distributed model and the associated capacitance is assumed to shunt the distributed model. A simplified schematic circuit diagram of the distributed parameter model of the hammer coil is shown in Figure A-2.

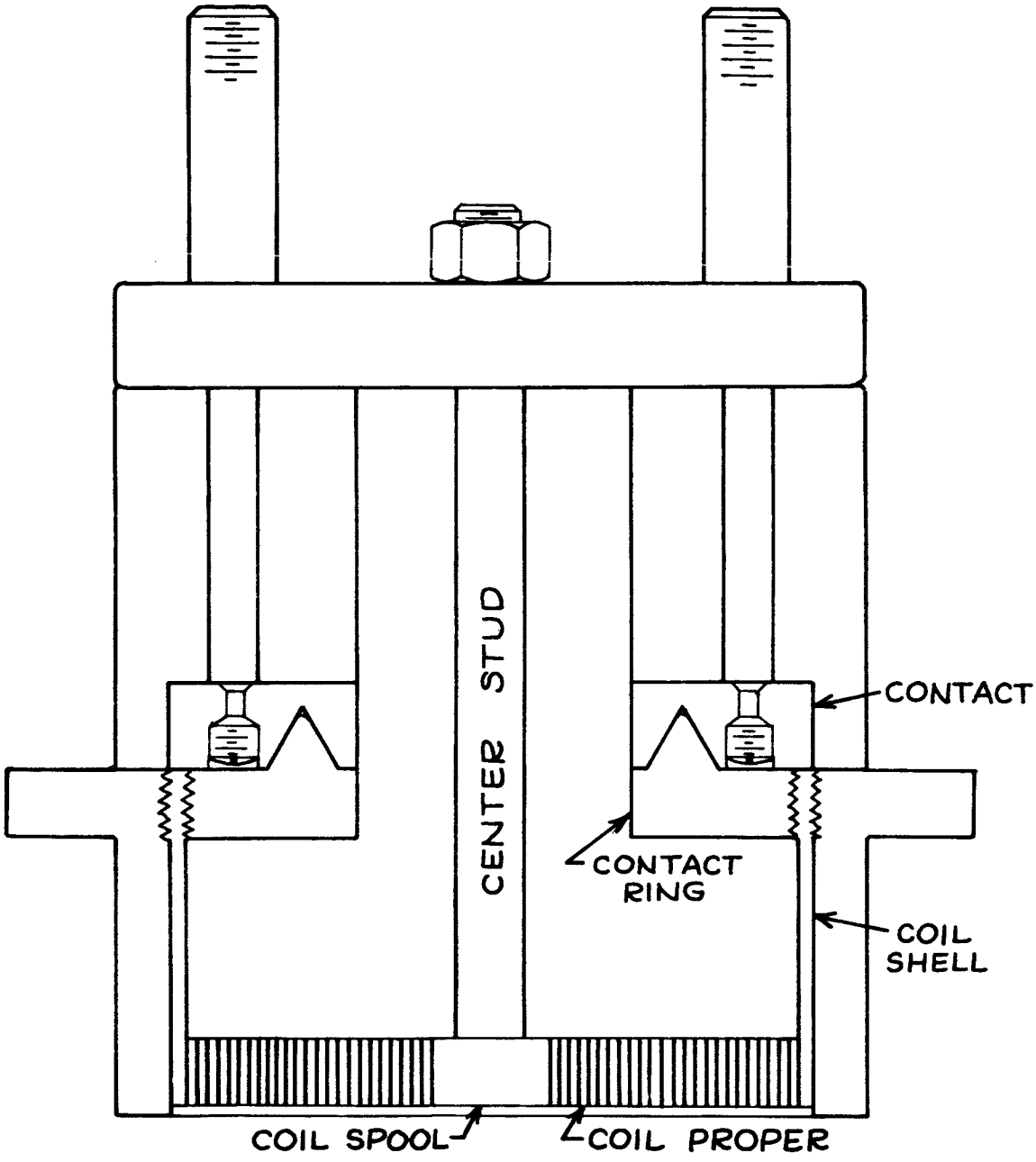

Figure A-1. Cross-Sectional View of the Hammer as Described in MR & T sk 182.

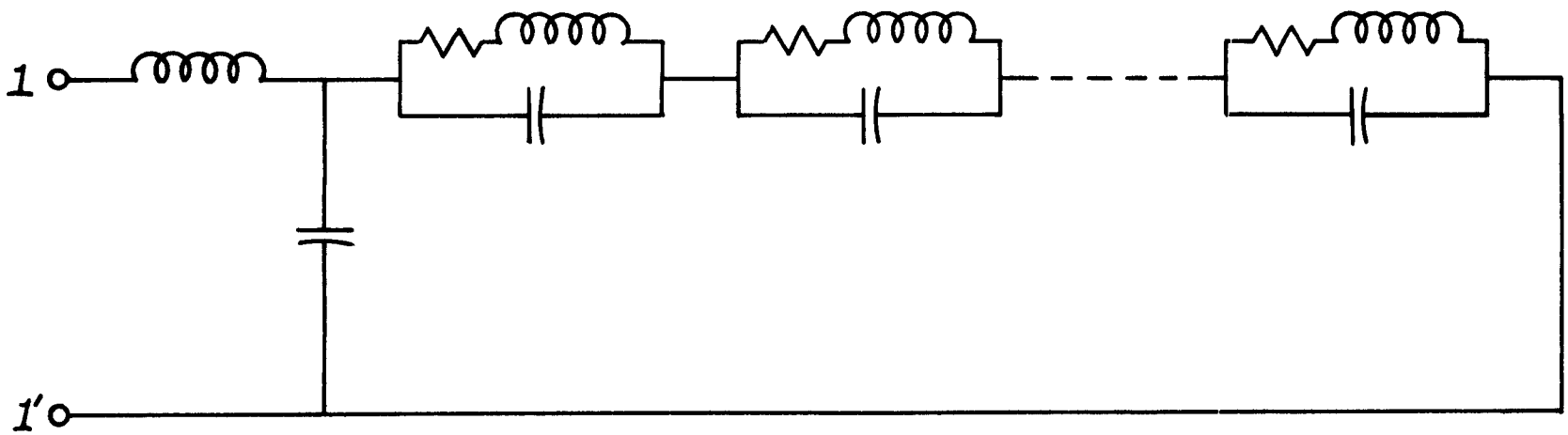

Figure A-2. Simplified Schematic Circuit Diagram of the Distributed Parameter Model of the Hammer Coil.

RESISTANCE DETERMINATION

The cross-sectional view of the hammer coil shown in Figure A-1 indicates four rather distinct areas for resistance determination. The areas included are the center stud and coil spool, the coil proper, the coil shell assembly, and the coaxial cable center conductors from their entrance point in the top cover plate to their termination in the coil shell assembly. The resistances of these areas are determined analytically from the physical characteristics of the material. In addition, the resistance values for the distributed parameter circuit outlined in the introduction are calculated.

The center stud and coil spool which collectively make up the ground or low potential terminal of the coil assembly are constructed of brass which has a resistivity, ρ, of 7×10^{-6} ohm-cm at zero degrees centigrade.[1] This resistivity is equivalent to a ρ of 2.76×10^{-6} ohm-inches. For a center stud radius, r, of 0.25 inches and effective current path length, L, of 5.187 inches* the low frequency stud resistance, R_s, may be calculated as

$$R = \rho \frac{L}{\pi r^2} = \rho \frac{L}{A} \qquad \text{(A-1)}$$

$$R_s = (2.76 \times 10^{-6}) \left(\frac{5.187}{\pi \times (.25)^2}\right) \qquad \text{(A-2)}$$

$$R_s = 72.7 \times 10^{-6} \text{ ohms.} \qquad \text{(A-3)}$$

The resistance of the coil spool is not so easily determined as that of the center stud because the geometry is not simple. As an approximation, the effective conductor area is taken as the average of the entry and exit conductor areas. The entry area, A, where the coil proper contacts the coil spool

*The above dimensions and all those following, except where noted, were obtained from the engineering drawings of the hammer coil provided by NASA, (MR&Tsk182).

has an area given as

$$A_1 = \frac{1}{4}\pi dh \tag{A-4}$$

where d is the diameter of the coil spool and h is the height of the spool. Hence,

$$A_1 = \frac{1}{4}\pi\left(\frac{7}{8}\right)\left(\frac{1}{2}\right) = .344 \text{ in.}^2 \tag{A-5}$$

The exit area A_2 is simply the area of the top of the coil spool or

$$A_2 = \pi(r)^2 \tag{A-6}$$

$$A_2 = \pi\left(\frac{7}{8}\right)^2 = .600 \text{ in.}^2 \tag{A-7}$$

The average area, A, is then calculated as

$$A = \frac{A_1 + A_2}{2} = \frac{.344 + .600}{2} = .472 \text{ in.}^2 \tag{A-8}$$

In a similar manner, an average conductor length can be determined to be .437 inches. From Equation (A-1) the low frequency resistance of the coil spool is then

$$R_{cs} = (2.76 \times 10^{-6})\left(\frac{.437}{.472}\right) = 2.55 \times 10^{-6} \text{ ohms.} \tag{A-9}$$

Thus, the combined resistance, R_{css}, of the center stud and the coil spool is

$$R_{css} = R_s + R_{cs} = 72.7 \times 10^{-6} + 2.55 \times 10^{-6} = 75.25 \times 10^{-6} \text{ ohms.} \tag{A-10}$$

At a temperature of 100 degrees centigrade, the resistance of the center stud and coil spool increases approximately as the temperature coefficient of resistivity of brass at 15 degrees centigrade which is .0020 per degree centigrade.[2] Thus, at 100 degrees centigrade, $[R_{css}]_{0°}$ becomes

$$[R_{css}]_{100°} = [R_{css}]_{0°} (100 \times .002 + [R_{css}]_{0°}) \tag{A-11}$$

$$[R_{css}]_{100°} = (75.25 + .2 \times 75.25) \times 10^{-6} \text{ ohms} \tag{A-12}$$

$$[R_{css}]_{100°} = 90.30 \times 10^{-6} \text{ ohms} \tag{A-13}$$

The skin effect phenomena which tends to cause electric currents to flow near the surface of conductors will increase the resistance of all the coil conductors as frequency is increased. A measure of the depth of the current penetration δ is given by Skilling as[3]

$$\delta = \sqrt{\frac{2\rho}{2\pi f\mu}} \tag{A-14}$$

where ρ is resistivity, f is frequency and μ is the absolute permeability of the medium (3.19×10^{-8} h/inch for nonferromagnetic material.)[4] For brass the current penetration is

$$\delta = \sqrt{\frac{2 \times 2.76 \times 10^{-6}}{2\pi f \times 3.19 \times 10^{-8}}} = 5.25 \sqrt{1/f} \tag{A-15}$$

or at 20,000 cps,

$$\delta = 5.25 \sqrt{\frac{1}{2x10^4}} = .0371 \text{ in.} \tag{A-16}$$

Reference to Skilling indicates that for a center stud conductor radius of 0.25 inches and a δ of .0371, the ratio of ac resistance to dc resistance $\frac{R_{ac}}{R_{dc}}$ is approximately 1.96, an increase of 96 percent. Hence, the total center resistances at 20,000 cps and 0 degrees and 100 degrees centigrade respectively become

$$[R_{css}]20kc\ 0° = (75.25 \times 10^{-6})(1.96) = 147.5 \times 10^{-6} \text{ ohms} \qquad (A\text{-}17)$$

$$[R_{css}]20kc\ 100° = (90.30 \times 10^{-6})(1.96) = 177.2 \times 10^{-6} \text{ ohms} \qquad (A\text{-}18)$$

The coil proper is constructed of a berillium-copper alloy ribbon manufactured under the trade name of Brylco 25. The resistivity of this alloy is dependent upon the type and duration of heat treatment applied during fabrication. According to the manufacturer, the resistivity ranges between four and five times the resistivity of copper.[5] For calculation purposes, a resistivity of four times that of copper was chosen as a good approximation. For commercial annealed copper at 20 degrees centigrade, ρ is 1.7241×10^{-6} ohm-cm.[6] Hence, ρ for Berylco 25 is approximately 6.90×10^{-6} ohm-cm., which is equivalent to 2.715×10^{-6} ohm-inches.

The coil is fabricated in the form of a constant pitch spiral starting at the coil spool in the center and terminating on the coil shell. The ribbon has a thickness of .072 inches and a width of .500 inches. The length, L, of the spiral may be calculated from the formula

$$L = \int_{o}^{\theta} r d\theta \qquad (A\text{-}19)$$

where r is the distance from the center of the center stud to the center of the ribbon and θ is the total angle of revolution. Reference to the engineering drawings shows that from contact point on the coil spool to the contact point on the coil shell, the coil has a total of 14.75 revolutions. This is equivalent to 29.5π radians. Futhermore, the distance, r, can be stated as

$$r = c + \frac{p\theta}{2\pi} \qquad (A\text{-}20)$$

where c is the distance from center stud to the center of the ribbon on the inner contact point, θ is the angle of revolution and p is the pitch of the coil. Hence, with an initial radius, c, of .4735 inches and a pitch of

.1074 inches,

$$r = .4735 + \frac{.1074\theta}{2\pi} \quad . \tag{A-21}$$

Substituting in Equation (A-19) the expression for the coil length becomes

$$L = \int_{o}^{29.5\pi} (.4735 + \frac{.1074\theta}{2\pi})d\theta \quad . \tag{A-22}$$

which upon integrating yields

$$L = 117.28 \text{ in.} \tag{A-23}$$

If the average length of the coil over the inner contact area where the coil spool joins the coil proper and outer contact area where the coil proper joins the coil shell is taken as the effective current length, the total effective length is

$$L = 117.28 + .344 + .548 = 118.112 \text{ in.} \tag{A-24}$$

The area, A, of each coil turn is found as

$$A = tw \tag{A-25}$$

where t is the turn thickness and w is the turn width. Hence, for a thickness of .072 inches and a width of 0.5 inches,

$$A = (.072)(.5) = .036 \text{ in.}^2 \tag{A-26}$$

The low frequency resistance of the coil proper at 20 degrees centigrade is then found by Equation (A-1) to be

$$[R_c]_{20^\circ} = (2.715 \times 10^{-6})(\frac{118.11}{.036}) \tag{A-27}$$

$$[R_c]_{20^\circ} = 8{,}910 \times 10^{-6} \text{ ohms} \tag{A-28}$$

At 100 degrees centigrade the coil resistance is increased by a factor proportional to the temperature coefficient of resistance α of Berylco 25. Since this coefficient is not available directly, it is assumed that the α of copper closely approximates it. Hence, the resistance of the coil at 100 degrees centigrade is

$$[R_c]_{100°} = [R_c]_{20°} + (80 \times .004)\ ([R_c]_{20°}) \tag{A-29}$$

$$[R_c]_{100°} = (8{,}910 \times 10^{-6}) + (.32 \times 8{,}910 \times 10^{-6}) \tag{A-30}$$

$$[R_c]_{100°} = 11{,}760 \times 10^{-6} \text{ ohms} \tag{A-31}$$

From Equation (A-14) the skin penetration depth δ for Berylco 25 as a function of frequency is

$$\delta = \sqrt{\frac{2 \times 2.715 \times 10^{-6}}{2\pi f \times 3.19 \times 10^{-8}}} = 5.21 \sqrt{1/f} \tag{A-32}$$

or at 20,000 cps

$$\delta = 5.21 \sqrt{\frac{1}{2 \times 10^4}} = .0369 \text{ in.} \tag{A-33}$$

Half the thickness of each turn of the coil is .036 inches.

Reference to Skilling shows that for a solid, round conductor of .036 inches radius the ratio of ac resistance to dc resistance $\frac{R_{ac}}{R_{dc}}$ is very nearly 1.02 at 20,000 cps, an increase of 2 percent over the resistance at zero frequency. The ratio of resistance increase in a rectangular conductor, due to the geometry, is somewhat less than for a round conductor and, therefore, will be considered negligible. Hence, the resistance of the coil proper is essentially constant throughout the frequency range of 20 cps to 20,000 cps.

Figure 3-A shows a top view of the coil including the coil spool and the outer shell. The quarter-section line A-A drawn through the coil was chosen as a good compromise from the aspect of symmetry. This line is the basis for developing the distributed parameter model of the coil, not only for

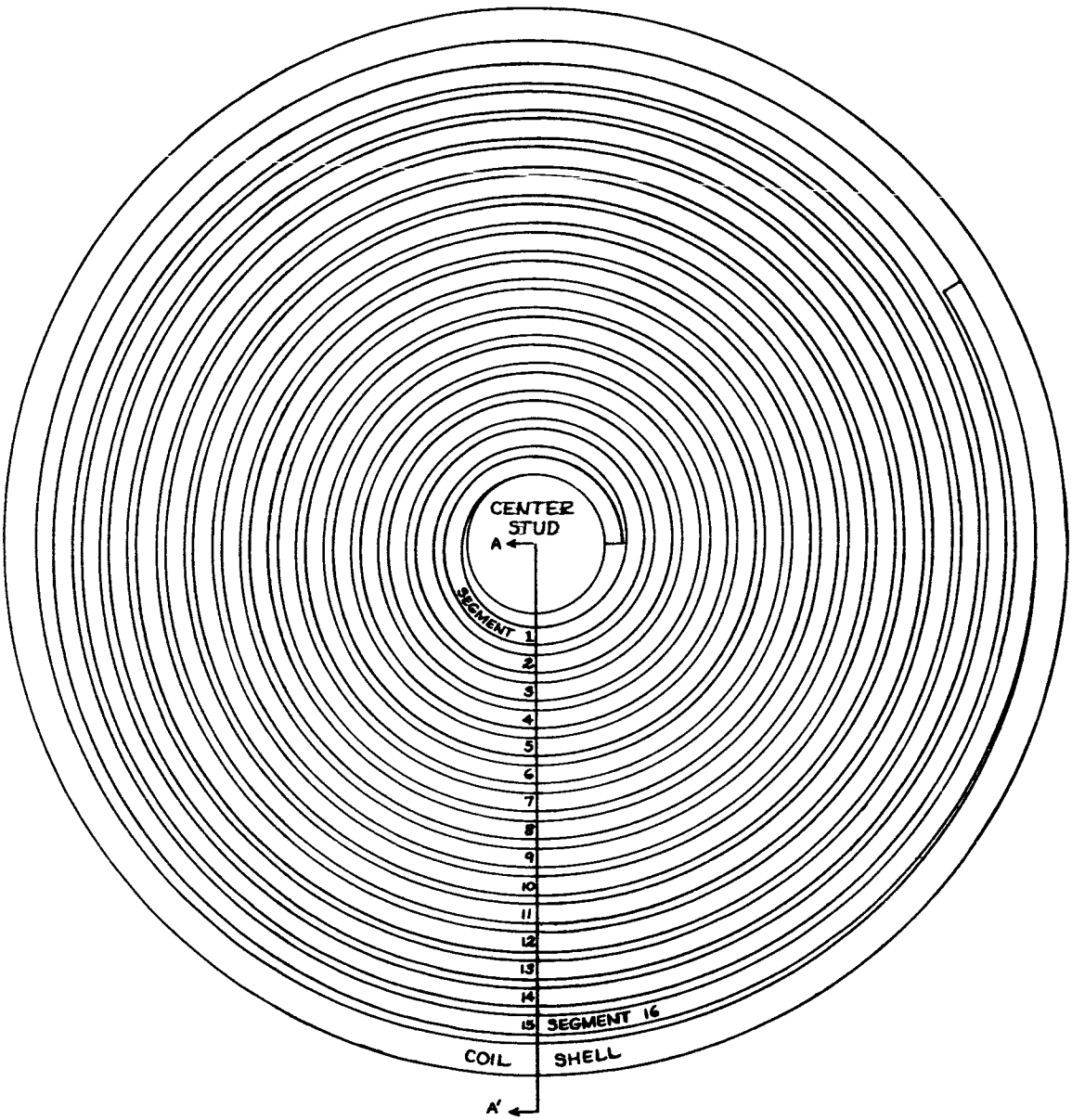

Figure A-3. Top View of Coil Section Showing Incremental Turn Segments.

the resistance parameter, but for the capacitance and inductance parameters as well. As outlined in the introduction, the parameters of the coil are considered to exist on a one turn basis. That is, the resistance, capacitance and inductance of each turn will be summed incrementally to determine the overall impedance of the coil.

To facilitate the determination of the parameters, the length of the spiral coil per turn and the resistance per turn were calculated by computer and appear in Table A-1. Reference to Figure A-3 shows that the coil is made up of sixteen segments adjacent to section line A-A. These segments include fourteen complete turns and two partial turns. The values given in the table are for these turns as numbered in the figure. The resistance values for the two partial turns include the effective contact area resistance also. The computer program and output data are in Appendix A.

The outer shell assembly or coil shell assembly consists of several component parts which include the coil shell, the contact ring, and the contact. Both the contact ring and contact are constructed of brass and are so massive that they have negligible resistance with respect to the remainder of the coil. The coil shell is constructed of Berylco 25 as is the coil proper. As a reasonable approximation, to determine the resistance of this shell, the effective current area is considered to be the average of the area of the contact strip where the coil contacts the coil shell and the area of the coil shell itself. The dimensions of the contact strip are .50 inches by 1.096 inches, which gives an area of .548 square inches. The coil shell is .125 inches thick and has a mean circumference of 4.25π. The shell area is then approximately 1.67 square inches. The average area A is then

$$A = \frac{1.67 + .548}{2} = \frac{2.218}{2} = 1.109 \text{ in.}^2 \qquad \text{(A-34)}$$

Incremental Segment	Length In Inches	Resistance in Ohms 20°C.	100°C.
1	1.571*	159.948	211.131
2	3.650	275.268	363.340
3	4.325	326.160	430.517
4	5.000	377.053	497.693
5	5.674	427.946	564.870
6	6.349	478.840	632.046
7	7.024	529.732	699.222
8	7.699	580.625	766.399
9	8.373	631.518	833.576
10	9.049	682.411	900.751
11	9.723	733.304	967.928
12	10.398	784.197	1035.105
13	11.073	835.090	1102.281
14	11.748	885.982	1169.456
15	12.422	936.876	1236.634
16	3.202*	268.400	354.288

*Lengths of the first and last segments do not include the length of the contact areas.

Table A-1. Length and Resistance Values For The Incremental Turn Segments Shown In Figure 3.

Similarly, the average length from the contact strip to points on the upper edge of the coil shell is approximately 8.4 inches. At 20 degrees centigrade the resistance of the coil shell, R_{shell}, is then

$$R_{shell} = (2.715 \times 10^{-6})(\frac{8.4}{1.109}) \quad \text{(A-35)}$$

$$R_{shell} = 20.55 \times 10^{-6} \text{ ohms} \quad \text{(A-36)}$$

At 100 degrees centigrade the resistance becomes

$$R_{shell} = (20.55 + .32 \times 20.55) \times 10^{-6} \quad \text{(A-37)}$$

$$R_{shell} = 27.12 \times 10^{-6} \text{ ohms} \quad \text{(A-38)}$$

At 20,000 cps the ratio of ac resistance to dc resistance according to Skilling is approximately 1.15 for the coil shell. Hence, the shell resistance at 20,000 cps and 20 degrees and 100 degrees centigrade respectively becomes

$$R_{shell} = 1.15\ R_{shell} = 23.6 \times 10^{-6} \text{ ohms} \quad \text{(A-39)}$$

$$R_{shell} = 1.15\ R_{shell} = 31.2 \times 10^{-6} \text{ ohms} \quad \text{(A-40)}$$

The final component of resistance to be taken into account in the hammer coil is that contributed by center conductors of the eight coaxial cables from their entry point in the top cover to their connection in the coil shell assembly. The cable is either RG-8 or a similar type. RG-8 has a center conductor composed of seven copper wires which have an individual diameter of .0296 inches each.[7] The total area of all seven wires is .003535 square inches. If this area is assumed to be concentrated in one solid round conductor, then the radius of that conductor is .124 inches. The resistivity of hard drawn copper at 20 degrees centigrade is 1.77×10^{-6} ohm-cm.;[8] which is equivalent to $.697 \times 10^{-6}$ ohm-inches. The penetration depth δ at 20,000 cps for copper is

$$\delta = \sqrt{\frac{2\rho}{2\pi f\mu}} = \sqrt{\frac{2 \times .697 \times 10^{-6}}{2\pi \times 2 \times 10 \times 3.19 \times 10^{-8}}} \quad \text{(A-41)}$$

$$\delta = \sqrt{3.48 \times 10^{-4}} = 1.865 \times 10^{-2} \quad \text{(A-42)}$$

$$\delta = .01865 \text{ in.} \quad \text{(A-43)}$$

The length of center conductors under consideration is 4.75 inches. Thus, the resistance, R_{cond}, for one conductor at 20 degrees centigrade is

$$R_{cond} = (1.77 \times 10^{-6})(\frac{4.75}{.124}) = 67.8 \times 10^{-6} \text{ ohms.} \quad \text{(A-44)}$$

For eight conductors in parallel the total resistance $R_{t\ cond}$ is

$$R_{t\ cond} = (\frac{67.8}{8}) \times 10^{-6} = 8.47 \times 10^{-6} \text{ ohms.} \quad \text{(A-45)}$$

The temperature coefficient of resistance for copper at 20 degrees centigrade is .00382. Hence, at 100 degrees centigrade $R_{t\ cond}$ becomes

$$[R_{t\ cond}]_{100°C.} = [R_{t\ cond}]_{20°C.} + (.00382 \times 80 \times [R_{t\ cond}]_{20°C.}) \quad \text{(A-46)}$$

$$[R_{t\ cond}]_{100°C.} = (8.47 + .306 \times 8.47) \times 10^{-6} = 11.06 \times 10^{-6} \text{ ohms} \quad \text{(A-47)}$$

From Skilling the ratio of ac resistance to dc resistance for the center conductors at 20,000 cps is approximately 2.62. Therefore, at 20,000 cps and 20 degrees and 100 degrees centigrade respectively, the center conductor resistances are

$$[R_{t\ cond}]_{20kc\ 20°C.} = 2.62 \times 8.47 \times 10^{-6} = 22.2 \times 10^{-6} \text{ ohms} \quad \text{(A-48)}$$

$$[R_{t\ cond}]_{20kc\ 100°C.} = 2.62 \times 11.06 \times 10^{-6} = 29.0 \times 10^{-6} \text{ ohms} \quad \text{(A-49)}$$

Component Discription and Symbol	Resistance in Microohms			
	20 cps		20,000 cps	
	20°C.	100°C.	20°C.	100°C.
Center Stud and Coil Spool - R_{css}	75.25*	90.28	147.5*	176.9
Coil Proper - R_c	8910	11,760	8910	11,760
Coil Shell - R_s	20.55	27.12	23.6	31.2
Coax Center Conductors - $R_{t\ cond}$	8.47	11.06	22.2	29.0
Totals	9014.27	11,889.46	9103.3	11,997.1

*Calculated at 0°C.

Table A-2. Resistance Values for the Hammer Coil Components Over the Frequency Range of 20 to 20,000 cps and the Temperature Range of 20° to 100° C.

CAPACITANCE DETERMINATION

The direct result of a difference of potential between any two physical points is the establishment of an electric field between those points. The hammer coil is a physical device which has the property of distributed resistance as was shown in a previous chapter. Hence, any current passing through the coil will cause a difference of potential to exist between the various components of the coil and establish an electric field. The determination and mapping of this field is essential to the determination of the capacitances associated with the coil. In the following, the electric field is determined and the resulting capacitance is related to the distributed parameter model.

The portion of the electric field that is easiest to evaluate and that leads to the majority of the capacitance is that field that exists between the individual turns of the coil. In fact, the field that exists deep inside the turns is linear and parallel and the resulting capacitance can be calculated directly. However, the field near the edge of the turns is not linear with distance and parallel, but bulges into what is usually called fringing, which is usually neglected in a typical problem. However, fringing is taken into account in this study to reduce the error as much as possible.

Figure A-4 shows a cross-sectional view of the edge of four turns of the coil. Since each of these turns has a uniform surface potential, purely geometric considerations dictate that equipotential lines, having the value of the surface potential, leave the center of the top edge of each turn of the angle of ninety degrees.[9] As a good approximation, these equipotential lines may be considered to extend perpendicular to the surface for a small distance. Hence, the electric field between any two turns is the same as that between two plates having the shape and dimensions of the conductor surfaces and their respective equipotentials. Figure A-5 shows two such plates.

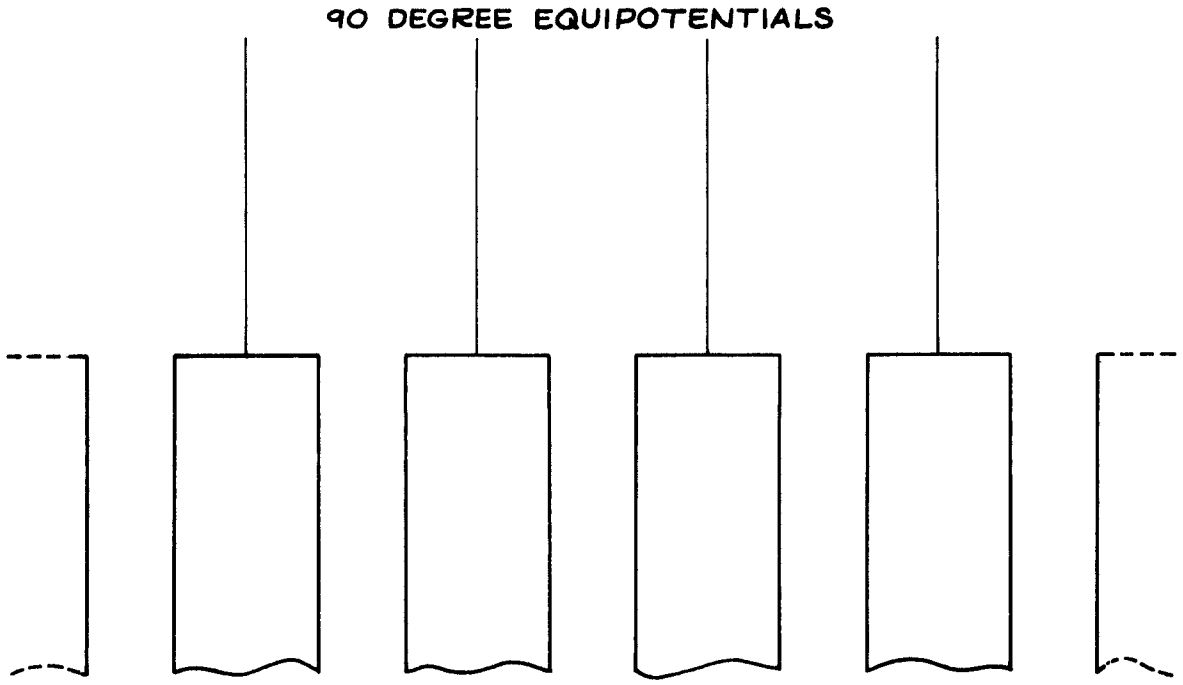

Figure A-4. Edge View of Four Turn Segments with 90 Degree Equipotential Lines Indicated.

Several methods are available for mapping of electric fields in both two and three dimensions. (The electric field of the hammer coil is, of course, three dimensional, but for any particular cross-section through the coil, the field may be considered to be purely two-dimensional with negligible error.) These methods include that of curvilinear squares, rubber sheet models, fluid-flow maps, iteration methods and relaxation methods.[10,11] All of the approaches have merit and are of varying degrees of difficulty, but in general lack the desired accuracy. Fortunately there is available another method utilizing an electrolytic tank which combines accuracy with ease of operation. The electrolytic tank is simply a shallow pool of water in which is placed a model of the device for which a field map is desired. In the case of the hammer coil, a potential source is placed across the two equipotential plates. A probe is then inserted in the water between the plates and the voltage picked up is nulled by means of a balanced bridge circuit. Now, so long as the probe is moved through the water in such a manner that the null is retained, a line of equal voltage will be traced. As many of these equal voltage or equipotential lines as are desired may be traced and plotted. The electrolytic tank apparatus used in this investigation is the property of the Aerophysics Department of Mississippi State University. A photograph of the tank appears in Figure A-6.

A pair of plates similar to those shown in Figure A-5 were placed in the electrolytic tank and equipotential field lines plotted. For calculating capacitance, it is necessary to have a plot of the electric flux lines. Following the procedure detailed by Hayt,[12] the flux lines were sketched and appear in Figure A-7 along with the corresponding equipotential lines.

For calculating the capacitance between turns, it is merely necessary to calculate the normalized resistance, R_{nt}, between turns and divide the quantity into the permittivity of the medium,[13] in this case nylon on one edge and air on the other. The normalized resistance, R_{nt}, is

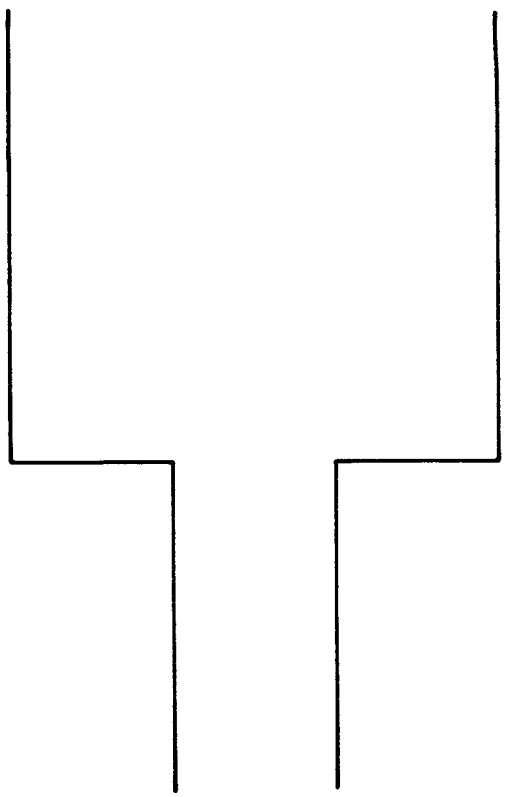

Figure A-5. Two Equipotential Plate Analogy for Determining the Electric Field in the Coil Section.

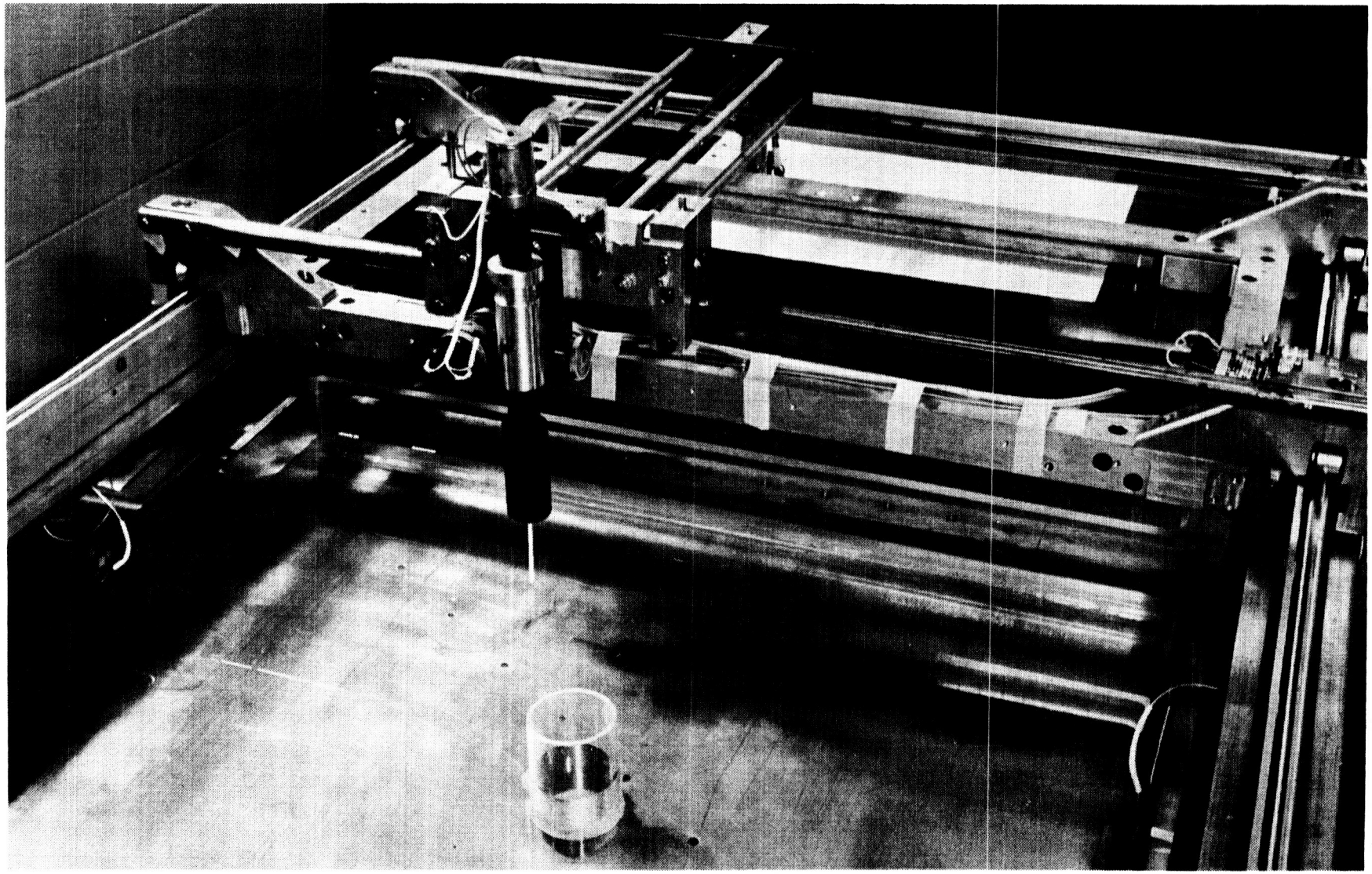

Figure A-6. Electrolytic Tank Assembly and Test Model.
(Photograph furnished by Aerophysics Department,
Mississippi State University)

$$R_{nt} = \frac{1}{\frac{1}{R_{n1}} \quad \frac{1}{R_{n2}} \quad \frac{1}{R_{n3}} + \ldots} \tag{A-50}$$

where R_{n1}, R_{n2}, ... are the normalized resistance of each flux tube connecting the turns. These resistances are equal to the number of curvilinear squares in each of the flux tubes.

For calculating the coil fringing capacitance to the depth shown in Figure A-7 the normalized resistance R_{nt} is

$$R_{nt} = \frac{1}{\frac{1}{8} + \frac{1}{8} + \frac{1}{8} + \frac{1}{8} + \frac{1}{7-5/8} + \frac{1}{8} + \frac{1}{16} + \frac{1}{12}} \tag{A-51}$$

$$R_{nt} = 1.109. \tag{A-52}$$

The permittivity of free space ε_o is 8.854×10^{-12} farads/meter.[14] The permittivity of air to four significant figures is also 8.854×10^{-12} farads/meter.[15] The relative dielectric constant ε_r for nylon is 3.7.[16] Hence, the permittivity of nylon, ε_{ny}, is 32.75×10^{-12} farads/meter. The medium in which the upper fringing capacitance exists is entirely nylon. Thus, the upper fringing capacitance, C_{uf}, is

$$C_{uf} = \frac{\varepsilon_{ny}}{R_{nt}} = \frac{32.75 \times 10^{-12}}{1.109} = 29.5 \times 10^{-6} \text{ f/m} \tag{A-53}$$

or

$$C_{uf} = \frac{29.5 \times 10^{-12}}{39.37} = 0.75 \times 10^{-12} \text{ f/in.} \tag{A-54}$$

As shown in Figure A-7, four of the flux tubes contributing to the lower fringing capacitance are in nylon while the remainder are in air. Substitution in Equation (A-50) gives a normalized resistance for those tubes in nylon of 2.0 and for those in air of 2.49. Hence, the lower fringing capacitance, C_{LF}, is

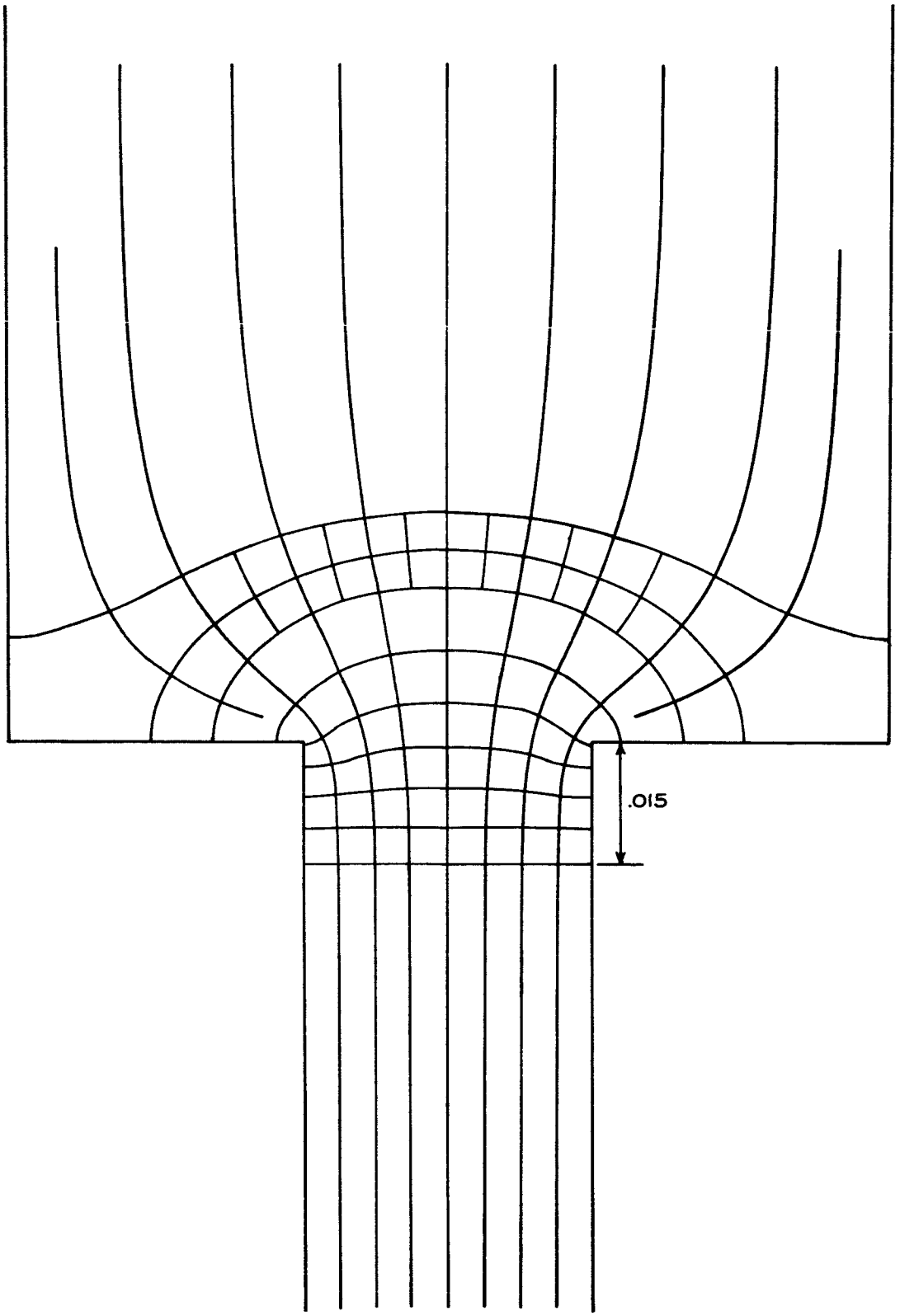

Figure A-7. Two Equipotential Plates with the Corresponding Equipotential Lines and Flux Lines.

$$C_{LF} = \frac{\epsilon_{ny}}{2} + \frac{\epsilon_{air}}{2.49} \tag{A-55}$$

$$C_{LF} = \frac{32.75 \times 10^{-12}}{2} + \frac{8.854 \times 10^{-12}}{2.49} \tag{A-56}$$

$$C_{LF} = (16.37 + 3.55) \times 10^{-12} = 19.92 \times 10^{-12} \text{ f/m} \tag{A-57}$$

or

$$C_{LF} = \frac{19.92 \times 10^{-12}}{39.37} = 0.506 \text{ f/in.} \tag{A-58}$$

Since the electric field is linear and parallel in the center area between the turns, the normal formula for the capacitance between two parallel plates can be used. The fringing capacitance calculated above extends to a depth of 0.015 inches. Thus, the center capacitance is

$$C_c = \frac{\epsilon_{ny} h}{d} \tag{A-59}$$

where h is the center section height and d is the spacing between turns. For an h of 0.47 inches and a d of 0.0354 inches,

$$C_c = \frac{(32.75 \times 10^{-8})(0.47)}{0.0354} = 435 \times 10 \text{ f/m} \tag{A-60}$$

or

$$C_c = \frac{435 \times 10^{-12}}{39.37} = 11.05 \times 10 \quad \text{f/in.} \tag{A-61}$$

The sum of both fringing capacitances and the center capacitance gives the total capacitance C_t as

$$C_t = (0.75 + .506 + 11.05) \times 10^{-12} \tag{A-62}$$

$$C_5 = 12.306 \times 10^{-12} \text{ f/in.} \tag{A-63}$$

For purposes of allocating the turn capacitance in the distributed parameter model, it is assumed that the total capacitance that exists between each turn

segment is in parallel with the resistance and inductance of that segment. Hence, referring to Table A-1 in the previous chapter, the resistance and inductance (not yet determined) of segment seven will be parallel with a capacitance equal to the segment length multiplied by C_t. A computed list of the segment capacitances for all sixteen segments is given in Table A-3.

The capacitances associated with the upper part of the coil assembly are obviously much smaller than those associated with the coil itself. Although they are probably neglibible, a reasonable approximation of their values can be obtained by assuming that the upper portions of the coil are segments of coaxial transmission line. The capacitance per inch of coaxial transmission line is [16a]

$$C = \frac{.613(k) \times 10^{-12}}{\log_{10} b/a} \quad \text{farads/in.} \qquad \text{(A-64)}$$

where a is the radius of the outer surface of the inner conductor, b is the radius of the inner surface of the outer conductor, and k is the relative dielectric constant of the region between the inner and outer conductors. The relative dielectric constant for nylon is 3.7. From Equation A-64 the capacitance per inch of the lower coil assembly composed of the center stud and coil shell is

$$C = \frac{.613(3.7) \times 10^{-12}}{\log_{10} \frac{2.09}{0.25}} = 2.46 \times 10^{-12} \text{ farads/in.} \qquad \text{(A-65)}$$

Hence, the capacitance C_L of the lower section is

$$C_L = 2.46 \times 10^{-12} \ (1.44) = 3.54 \times 10^{-12} \text{ farads} \qquad \text{(A-66)}$$

The capacitance per inch of the center section composed of the center stud, the contact and the contact ring is

$$C = \frac{.613(3.7) \times 10^{-12}}{\log_{10} \frac{1.0}{0.25}} = 3.77 \times 10^{-12} \text{ farads/in.} \qquad \text{(A-67)}$$

Incremental Segment	Capacitance In Bicofarads	Incremental Segment	Capacitance In Picofarads
1	19.343	9	103.046
2	44.916	10	111.349
3	53.220	11	119.654
4	61.524	12	127.959
5	69.828	13	136.262
6	78.133	14	144.567
7	86.437	15	152.871
8	94.741	16	39.404

Table A-3. Computed Table of the Distributed Capacitance Components for the Incremental Turn Segments of the Hammer Coil.

Hence, the capacitance C_c of the center section is

$$C_c = 3.77 \times 10^{-12} \ (1.25) = 4.71 \times 10^{-12} \text{ farads} \qquad \text{(A-68)}$$

If the eight coaxial center conductors are assumed to be the outer conductor of a coaxial line, then the capacitance per inch between them and the center stud is

$$C = \frac{.613(3.7) \times 10^{-12}}{\log \frac{1.87}{0.25}} = 2.60 \times 10^{-12} \text{ farads/in.} \qquad \text{(A-69)}$$

which yields a capactance C_u of the upper section as

$$C_u = 2.60 \times 10^{-12} \ (2.0) = 5.20 \times 10^{-12} \text{ farads} \qquad \text{(A-69a)}$$

An electric field map for an entire quarter section of the coil is shown in Figure A-8 . This map was obtained from a brass model of the coil placed in the electrolytic tank described previously. Potentials for the various turns of the coil were calculated and applied through a potentiometer voltage dividing network from the tank's internal power supply. A very accurate determination of the upper section capacitances can be obtained from this map. However, due to the small magnitude of these capacitances, this accuracy is not required.

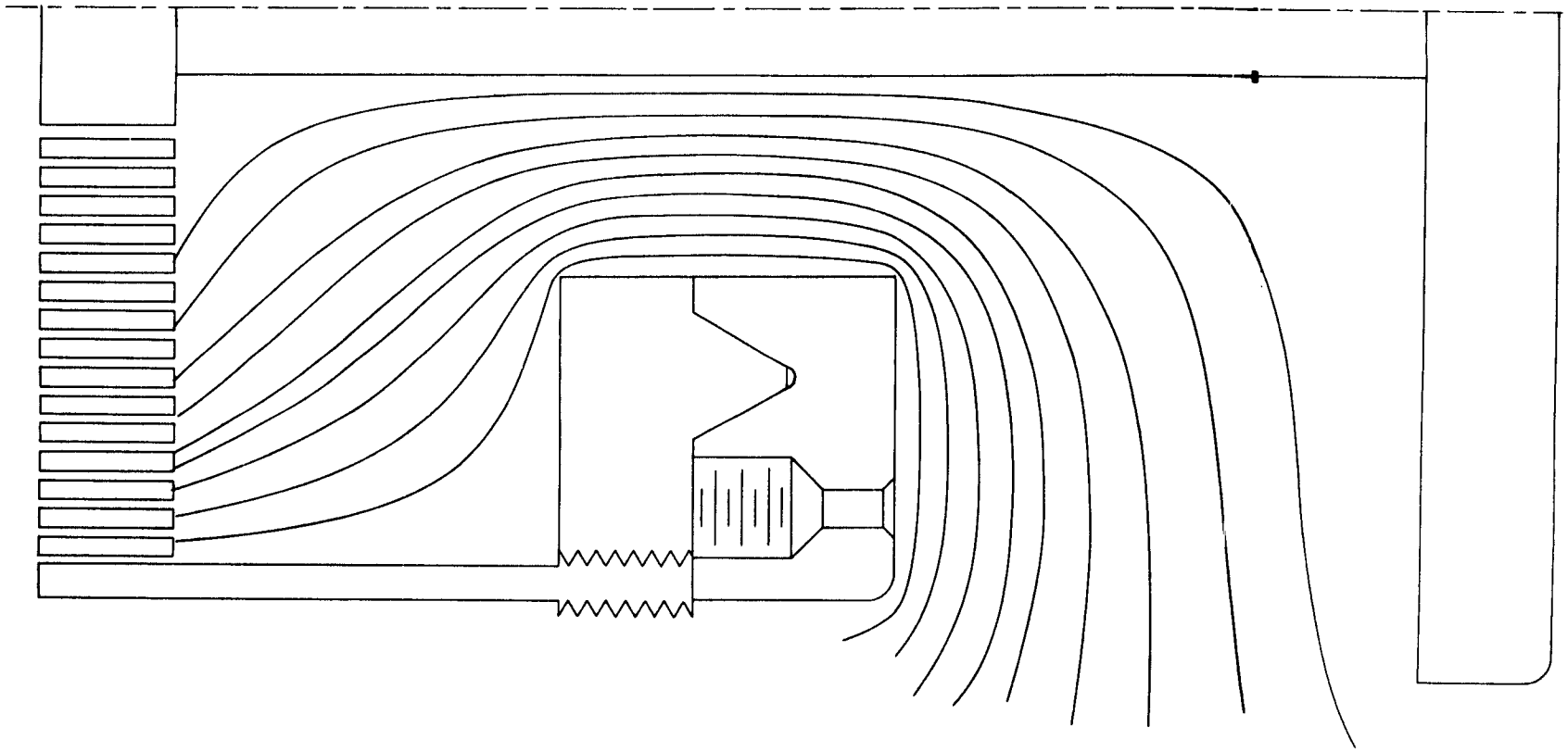

Figure A-8. Electric Field Map of a Quarter-Section of the Hammer Coil.

INDUCTANCE DETERMINATION

Inductance may be defined in any one of several ways, each of which are equally valid and correct. The degree to which a particular definition is useful in a given application depends upon the form of the definition and the form of the problem. As an example, from an energy standpoint inductance, L, can be defined as [17]

$$L = \frac{2W_H}{I^2} \tag{A-70}$$

where I is the total current flowing in a closed path and W_H is the energy in the magnetic field produced by this current. This form requires that the field energy be known or be available through calculation. Provided either magnetic field intensity, H, or field density, B, are known, the field energy is directly

$$W_H = 1/2 \int_{vol} (B.H)\ dv. \tag{A-71}$$

B or H may or may not be easy to determine depending upon geometry and symmetry. Even simple cases often produce integrals whose solutions are very difficult.

The vector magnetic potential approach, in general, simplifies the problems encountered in working directly with B and H, although it is certainly not a guaranteed method. A familiar form for inductance using vector potential A is that for a filamentary conductor of uniform current distribution and small cross section given as

$$L = \frac{1}{I} \int A \cdot dl. \tag{A-72}$$

Applying Stokes' theorem

$$L = \frac{1}{I} \int_S (\Delta XA)\ .dS \tag{A-73}$$

$$L = \frac{1}{I} \int_s B \cdot dS \qquad \text{(A-74)}$$

or

$$L = \frac{\Phi}{I} \qquad \text{(A-75)}$$

Now L is dependent only upon the total flux, Φ, surrounding the conductor and the current, I, through the conductor.

If a true filamentary current is chosen, then the inductance for any current flowing in the conductor is infinite.[18] This fact is readily apparent when it is realized that the magnetic field intensity varies inversely with distance from the conductor, and for a conductor of infinitesimal radius a simple integration shows that an infinite amount of flux is contained within any cylinder of finite radius about the conductor. If a filament of finite radius is chosen, then this problem is eliminated and the inductance becomes finite. However, there is an additional internal inductance generated as a result of the field inside the conductor. This internal inductance, L_i, takes the form of [19]

$$L_i = \frac{\mu}{8\pi} \qquad \text{(A-76)}$$

Thus, the total inductance, L, of a filamentary conductor of finite radius is the sum of the internal inductance L_i and the external inductance L_e.

The physical structure of a Hammer Coil includes two factors that make determination of inductance especially complicated and somewhat difficult. The first of these is the fact that the conductor which makes up the coil proper is of rectangular cross-section, not a round filamentary conductor, and the second is that the geometry of the coil is that of a spiral. The only obvious solution to the first problem is to consider the rectangular conductor composed of many round filamentary conductors tightly packed together. If a sufficient number of filaments are chosen such that the diameter of each

filament is much smaller than the smallest dimension of the rectangular conductor, then, to a good approximation, the magnetic field resulting from the closely packed round filaments is the same as that from the rectangular conductor. The second problem concerning the spiral configuration of the coil has no such simple solution. As will be seen shortly, even the simple geometry of a circular current loop leads to an elliptic integral expression for the vector potential. If, instead of a spiral configuration, the coil is assumed to be a set of concentric, coplaner cylinders, the problem is reduced to that of finding the vector potential for a large number of circular current filaments and summing to find the resultant potential.

Figure A-9 is a circular current loop of some finite radius lying in the x - y plane and whose axis corresponds with the z axis of the coordinate system. The general point p is assumed to lie in the x - y plane, and a current I is assumed to be flowing in the loop. The vector potential at the point p has a component in the ϕ direction only, which for p in the y - z plane means that $A_\phi = -A_x$. The differential vector potential dA_x from a current element Ids is[20]

$$dA_x = - \frac{Ids \sin \phi}{4\pi r} \tag{A-77}$$

The total vector potential at the point p will be summation of all the differential potentials around the current loop or

$$A_x = - \int \frac{I \sin \phi ds}{4\pi r} = - \frac{Ia}{4\pi} \int_o^{2\pi} \frac{\sin \phi d\phi}{r} \tag{A-78}$$

Now referring to Figure A-9

$$\bar{r} = \bar{R} - \bar{a} \tag{A-79}$$

and

$$r^2 = \bar{r} \cdot \bar{r} = (\bar{R} - \bar{a}) \cdot (\bar{R} - \bar{a}) = R^2 - 2\bar{R} \cdot \bar{a} + a^2 \tag{A-80}$$

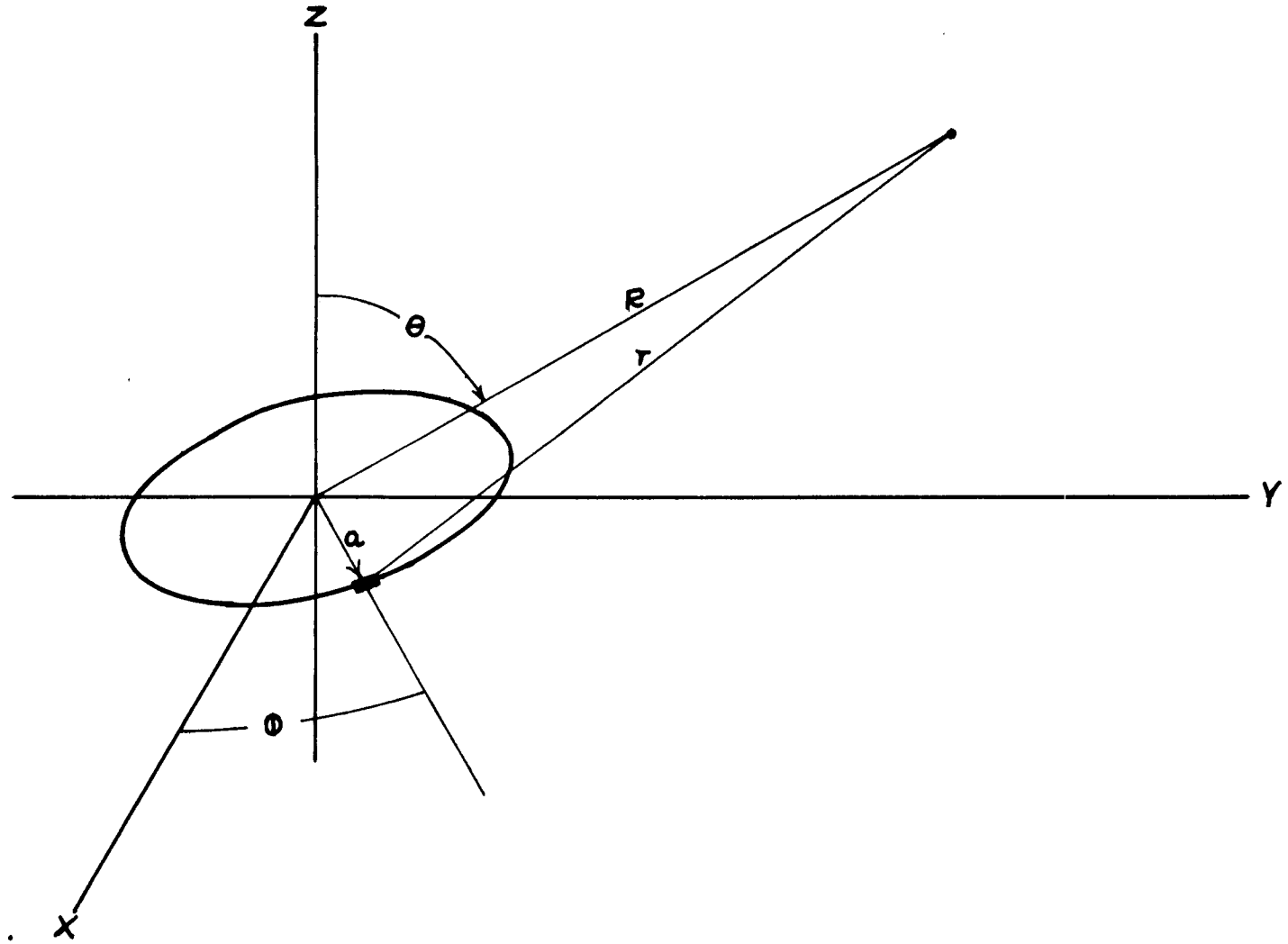

Figure A-9. Circular Current Element in Spherical Coordinates.

The quantity $\bar{R} \cdot \bar{a}$ is R times the projection of $\bar{a}$ on $\bar{R}$ and has a value

$$\bar{R} \cdot \bar{a} = Ra \sin \phi \sin \theta$$

Then

$$\frac{1}{r} = \frac{1}{\sqrt{R^2 + 2\,Ra \sin \phi \sin \theta + a^2}} \qquad \text{(A-81)}$$

and

$$A_x = - \frac{Ia}{4\pi} \int_o^{2\pi} \frac{\sin \phi \, d\phi}{\sqrt{R^2 + a^2 - 2\,Ra \sin \phi \sin \theta}} \qquad \text{(A-82)}$$

From symmetry with respect to the y - z plane

$$A_x = - \frac{2\,Ia}{4\pi} \int_o^{\pi} \frac{\sin \phi \, d\phi}{\sqrt{R^2 + a^2 - Ra \sin \phi \sin \theta}} \qquad \text{(A-83)}$$

Now, since

$$\bar{H} = \text{Curl } \bar{A} \qquad \text{(A-84)}$$

it is only necessary to evaluate Equation (A-83), take the curl of the resultant, find field intensity B from the permittivity of the medium, evaluate the flux Φ and solve directly for the inductance by Equation (A-75). Unfortunately, however, the expression for vector potential in Equation (A-83) appears to be an elliptic integral for which no general solution exists.* A table solution is possible for each set of parameters; however, to reach this table solution requires that Equation (A-83) be reduced through three subsequent elliptic integrals before a table lookup can be achieved.[21] This process is quite

*In actuality, the elliptic integral of Equation (A-83) may be reduced to a sum of simple integrals by division. However, the process of evaluating the curl of these integrals is extremely complex and time-wise is less economical than the solution proposed later.

difficult and time consuming.

An alternate solution to the integral can be obtained numerically. This solution merely involves evaluating the integral by Simpson's rule over the range specified. Examination shows that for any particular evaluation, R, a, I, and θ are constant and that ϕ is the variable of integration, appearing as sin ϕ. For evaluation using Simpson's rule, it is necessary to have an odd number of ordinates, the first point at the near extreme of the range and the last point at the other extreme of the range. This arrangement assures an even number of panels as is required. An additional requirement is that the points be evenly spaced, the number depending entirely upon the accuracy desired.[22] At a spacing of .1 radian the error for $\int_o^\pi \sin\phi \, d\phi$ is less than .000002.[23] This high degree of accuracy indicates that a much larger increment would be permissable with a commensurate saving of time. With an increment spacing of $\pi/10$ and for the integral

$$A = C \int_o^\pi \left(\frac{\sin \phi}{a - b \sin \phi} \right) d\phi \qquad \text{(A-85)}$$

which is equivalent to Equation (A-83) for the vector potential, the error is less than .1 percent. Hence, an ordinate spacing of $\pi/10$ is adequate for the accuracy desired.

One form of Simpson's Rule is[24]

$$\int_{x_o}^{x_{2m}} y\,dx = (y_0 + 4y_1 + 2y_2 + 4y_3 + 2y_4 + 4y_5 + \ldots + 4y_{2m-1} + y_{2m}) - \frac{m y^{(4)} h^5}{90} \qquad \text{(A-86)}$$

In the remainder term $y^{(4)}$ denotes the value of the fourth derivative at some point between x_o and x_{2m}. The total remainder term is a measure of the probable error which may be omitted if it is less than the required accuracy for the integral.

Now that a method has been decided upon for the evaluation of the integral that represents the vector potential, the next task that arises is that of specifying the configuration of the filamentary conductors that make up each turn of the coil. Good judgement seems to dictate that each filament be of symmetrical cross-section, that is either round or square. Since the turn itself is of rectangular cross-section, the logical choice is for the square filamentary conductors. Assuming square conductors are used, many packing densities would fill the space occupied by the rectangular turn, which has dimensions of 0.5 inches and 0.072 inches. Several possibilities are five filaments wide by thirty-five filaments high, three wide by twenty high, or in the simplest case, one wide by seven high. As a starting point and in the interest of saving computing time, a density of three wide by twenty high gives a total number of sixty filaments per turn. If it is assumed that coil is made up of fifteen concentric turns spaced as along the section A-A line in Figure A-3, then the total number of filaments is 900. Since the vector potential for each of these filaments must be evaluated for each field point required, the computing task becomes quite large. This fact is especially evident when it is realized that a good field map for the hammer coil would require at least 500 vector potential field points.

To alleviate the problem, the number of filaments to be evaluated must be reduced in some manner. One approach is to consider each coil turn as being made up of rectangular rather than square filaments. For example, the filament density in the preceeding case could be reduced from three wide by twenty high to three wide by ten high. The best way to determine if the latter configuration is acceptable is to evaluate both configurations and note the difference between the two. A suitable evaluation test is to determine the difference in the near field vector potential as a result of the two filament configurations since the near field is most sensitive to conductor arrangement. For a test composed of a test point located 0.125 inches above the center of the second turn of the

coil, the vector magnetic potential contributed by the first three turns is as follows: For a filament packing of three wide by twenty high the vector potential equals 40.3718; for a filament packing of three wide by ten high the vector potential equals 42.1822. The results show a 4.2 percent difference of vector potentials in the near field. Since the far field is unchanged by the two methods and the two are added, this amount of error is completely tolerable.

Three computer programs for evaluating the vector magnetic potential at a series of points surrounding the coil are listed in Appendix A. Each of these programs is simply a formalized routing for calculating the vector potential from each filament in sequential order. The first program requires that points at which the potential field is to be determined be read into the computer from punched cards. The output from this program is simply the vector potential at the point in question. The two remaining programs have the special capacity for automatically generating input data points and for numerically evaluating the curl of the A field to obtain the H field. The first of thse programs is concerned with the near A field points indicated in Figure A-10 by dots. The crosses indicate points in the numerically obtained H field. The second of these programs is entirely similar to the first with the exception that the A field points and H field points are further spread and,hence,represent the far field of the coil. Figure A-11 is a graphic representation of the far field points and their physical relation to the coil itself.

The output data for these last two programs contain the y and z coordinates of the field point in question, the y component of the H field, the z component of the H field, the resultant component and the angle of this resultant with the y axis. This is all the data that is necessary for plotting a magnetic field map of the hammer coil and obtaining the resulting inductance.

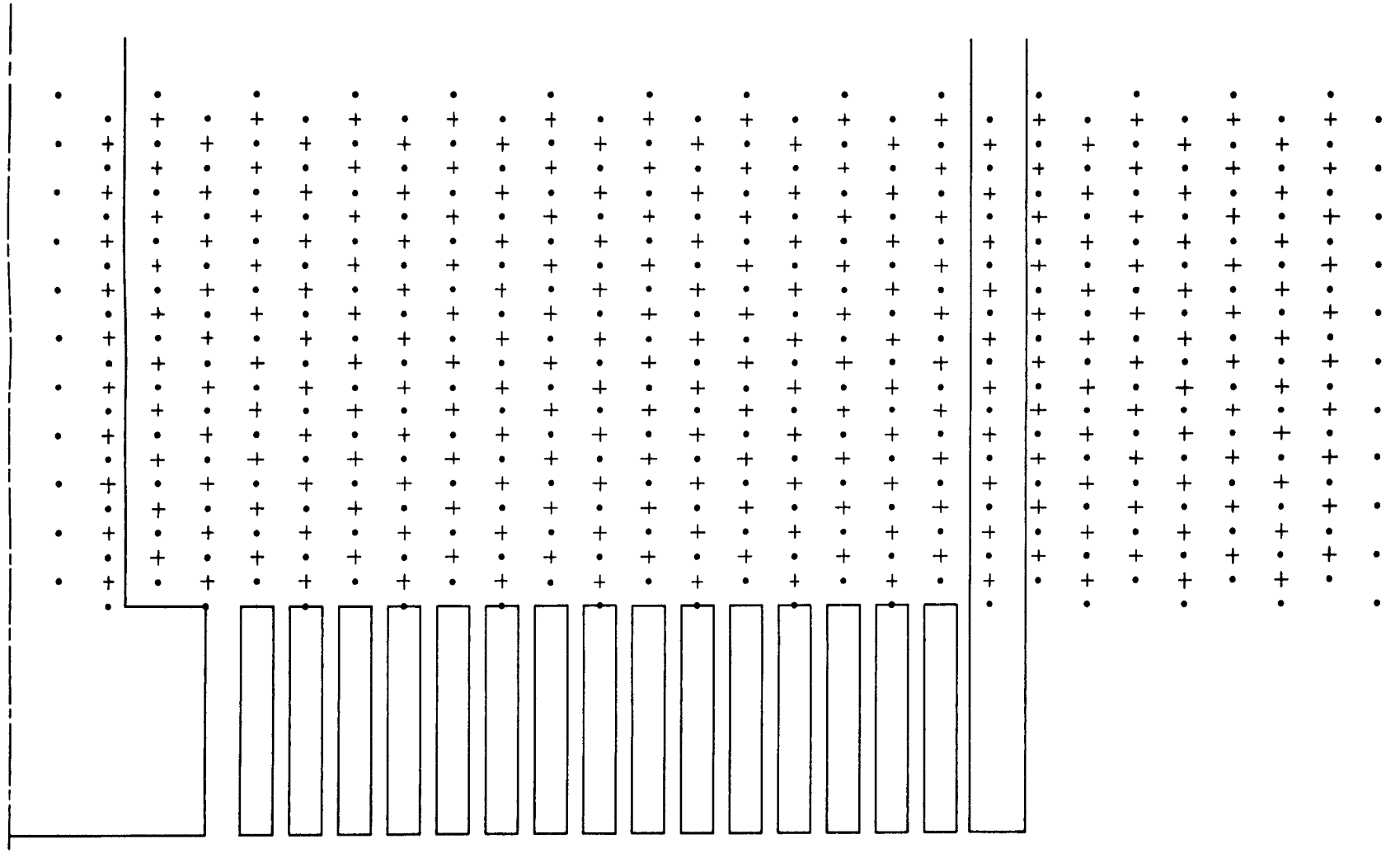

Figure A-10. A-Field and H-Field Points Generated in the Near Field.

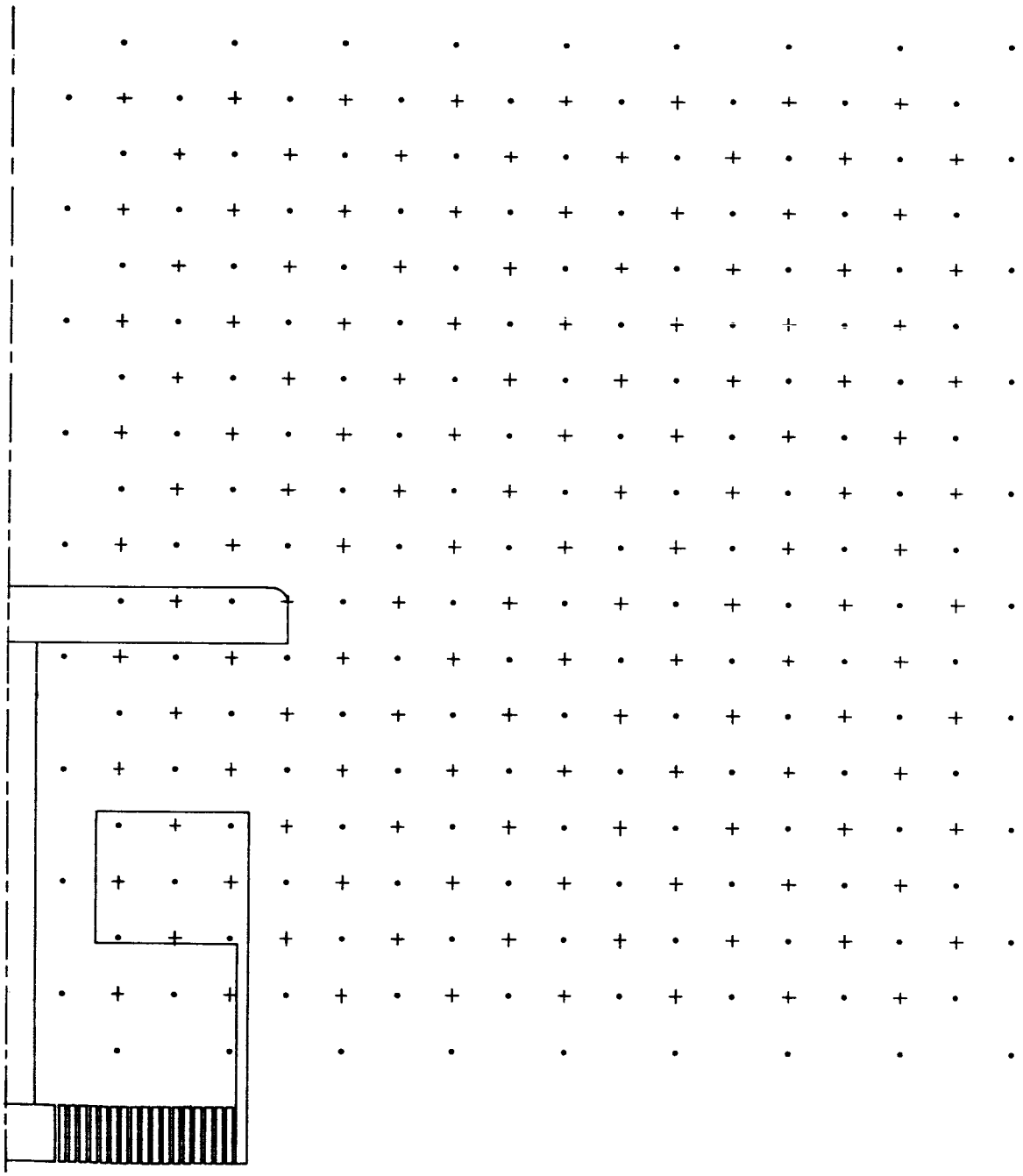

Figure A-11. A-Field and H-Field Points Generated in the Far Field.

Once the H field for a coil has been determined it is only necessary to multiply by μ to obtain the flux density, integrate this over an open surface whose perimeter is the coil in question and divide the resulting flux by the coil current to obtain the coils total inductance. In relation to the hammer coil,an infinite number of surfaces are available over which the integral yielding flux may be calculated.[25] One of these surfaces over which the integral is particularly easy to evaluate is a cylinder extending from each individual coil turn to infinity in either the positive or negative z direction. All of the flux which is either common only to the coil over which the cylinder sits or to that coil and any other coils must pass through the cylinder. Furthermore, it is only necessary to consider the flux normal to the cylinder surface. This normal flux results only from the H field component in the y direction. Hence, it is merely necessary to find an expression for H_y as a function of z and perform the double integration

$$\Phi = 2\mu \int_o^{\pi} \int_o^{\infty} H_y(z)\, r dz d\Phi \tag{A-87}$$

But

$$H = \text{curl } A \tag{A-88}$$

which in the z direction becomes

$$H_y(z) = -\frac{\partial A}{\partial z} = -\frac{dA}{dz} \tag{A-89}$$

Hence,

$$\Phi = 2\mu \int_o^{\pi} \int_o^{\infty} -\frac{dA}{dz}\, r dz d\Phi$$

or

$$\Phi = 2\mu \int_o^{\pi} \int_{[A]_r = o}^{[A]_r = \infty} - r dA d\Phi \tag{A-91}$$

Since r is constant for each cylinder

$$\Phi = 2\mu r \int_0^{\pi} \int_0^{\infty} dA d\Phi \tag{A-92}$$

Now, A is a monotonically decreasing function which has its maximum value at z = 0 and decreases to zero at z = ∞. Hence,

$$\Phi = 2\mu r \int_0^{\pi} A_{max} \, d\Phi \tag{A-93}$$

where A_{max} is the value of A at z = 0. Futhermore,

$$\Phi = 2\pi\mu r \, A_{max} \tag{A-94}$$

Equation (A-94) leads to the startling conclusion that the total flux surrounding a coil, including both internal and external flux, is dependent only upon the vector magnetic potential at the center of the coil turn. Equation (A-94) leads directly to a total inductance of one turn being

$$L = \frac{2\pi\mu r \, A_{max}}{I} \tag{A-95}$$

This important result shows that for calculating inductance it is entirely unnecessary to have any information concerning the field about an inductor with the exception of the vector potential in the turn center, providing the medium surrounding the inductor has a constant permeability.

The results of the inductance determination for the fifteen coaxial, coplaneer cylindrical coil turns which approximate the hammer coil are shown in Table A-4. The total inductance of 11.5290×10^{-6} henries is quite reasonable for a coil of this size and configuration. Since the distributed parameter model is composed of sixteen coil segments, the actual values for the model are slightly different from those given in Table A-4. Each segment of the distributed model actually lies between the circular turns of approximate inductance model. Hence, the mean inductance of each two adjacent coil inductances is taken as the actual distributed parameter inductance. The inductance of the

Cylinder	Inductance in Microhenries	Cylinder	Inductance in Microhenries
1	.2070	9	.9199
2	.2949	10	.9866
3	.3866	11	1.0456
4	.4803	12	1.0879
5	.5745	13	1.1113
6	.6673	14	1.1081
7	.7572	15	1.0578
8	.8420	Total	11.5290

Table A-4. Computed Table of the Inductances of The Fifteen Coaxial Coplanar Cylinder Which Approximate the Hammer Coil.

two end segments is taken as the proportional extrapolated inductance of the adjacent segments. A tabulation of the distributed parameter inductance components for each segment is given in Table A-5.

In addition to the inductance of the coil proper which accounts for the bulk of the hammer coil inductance, a somewhat smaller amount of distributed inductance exists in the center stud, the coil shell assembly and the coaxial cable center conductors. As an approximation it seems reasonable to consider that the center stud and the coil shell assembly including the eight coaxial cable center conductors form an equivalent coaxial transmission line. For such a line the inductance L_{TL} is[26]

$$L_{TL} = (.461 \log_{10} \frac{b}{a} + .050 K_{\phi}) \times 10^{-6} \text{ henries/m} \qquad \text{(A-96)}$$

where a is the radius of the outer surface of the inner conductor, b is the radius of the inner surface of the outer conductor and $K\phi$ is the permeability and skin effect constant which is equal to one for nonmagnetic wire at zero frequency. Thus, for an inner coil shell radius of 2.09 inches and a center stud radius of 0.25 inches, the inductance of the lower section adjacent to the coil is

$$L_{TLL} = [(.461) \log_{10} \frac{2.09}{.25} + (.050)(1.0)] \times 10^{-6} \qquad \text{(A-97)}$$

$$L_{TL} = [(.461)(.968) + .05] \times 10^{-6} \qquad \text{(A-98)}$$

$$L_{TL} = .497 \times 10^{-6} \text{ henries/m} \qquad \text{(A-99)}$$

or

$$L_{TL} = .01236 \times 10^{-6} \text{ henries/in.} \qquad \text{(A-100)}$$

Similarly, the inductance, L_{TLC}, between the coil assembly center section and the center stud is

Incremental Segment	Inductance in Microhenries	Incremental Segment	Inductance in Microhenries
1	.0809	10	.9542
2	.2509	11	1.0171
3	.3407	12	1.0667
4	.4334	13	1.0996
5	.5254	14	1.1097
6	.6209	15	1.0929
7	.7122	16	.2700
8	.7996		
9	.8809	Total	11.2651

Table A-5. Computed Table of the Distributed Inductance Components for the Incremental Turn Segments of the Hammer Coil.

$$L_{TLC} = [(.461)\ \log_{10} \frac{1.0}{.25} + (.050)(2.0)] \times 10^{-6} \qquad \text{(A-101)}$$

$$L_{TLC} = [(.461)(.602) + .05] \times 10^{-6} \qquad \text{(A-102)}$$

$$L_{TLC} = .328 \times 10^{-6} \text{ henries/m} \qquad \text{(A-103)}$$

or

$$L_{TLC} = .00833 \times 10^{-6} \text{ henries/in.} \qquad \text{(A-104)}$$

If the inductance, L_{TLU}, associated with the center stud and coaxial cable center conductors is assumed to be that of a coaxial cable of the same dimensions, then

$$L_{TLU} = [(.461)\ \log_{10} \frac{1.87}{.25} + (.050)(1.0)] \times 10^{-6} \qquad \text{(A-105)}$$

$$L_{TLU} = [(.461)(.874) + .05] \times 10^{-6} \qquad \text{(A-106)}$$

$$L_{TLU} = .453 \times 10^{-6} \text{ henries/m} \qquad \text{(A-107)}$$

or $$L_{TLU} = .0115 \times 10^{-6} \text{ henries/in.} \qquad \text{(A-108)}$$

For the distributed parameter model the inductance of the coil shell, etc., is considered to exist in two parts: one part which includes the coil shell, the contacting and the center stud from the coil spool to the point opposite the contact and contact ring junction; a second part which includes the contact, the coaxial cable center conductors and that portion of the center stud above the contact ring. The inductance, L_L, of the first portion is found from Equations (A-100) and (A-104) as

$$L_L = L_{TLL}\ (1.438) + L_{TLC}\ (0.5) \qquad (A\text{-}109)$$

$$L_L = (.01236 \times 10^{-6})(1.438) + (.00833 \times 10^{-6})(0.5) \qquad (A\text{-}110)$$

$$L_L = .02193 \times 10^{-6} \text{ henries} \qquad (A\text{-}111)$$

The inductance, L_U, of the second portion is found from Equations (A-104) and (A-108) as

$$L_U = L_{TLC}\ (0.75) + L_{TLU}\ (2.00) \qquad (A\text{-}112)$$

$$L_U = (.00833 \times 10^{-6})(0.75) + (.0115 \times 10^{-6})(2.00) \qquad (A\text{-}113)$$

$$L_U = .02925 \times 10^{-6} \text{ henries} \qquad (A\text{-}114)$$

These calculations complete all those necessary for the inductive components of the distributed parameter model of the hammer coil.

CONCLUSION - TOTAL IMPEDANCE DETERMINATION

The finalized distributed parameter circuit for the hammer coil is shown in Figure A-12. The parameter values for the parallel RLC circuits may be found in Tables A-1, A-3, and A-5. The values for the remaining circuit elements may be found under the appropriate headings earlier in this report.

To facilitate the evaluation of the impedance seen at the input terminals, 1-1', a routine for reducing the network of Figure A-12 was written and appears in Appendix. Four unique cases of impedance can be determined from the information derived earlier. These are the impedances at 20 cps and 20 degrees centigrade, at 20 cps and 100 degrees centigrade, at 20,000 cps and 20 degrees centigrade, and at 20,000 cps and 100 degrees centigrade. Impedances and their corresponding angles over the frequency range of 20 cps to 20,000 cps, as determined from the computer routine, are shown in Table A-6 for the four cases mentioned. Obviously, the data used for the 20 cps computations will not yield accurate results at 20,000 cps and vice-versa. However, for comparison both extremes are shown in the table.

As can be seen, the only factor that causes any appreciable difference between the four cases is temperature and that only at low frequencies. The skin effect phenomena is complete negligible. Plots of the input impedance and impedance angle are shown in Figures A-13, A-14, and A-15. Figure A-13 is a plot of the magnitude of the input impedance from 20 to 20,000 cps. Figure A-15 shows the impedance phase angle over the entire range. The most obvious facts resulting from studying these curves are that the impedance has no capacitive component and that the magnitude of the inductance reactance dominates entirely in the frequency range over 1000 cps. The magnitudes of the shunting capacitve reactances are much greater than either the resistances or the inductive reactances. Hence, the coil can accurately be described by

Frequency in cps	Impedance in Milliohms at 20° C.			
	20 cps		20,000 cps	
	Magnitude	Angle	Magnitude	Angle
20	9.128	8.95	9.216	8.86
25	9.190	11.14	9.278	11.03
40	9.454	17.49	9.539	17.32
63	10.067	26.39	10.146	26.17
100	11.479	38.23	11.549	37.95
160	14.508	51.57	14.564	51.29
250	19.918	63.08	19.958	62.85
400	29.812	72.39	29.839	72.23
630	45.654	78.60	46.671	78.49
1000	71.609	82.76	71.620	82.69
1600	114.020	85.46	114.027	85.41
2500	117.827	87.09	177.832	87.06
4000	284.301	88.18	284.304	88.16
6300	447.639	88.84	447.641	88.83
10,000	710.453	89.27	710.454	89.26
16,000	1136.668	89.54	1136.669	89.54
20,000	1420.821	89.63	1420.821	89.63

Frequency in cps	Impedance in Milliohms at 100°C			
	20 cps		20,000 cps	
	Magnitude	Angle	Magnitude	Angle
20	11.978	6.81	12.087	6.75
25	12.025	8.49	12.134	8.41
40	12.228	13.43	12.335	13.31
63	12.707	20.62	12.810	20.44
100	13.853	30.84	13.948	30.61
160	16.451	43.70	16.530	43.43
250	21.374	54.19	21.435	55.94
400	30.804	67.28	30.847	67.10
630	46.308	75.11	46.336	74.98
1000	72.028	80.49	72.046	80.40
1600	114.283	84.02	114.295	83.97
2500	177.996	86.16	178.003	86.13
4000	284.406	87.60	284.411	87.58
6300	447.706	88.47	447.709	88.46
10,000	710.495	89.04	710.497	89.03
16,000	1136.695	89.40	1136.696	89.39
20,000	1420.84	89.52	1420.842	89.51

Table A-6. Terminal Impedance Magnitude and Angle for the Hammer Coil over the Frequency Range of 20 to 20,000 cps and the Temperature Range of 20° to 100°C.

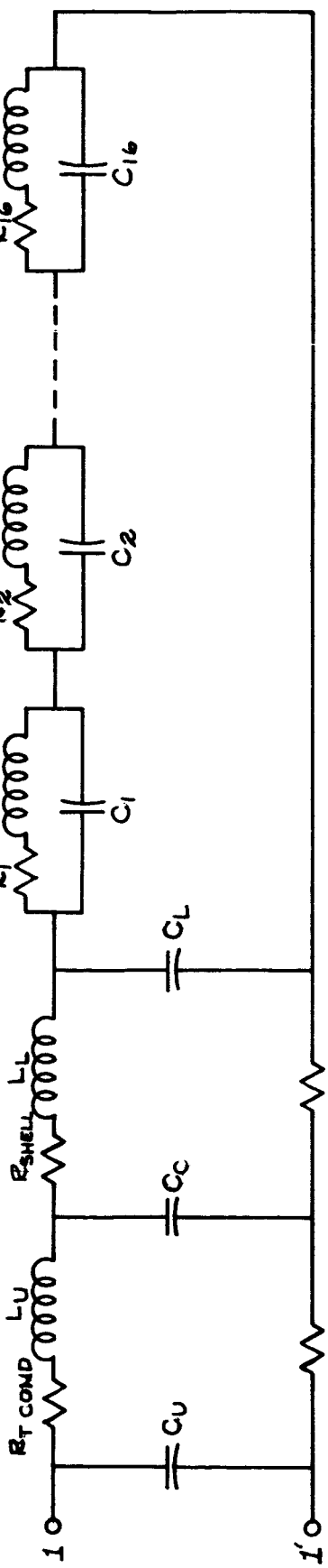

Figure A-12. Actual Schematic Circuit Diagram of the Distributed Parameter Model of the Hammer Coil.

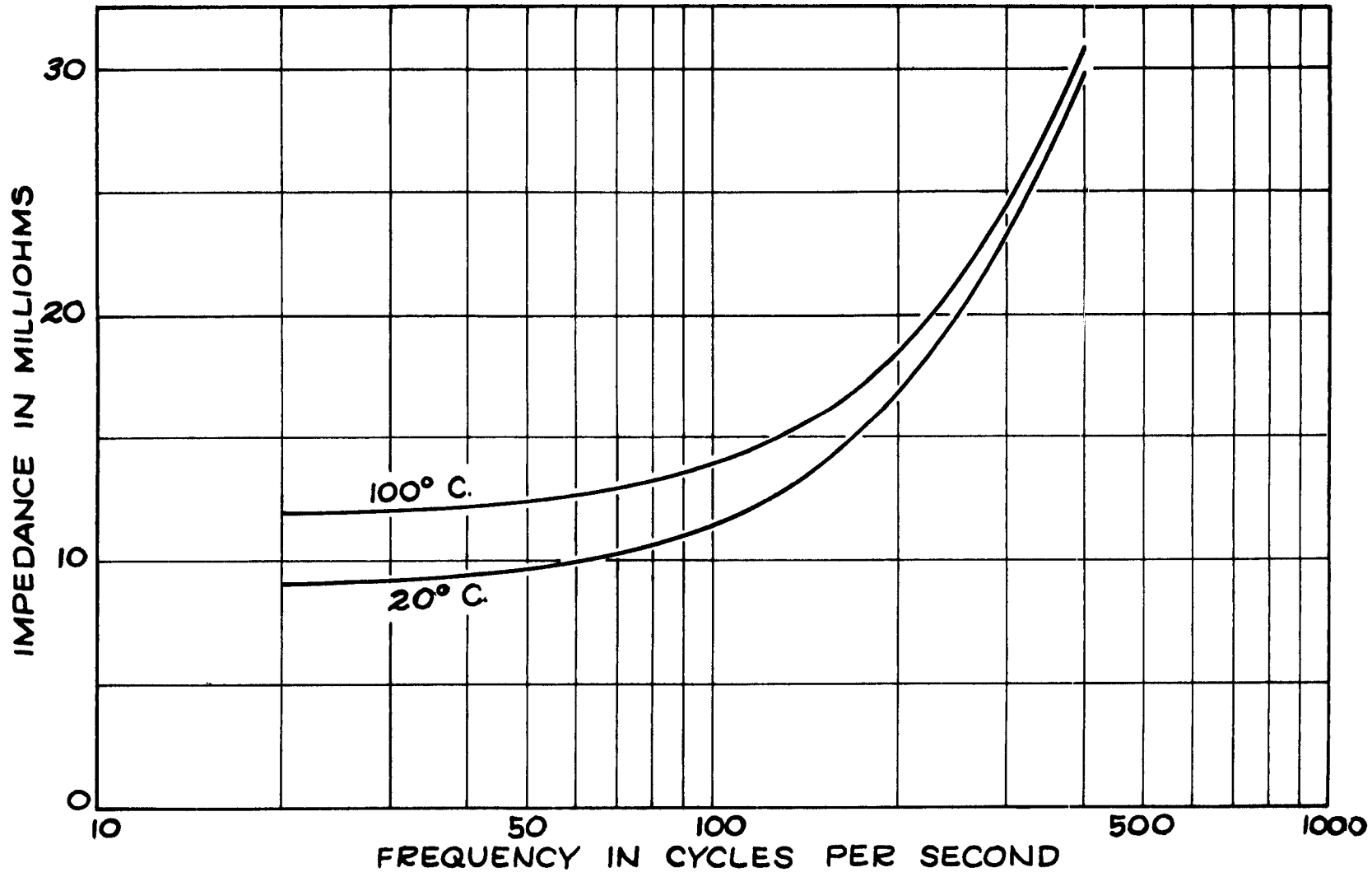

Figure A-13. Low Frequency Terminal Impedance of the Hammer Coil Indicating Variation with Temperature.

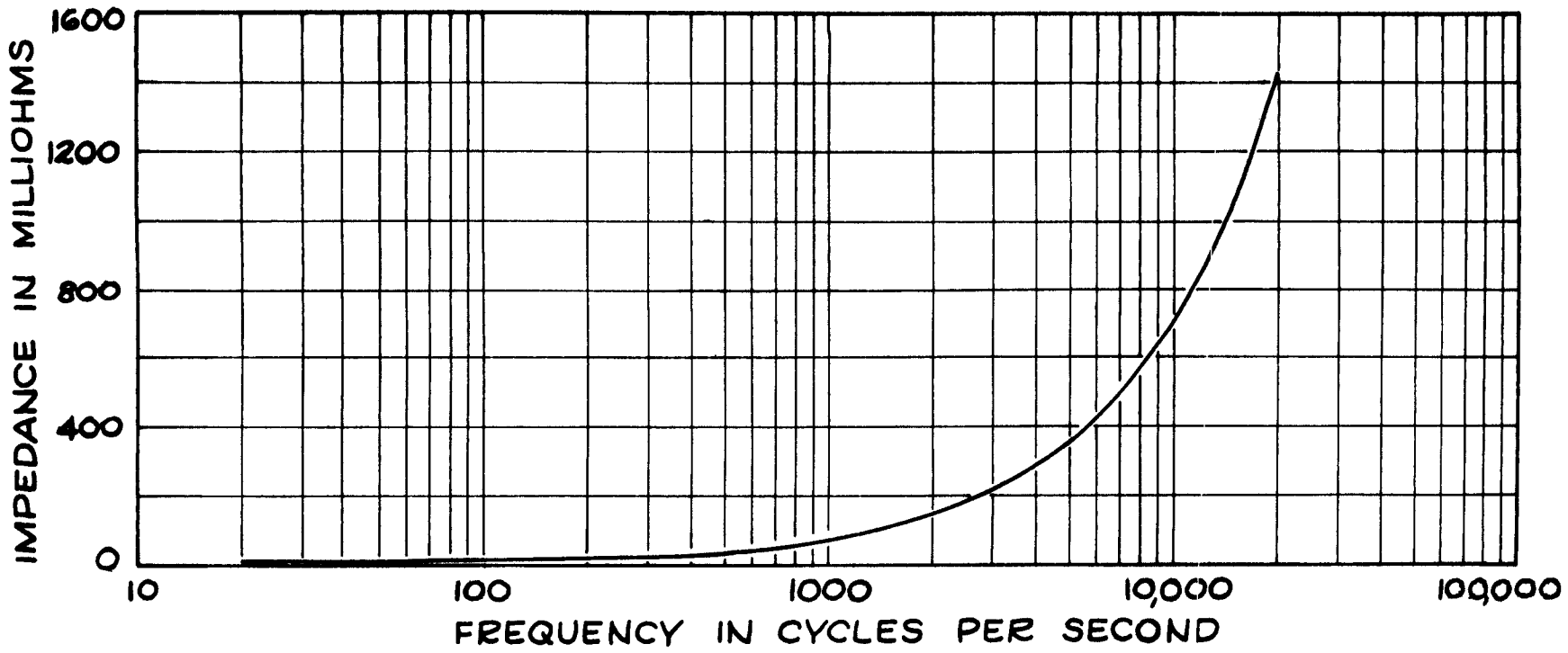

Figure A-14. Terminal Impedance of the Hammer Coil Over the Frequency Range of 20 to 20,000 cps.

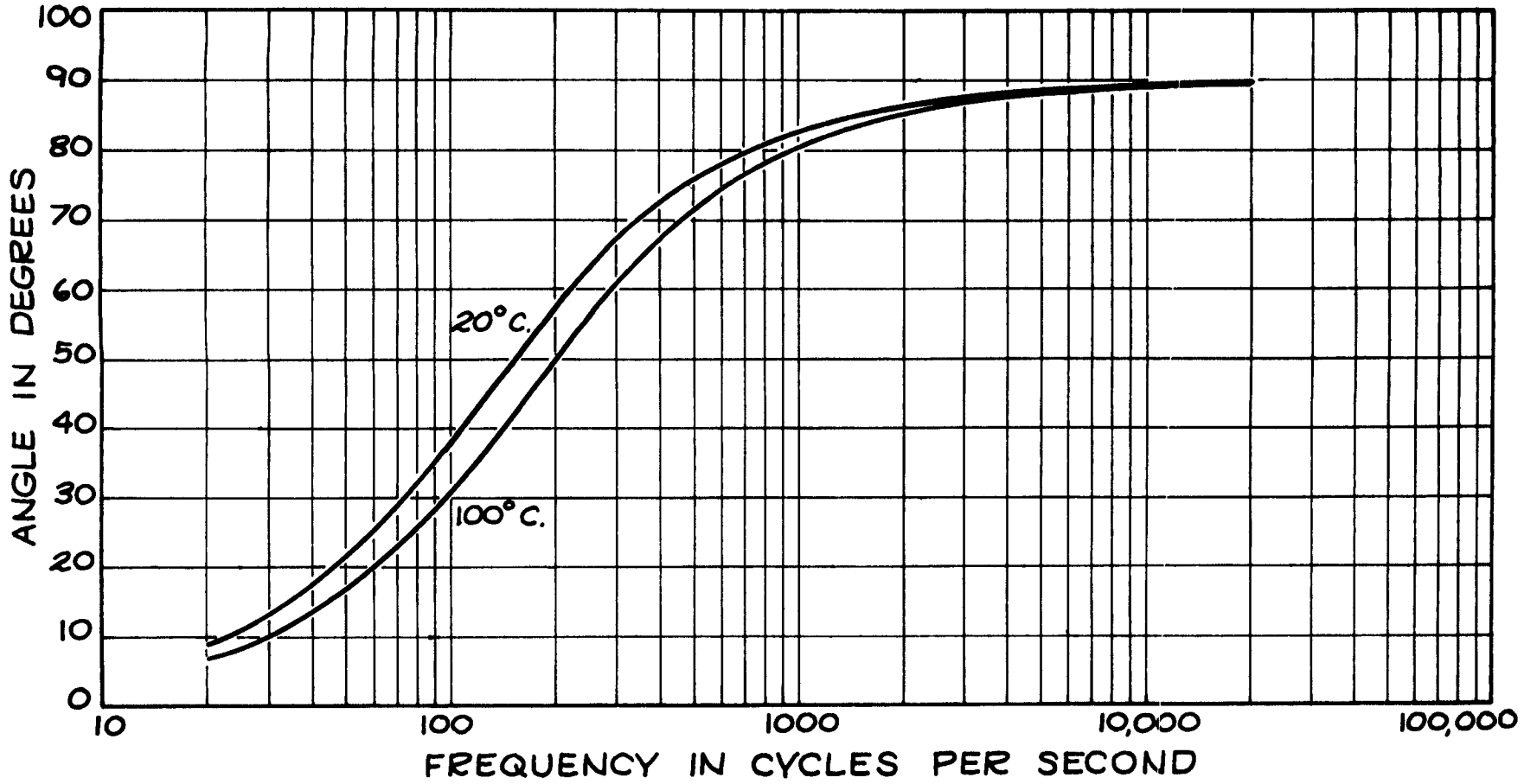

Figure A-15. Angle of the Terminal Impedance of the Hammer Coil Over the Frequency Range of 20 to 20,000 cps at 20° and 100° Centigrade.

a simple series RL circuit with complete disregard to all capacitive elements. The most prominant circuit parameter at the higher frequencies is the net inductance of 11.3163×10^{-6} henries.

For purposes of directly scaling the hammer coil from those dimensions given in MRT sk 182, the following formulae apply. For any scaled resistive component, R_{scale},

$$R_{scale} = (R)\ (\frac{1}{S}) \tag{A-115}$$

where R is the unscaled resistance and S is the scale factor. For any scaled inductive component, L_{scale},

$$L_{scale} = (L)\ (S) \tag{A-116}$$

where L is the unscaled resistance. All scaled capacitive components, C_{scale}, are related by

$$C_{scale} = (C)\ (S) \tag{A-117}$$

where C is the unscaled capacitance.

Table A-2 is a compilation of the resistive components of the hammer coil over the frequency range of 20 to 20,000 kcs including changes of resistance with temperature.

SECTION B

CRYOGENIC SEALING COIL

INTRODUCTION

This section of the report is concerned with the Cryogenic Sealing Coil. The coil is designed to make use of the magnetomotive forming process as currently employed by the National Aeronautics and Space Administration's Marshall Space Flight Center.

Specifically, this section of the report will determine the distributed parameter equivalent circuit of both a typical coil, for which dimensions have been provided, and for a coil which a mean diameter coil turn dimension, D_m, exists. The later equivalent circuit is considered in order that a linear scaled version of the typical coil might be more rapidly analyzed.

From the typical coil equivalent circuit, the frequeney response throughout the audio frequency spectrum will be determined.

DETERMINATION OF RESISTANCES

In order to be able to determine the incremental resistances associated with the cryogenic coil assembly, it is first necessary to examine the coil's geometry. To do this, a cross section of the typical coil assembly, as seen in Figure B-1 proves quite useful.

Several points in the form of explanations need to be made concerning Figure B-1. First, the assembly basically included four materials;"Brylco 25" a registered trademark for Beryllium Corporation's beryllium - copper - cobalt alloy, copper, brass, and nylon. In addition, the entire coil assembly configuration is "potted" in nylon as bounded by the dashed line shown about the assembly in Figure B-1. For detailed drawings see Figures B-I-1 through B-I-6 in Appendix B-I.

The entire coil assembly, referred to hereafter as the coil, provides a closed electrical circuit. Figure B-2 shows the coil with current vectors which would exist under normal operation.

Current enters the coil through six coaxial cable inputs spaced at 60 degree angular increments about the coil base plate. From the base plate, the current enters the eight turn solenoidal section of the coil. It is assumed to leave each lower segment of the soleonoid cross-section perpendicularly and enter each upper segment perpendicularly. After traveling through the ground plate, it is returned to relative ground potential through the center bolt.

Before proceeding further, it is necessary to examine the two types of conducting materials employed in coil construction. Published information by the Beryllium Corporation indicated that "Brylco 25", hereafter referred to as B-25, is composed of 1.80 - 2.05 percent beryllium and 0.20 - 0.30 percent cobalt. The balance of the alloy is copper.[5]

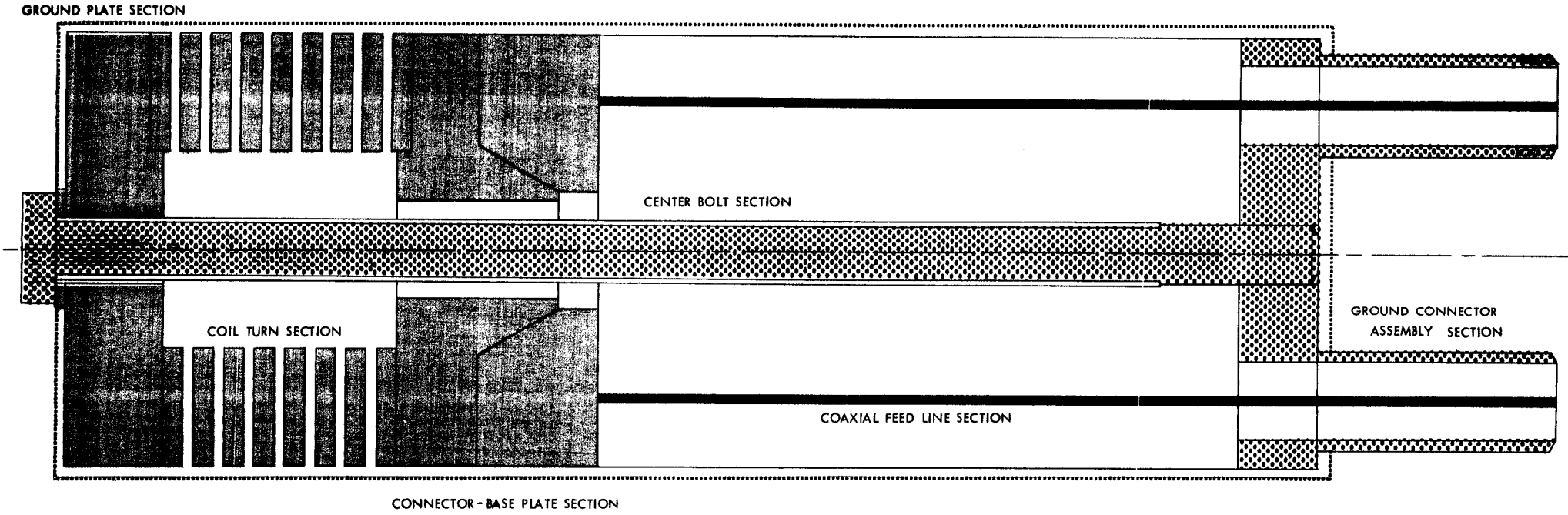

LEGEND

- BRASS
- NYLON
- BRYLCO-25
- COPPER

Figure B-1. Cryogenic Coil Assembly Cross Section Showing Materials Used in Construction

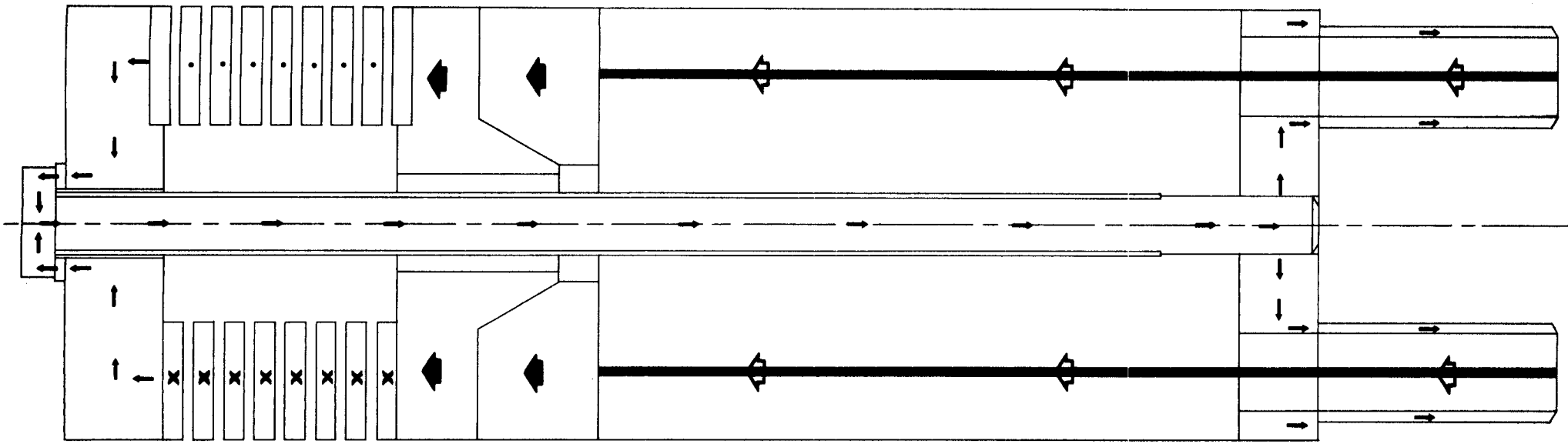

Figure B-2. Cryogenic Coil Assembly Cross Section Showing Current Vectors Present Under Normal Operation

Further published information by the Beryllium Corporation indicated that the conductivity of the B-25 is a function of heat treatment which the material undergoes. All B-25 employed in this coil is heat treated at 650 - 700 degrees Fahrenheit for two hours. Referring to published information, the expected conductivity after such heat treatment would be 22 percent that of standard annealed copper.[5] Taking 6.78×10^{-6} ohm-inches (or 1.724×10^{-8} ohm-meters[8]) as the standard conductivity of annealed copper and neglecting any variations with respect to temperature, gives a resistivity of 3.081×10^{-6} ohm-inches for B-25. The conductivity of brass under similar conditions is 2.64×10^{-6} ohm-inches.[27]

With resistivity values of the coil's materials now established, determination of the various incremental dc resistance within the coil can be made. Resistances are determined from the equation,

$$r = \rho \frac{L}{A} \qquad \text{(B-1)}$$

where r is the resistance in ohms, ρ is resistivity of conducting material in ohm-inches, L is the length of the conducting material in inches, and A is cross-sectional area of conducting material in square inches. The results of these calculations (see Appendix B-I) are shown in Table B-1.

Upon examination of the relative values of resistance in Table B-1 three components are found to be of importance. These are respective resistances of the coaxial feed lines, the coil turn section, and the center bolt. Therefore, all calculations to be made involving resistances of the coil included these three sections.

In order to discuss how skin effect changes incremental values of resistances for the coil, it is necessary to introduce a penetration factor δ. By definition, in the work done by Skilling,

$$\delta = 39.37 \sqrt{\frac{2\rho}{\omega\mu}} \qquad \text{(B-2)}$$

Section of Coil	Material	Resistance of Section	Total Series Equivalent Resistance of Section
Coaxial Feed Lines	Copper	775.000×10^{-6} ohms	125.500×10^{-6} ohms
Connector - Base Plate	B-25	0.702×10^{-6} ohms	0.702×10^{-6} ohms
Coil Turn Section	B-25	208.800×10^{-6} ohms	1670.400×10^{-6} ohms
Ground Plate	B-25	$.956 \times 10^{-6}$ ohms	0.956×10^{-6} ohms
Center Bolt	Brass	218.000×10^{-6} ohms	218.000×10^{-6} ohms
Ground Connector Assembly	Brass	1.179×10^{-6} ohms	1.179×10^{-6} ohms
TOTAL RESISTANCE			2016.737×10^{-6} ohms

Table B-1. D. C. Resistance of Cryogenic Coil Sections

where ρ is resistivity in ohm-meters, ω is radian frequency, μ is absolute permeability of material in henries per meter, and 39.37 is the constant needed to allow δ to be expressed in inches.[3]

To consider what changes occur in the various coil sections, δ as a function of frequency must be determined for copper, B-25, and brass. Since three materials are non-magnetic, the value of μ equals 1.257×10^{-6} henries/meter. Calculation of the respective δ's gives

$$\delta \text{ Copper} = 2.605 \sqrt{\frac{1}{f}} \qquad \text{(B-3a)}$$

$$\delta \text{ B-25} = 5.55 \sqrt{\frac{1}{f}} \qquad \text{(B-3b)}$$

$$\delta \text{ Brass} = 5.13 \sqrt{\frac{1}{f}} \; . \qquad \text{(B-3c)}$$

Each of the above equations indicates that penetration depth decreases inversely as the square root of frequency. Thus, penetration depth will be minimum at the highest frequency under consideration. In this study, which is restricted to consideration of audio frequency spectrum, the maximum frequency for consideration is 20,000 cps. At 20,000 cps the respective values of penetration are:

$$\text{for copper} \quad \delta = .0154 \text{ inches} \qquad \text{(B-4a)}$$

$$\text{for B-25} \quad \delta = .0392 \text{ inches} \qquad \text{(B-4b)}$$

$$\text{for brass} \quad \delta = .0362 \text{ inches.} \qquad \text{(B-4c)}$$

Examination of each of the three important resistance elements in the coil can not be made with reference to skin effect and associated penetration depths.

The inner conductor of the coaxial feed line which is equivalent to RG-8A/U cable, has an effective radius of .302 inches.[7] For studying the skin effect changes in resistance for solid round conductors, a ratio, $\sqrt{2\, r/\delta}$ is used to relate r_{ac} to r_{dc}.[28] The term r is the radius of the conductor.

At 20,000 cps, the inner coaxial conductor has a ratio of .952, the equivalent ac resistance is 1.004 times the dc resistance.[28]

Since the scope of this study involves solution for circuit parameters within five percent of their absolute values, the 0.4 percent change in the inner coaxial conductor resistance will be neglected.

The center bolt section with a radius of .1675 inches has a $\sqrt{2\ r/\delta}$ ratio of 2.072 at 20,000 cps. The corresponding ac resistance for this value is 1.09 times the dc resistance.[28] This percent increase must be taken into consideration.

It is important to note that when the penetration depth, δ, is large enough so that the ratio $\sqrt{2\ r/\delta}$ is .4 or less, the ac resistance is equal to the dc resistance.[28] For the center bolt section, the ratio $\sqrt{2\ r/\delta}$ equals .4 when δ equals .592. This corresponds to a frequency of 75 cps. There must, therefore, be two expressions for the center bolt resistance. The first defining the center bolt resistance between 20 cps and 75 cps would simply be r_{ac} equals r_{dc}. The second must include the variation of r_{ac} with respect to frequency between 75 cps and 20,000 cps.

Table B-2 shows calculated values of r_{ac} with respect to r_{dc} between 75 cps and 20,000 cps.[28]

From Table B-2, a reference to the work of Skilling leads the investigator to believe that a general relationship of r_{ac} in terms of r_{dc} exists for the frequency range from 75 cps to 20,000 cps. The results appear to be of the form,

$$r_{ac} = (A + Be^{Kf-1/2})\ r_{dc}. \qquad \text{(B-5)}$$

It must be noted that the equation would be valid only for frequencies between 75 cps and 20,000 cps; specific values of r_{ac} may be found from interpolation in Table B-2. Below 75 cps, r_{ac} equals r_{dc}.

Frequency	δ	$\sqrt{2}\ r/\delta$	r_{ac}
75 cps	.5930	.4000	1.000000 r_{dc}
100 cps	.5130	.4620	1.000031 r_{dc}
200 cps	.3620	.6650	1.001275 r_{dc}
400 cps	.2560	.9260	1.004000 r_{dc}
800 cps	.1814	1.3040	1.016000 r_{dc}
1000 cps	.1620	1.4620	1.024000 r_{dc}
2000 cps	.1146	2.0680	1.089000 r_{dc}
4000 cps	.0811	2.9200	1.311000 r_{dc}
8000 cps	.0573	4.1400	1.729000 r_{dc}
10,000 cps	.0513	4.6200	1.904000 r_{dc}
20,000 cps	.0362	6.5500	2.441000 r_{dc}

Table B-2. Resistance Variations of Center Bolt Section of Cryogenic Coil Due to Skin Effect

The remaining resistance to be considered is that of the coil turn section. In order to determine how the skin effect changes the resistance of this section, it is necessary to reduce the rectangular cross-section of the coil turn to an equivalent circular cross-section. This reduction is accomplished by considering a circular cross-section which has the same total area as the rectangular cross-section. Following reduction to this form, (see Appendix), the data in Table B-3 is obtained.[28]

From Table B-3, a study of Skilling's work leads to the following general equation for r_{ac} as a function of frequency.

$$r_{ac} = (D + Ec^{Kf-1/2})r_{dc} \qquad \text{(B-6)}$$

This equation would be valid only for frequencies between 1000 cps and 20,000 cps. Specific values of r_{ac} may be found from interpolation in Table B-3. Below 10,000 cps, r_{ac} equals r_{dc}.

In summary, there are three resistances of importance in the coil. They are:

(1) The Center Coaxial Feed Lines Section,

(2) The Center Bolt Section,

(3) The Coil Turn Section.

The corresponding resistances of the sections are:

(1) Center Coaxial Feed Lines:

r_{ac}			
Each line	Total Equivalent	Frequency Range	
775×10^{-6} ohms	125.5×10^{-6} ohms	$20 \text{ cps} \leq F \leq 20{,}000 \text{ cps}$	(B-7a)

(2) Center Bolt Section

r_{ac}	Frequency Range	
218×10^{-6} ohms	$20 \text{ cps} \leq F \leq 75 \text{ cps}$	(B-7b)
218×10^{-6} (Equations B-5) ohms	$75 \text{ cps} \leq F \leq 20{,}000 \text{ cps}$	(B-7b)

(3) Coil Turn Section

r_{ac}			
Per Turn	Total Section	20 cps $\leq$ F $\leq$ 1000 cps	(B-7c_1)
208.9×10^{-6} ohms	1620.4×10^{-6}		
208.8×10^{-6} (Equation B-6)	1670.4×10^{-6} (Equation B-6)	100 cps $\leq$ F $\leq$ 20,000 cps	(B-7c_2)

Frequency	$\delta_{effective}$	$\sqrt{2}\ r/\delta$	r_{ac}
1000 cps	.5930	.4000	1.000 r_{dc}
1420 cps	.4050	.6000	1.001 r_{dc}
2000 cps	.2790	.8700	1.003 r_{dc}
4000 cps	.2620	.9250	1.015 r_{dc}
8000 cps	.1572	1.5400	1.029 r_{dc}
10,000 cps	.1204	2.0130	1.080 r_{dc}
20,000 cps	.0722	3.3640	1.366 r_{dc}

Table B-3. Resistance Variations of Coil Turn Section of Cryogenic Coil due to Skin Effect

DETERMINATION OF CAPACITANCE

Having established the location and relative values of resistance, an inspection of Figure B-3 may be made in order to determine information concerning the electric fields which exist while the coil is under normal operation.

If an applied potential, "V", is assumed to exist where the coaxial center feed lines enter the coil assembly, Figure B-3 indicates the relative potentials throughout the various component sections. The geometry of the coil lends itself to division into six separate regions for the determination of electric fields. These regions are designated by the letters A through F on Figure B-3.

Capacitance values associated with each of the regions A through F must be determined. The capacitance between any two points, although requiring a difference in potential, is independent of the potential difference which causes it. Thus, the values of the relative potentials are not a factor in capacitance calculations.

Several methods for determing values of capacitance are available. However, with the geometry of the coil assembly given, the most logical method for determination is that based on the work of A. D. Moore.[9 11 13] Moore's method involves first obtaining in some manner an electric field map of the area for which it is desired to determine capacitance. The method further requires that only the electric flux lines be determined. For the study of

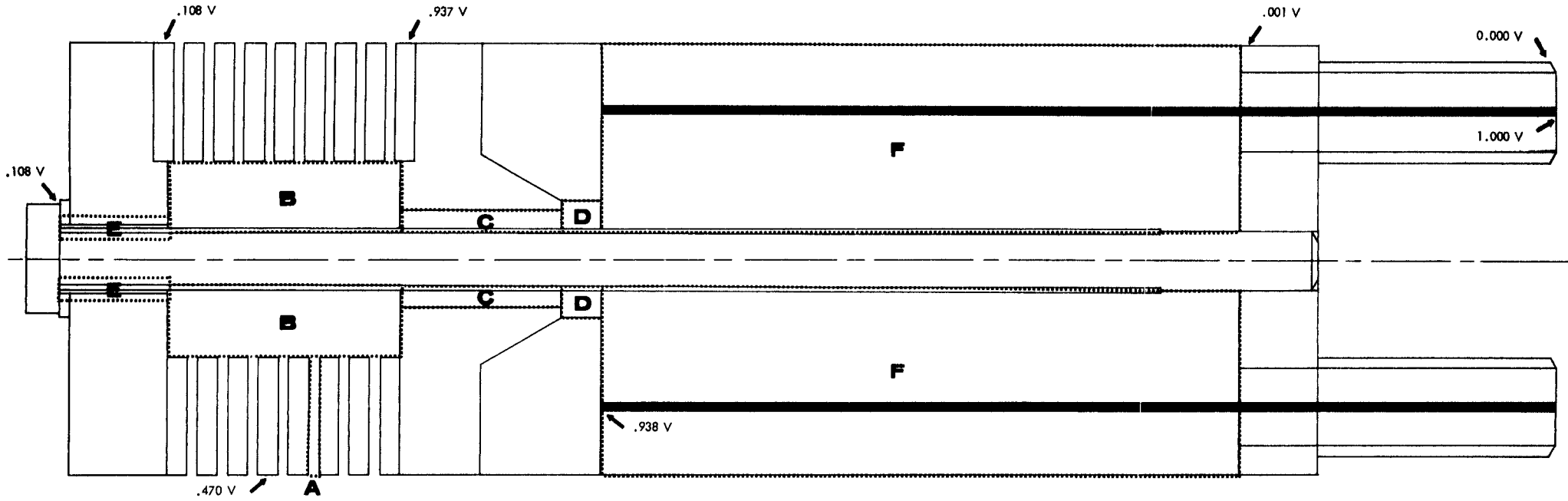

Figure B-3. Cryogenic Coil Assembly Cross Section Showing Various Relative DC Potentials and Regions of Capacitance

this coil assembly, Moore's methods will be used.

The method requires that, following the determination and mapping of the electric flux lines, inscribed circles be drawn between each pair of adjacent flux lines.[13] After all circles have been inscribed between flux lines in any region, the capacitance may be determined per unit depth by the following equation:

$$C = \varepsilon / R_{NT} \tag{B-8}$$

where C is capacitance in micro-micro farads, ε is absolute permittivity in micro-micro farads per inch, and R_{NT} is defined as,

$$\frac{1}{1/Nc_1 + 1/Nc_2 + 1/Nc_3 + \ldots + 1/Nc_j} \quad . \tag{B-9}$$

In Equation B-9, Nc represents the number of inscribed circles between two adjacent flux lines. The subscripts represent each series of circles from those inscribed between the first pair of adjacent flux lines, 1, to the last pair, j.[13]

After determination of the capacitance per unit depth, it then becomes necessary to multiply the results of Equation B-8 by the equivalent depth in order to obtain the total capacitance in the region under consideration. Moore's method is commonly referred to as the circle method of solution.

Determination of the electric field required in order to ultimately arrive at capacitances in the regions of the coil, and the accuracy with which each region's electric field map is determined must depend on the relative capacitance which it will contribute to the defining equation for the coil.

Although rigorous mapping techniques could be undertaken, a brief study of the essentials of electric field mapping will indicate some deviation from the rigorous procedures to be acceptable. There are two basic restrictions placed on electric field maps. First, all flux lines leave perpendicularly

from one surface and arrive perpendicularly at the second surface. Second, if equal potential lines are included, the intersection of the electric flux lines with the equal potential lines must produce curvilinear squares.[11] Also, flux lines leaving or arriving at a discontinuous point, such as a right angle, will bisect the discontinuity from which it originates or at which it terminates.

After reviewing the points mentioned above and a considerable number of field maps, which were prepared by Moore, it was decided that the mapping for all areas of the cryogenic coil could be done without resorting to any of the extremely rigorous methods.[9 11 13]

The capacitances in region A between each of the coil turns, may be determined by accurately plotting flux lines between turn surfaces. Figure number B-4 shows the plotting of the field lines in upper and lower cross-sections. Both cross-sections must be considered due to non-symmetry in the coil turn section. The averaged values of capacitance per unit depth for the upper and lower sections over the total area is divided by the total number of turns, 8, in order to arrive at a per turn capacitance value. Moore's method is used to consider the fringing of both upper and lower cross-sections. Although there may be some slight variation in the actual individual turn capacitance, the averaging procedure will produce results well within the desired accuracy.

Table B-4 lists the results obtained in determining the capacitances in region A. The results for capacitance are obtained by solution of Equation B-8. The dielectric material between all turns being nylon, yields a relative permittivity of 3.7.[16] Absolute permittivity may be found by Equation B-10a.

$$\varepsilon = (\varepsilon_o)\ (\varepsilon_r) \qquad \text{(B-10a)}$$

where ε_o is the permittivity of free space and ε_r is the relative permittivity of the medium.[14] For nylon

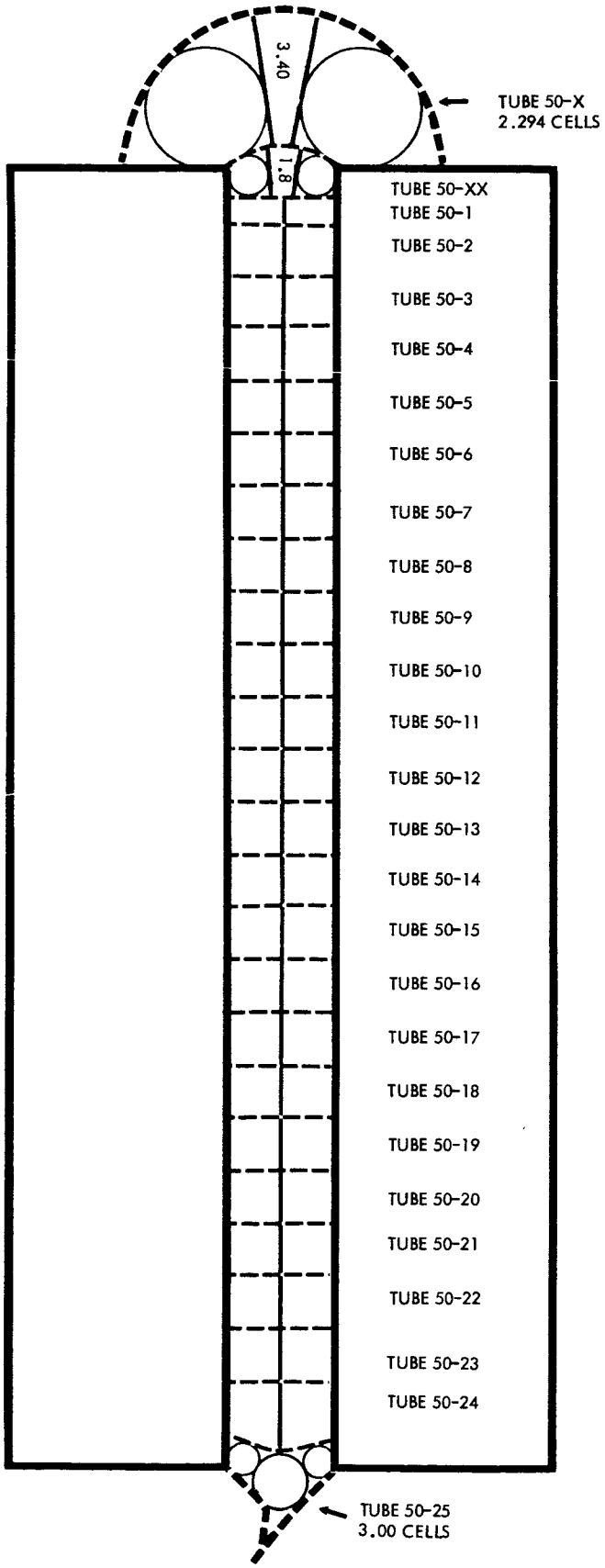

NOTE: 1. CELLS PER TUBE
50-XX, 2.555 CELLS
50-1 through 50-24
each have 2.000 CELLS.
2. THIS FIGURE REPRESENTS
REGION A FOR EACH
PAIR OF COIL TURNS
FOR BOTH UPPER AND
LOWER CROSS SECTIONS.

Figure B-4. Cross Section Between Coil Turns for Region A Used to Determine Capacitance in Cryogenic Coil

REGION A

Lower Cross Section		
Tube No.	No. Cells	1/(No. Cells)
50-X	2.294	.4359
50-XX	2.555	.3914
50-1	4.000	.2500
50-2	2.000	.5000
50-3	2.000	.5000
50-4	2.000	.5000
50-5	2.000	.5000
50-6	2.000	.5000
50-7	2.000	.5000
50-8	2.000	.5000
50-9	2.000	.5000
50-10	2.000	.5000
50-11	2.000	.5000
50-12	2.000	.5000
50-13	2.000	.5000
50-14	2.000	.5000
50-15	2.000	.5000
50-16	2.000	.5000
50-17	2.000	.5000
50-18	2.000	.5000
50-19	2.000	.5000
50-20	2.000	.5000
50-21	2.000	.5000
50-22	2.000	.5000
50-23	2.000	.5000
50-24	2.000	.5000
50-25	3.000	.3333
Total		12.9016
Total x 7 turns in section		90.3742
$1/(7 \cdot T) = R_{NT_1}$		.01106

Upper Cross Section		
Tube No.	No. Cells	1/(No.Cells)
50-X'	2.294	.4359
50-XX'	2.555	.3914
50-1'	4.000	.2500
50-2'	2.000	.5000
50-3'	2.000	.5000
50-4'	2.000	.5000
50-5'	2.000	.5000
50-6'	2.000	.5000
50-7'	2.000	.5000
50-8'	2.000	.5000
50-9'	2.000	.5000
50-10'	2.000	.5000
50-11'	2.000	.5000
50-12'	2.000	.5000
50-13'	2.000	.5000
50-14'	2.000	.5000
50-15'	2.000	.5000
50-16'	2.000	.5000
50-17'	2.000	.5000
50-18'	2.000	.5000
50-19'	2.000	.5000
50-20'	2.000	.5000
50-21'	2.000	.5000
50-22'	2.000	.5000
50-23'	2.000	.5000
50-24'	2.000	.5000
50-25'	3.000	.3333
Total		12.9016
Total x 8 turns in section		103.9016
$1/(8 \cdot T) = R_{NT_2}$		.00968

Average of R_{NT_1} and R_{NT_2} .01033

Table B-4. Information Used in Determining Per-Unit Depth Capacitance in Region A of Cryogenic Coil

$$\varepsilon = (.2248\ \mu\mu f/inch)\ (3.7) = .8318\ \mu\mu f/inch \qquad (B\text{-}10b)$$

The resulting value of total capacitance per unit depth for the coil turn section, region A, is

$$C_{A\ pud} = \frac{.8318}{.01033} = 80.523\ \mu\mu f/inch.$$

Total capacitance for this region is

$$C_{coil\ turn\ section} = \pi\ (1.9875)(80.523) = 502.778\ \mu\mu f/inch,$$

where 1.9875 inches is the mean diameter of the coil turn section. The corresponding value of capacitance per turn is

$$C_{coil\ turn\ section/turn} = 502.778 = 62.847\ \mu\mu f$$

For the capacitance in region B, between the coil turn section and the center bolt, it is necessary to again obtain both upper and lower cross sectional electric field maps - due to non-symmetry in the region.

The resulting maps with plotted circles are shown in Figures B-5$_a$ and B-5b. Electric flux lines for both figures were sketched using knowledge obtained from Moore's work to maximize accuracy.[13 27 28] It is again necessary to average the results of both upper and lower cross-sections to arrive at the final value of capacitance. Further, the results must be distributed on a per turn basis for the eight coil turns.

The results of mapping in Region B are tabulated in Table B-5.

It is important to note that the heat shrinkable tubing used to insulate the center bolt (Temlock #TL-E-393) is, for this study, considered to have a relative permittivity of 3.7, thus, making it equivalent to nylon. The entire dielectric medium in Region B will, therefore, be considered to be nylon. If a material with a permittivity not appreciably different from nylon is used, the error will be negligible.

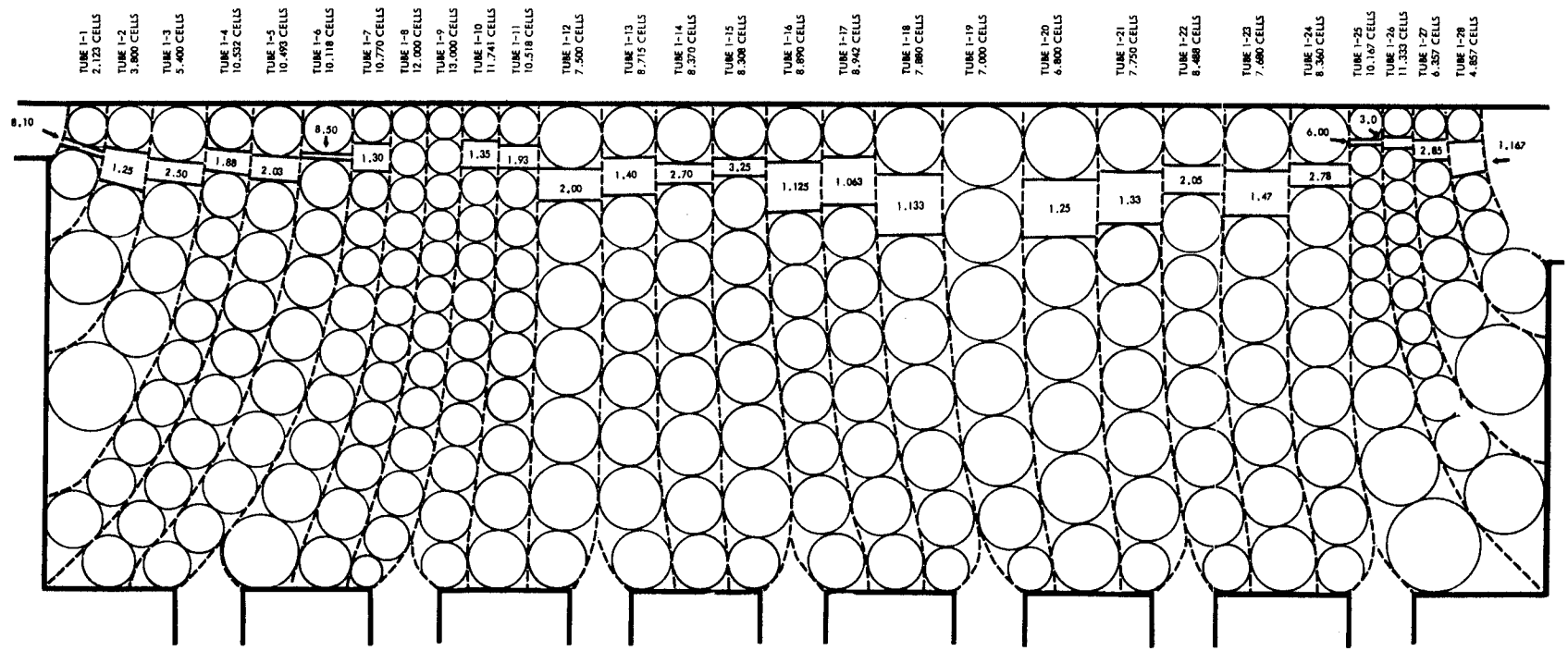

Figure B-5a. Lower Cross Section of Region B Used to Determine Capacitance In Cryogenic Coil

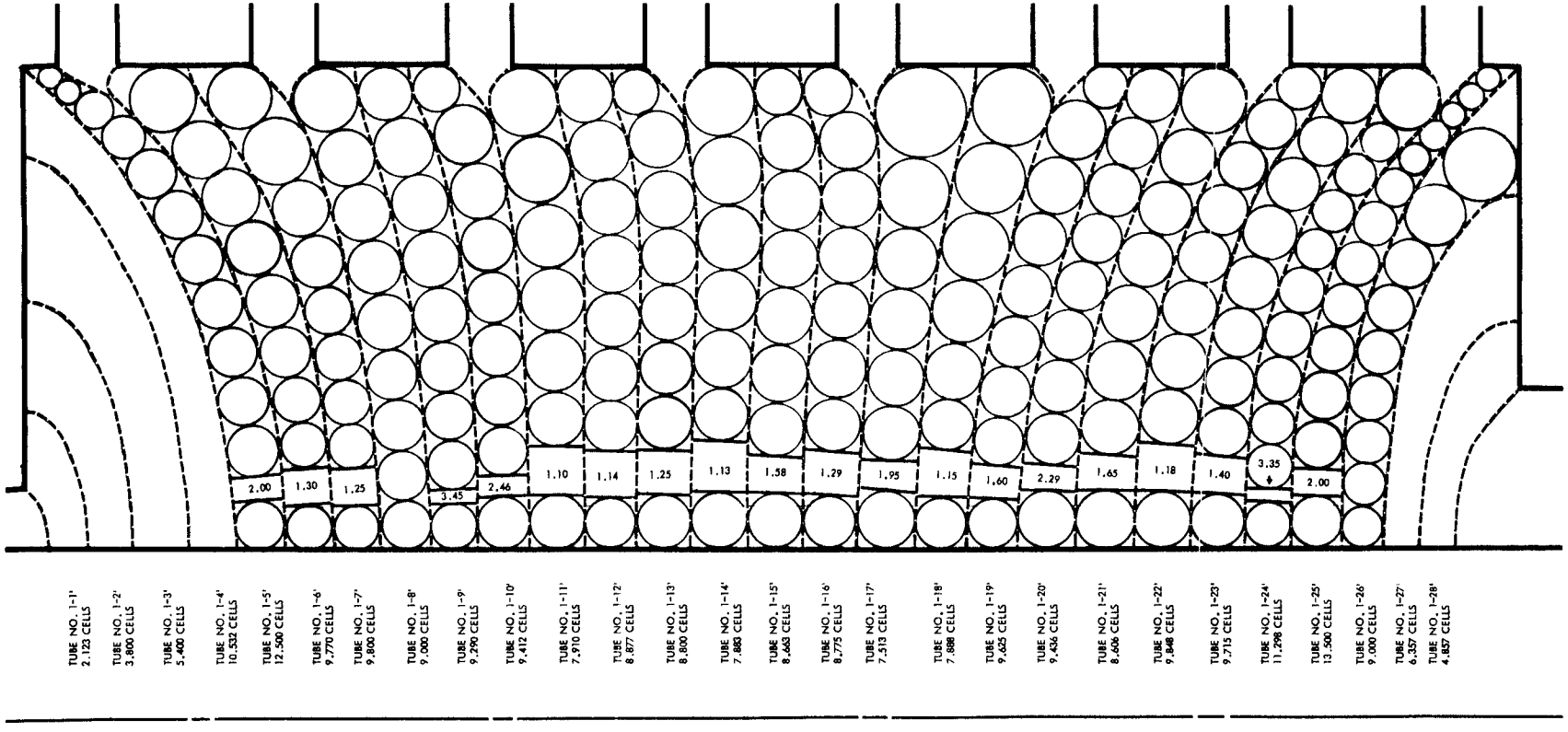

NOTE: TUBES 1-1' - 1-4' ARE EQUIVALENT RESPECTIVELY TO TUBES 1-1 - 1-4 IN FIGURE B-5a
TUBES 1-27' & 1-28' ARE EQUIVALENT RESPECTIVELY TO TUBES 1-27 & 1-28 IN FIGURE B-5a

Figure B-5b. Upper Cross Section of Region B Used to Determine Capacitance In Cryogenic Coil

Lower Cross Section		
Tube No.	No. Cells	1/(No.Cells)
1-1	2.123	.4710
1-2	3.800	.2632
1-3	5.400	.1852
1-4	10.532	.0949
1-5	10.493	.0953
1-6	10.118	.0988
1-7	10.770	.0929
1-8	12.000	.0833
1-9	13.00	.0769
1-10	11.741	.0852
1-11	10.518	.0908
1-12	7.500	.1333
1-13	8.715	.1147
1-14	8.370	.1195
1-15	8.308	.1204
1-16	8.890	.1125
1-17	8.942	.1118
1-18	7.880	.1269
1-19	7.000	.1429
1-20	6.800	.1471
1-21	7.750	.1290
1-22	8.488	.1178
1-23	7.680	.1302
1-24	8.360	.1196
1-25	10.167	.0984
1-26	11.333	.0882
1-27	6.357	.1575
1-28	4.857	.2059
Total		3.8132
1/Total		.2622
Average of 1/Total = R_{NT}		

Upper Cross Section		
Tube No.	No. Cells	1/(No.Cells)
1-1'	2.123	.4710
1-2'	3.800	.2632
1-3'	5.400	.1852
1-4'	10.532	.0949
1-5'	12.500	.0800
1-6'	9.770	.1024
1-7'	9.800	.1020
1-8'	9.000	.1111
1-9'	9.290	.1076
1-10'	9.412	.1062
1-11'	7.910	.1264
1-12'	8.877	.1127
1-13'	8.800	.1136
1-14'	7.883	.1269
1-15'	8.663	.1154
1-16'	8.775	.1140
1-17'	7.513	.1331
1-18'	7.888	.1268
1-19'	9.625	.1040
1-20'	9.436	.1060
1-21'	8.606	.1162
1-22'	9.848	.1015
1.23'	9.715	.1029
1-24'	11.298	.0885
1-25'	13.500	.0741
1-26'	9.000	.1110
1-27'	6.357	.1575
1-28'	4.857	.2059
Total		3.7602
1/Total		.2659
.2641		

Table B-5. Information Used in Determining Per-Unit Depth Capacitance in Region B of Cryogenic Coil

For region B, the total equivalent capacitance per unit depth is

$$C_{B\ pud} = \frac{.8318}{.2641} = 3.150\ \mu\mu f/inch$$

The corresponding total capacitance is

$$C_B = \pi\ (.7925)\ 3.150 = 7.843\ \mu\mu f.$$

where .7925 inches is the mean diameter of the region. The capacitance distributed in the seven spaces between the eight turns is

$$C_{B/turn} = \frac{7.843}{7} = 1.120\ \mu\mu f.$$

Regions C and D can most easily be considered at the same time. Due to the symmetry of upper and lower cross-sections, only the lower one will be used. The results of plotting and sketching the electric field and needed circles for these regions are shown in Figure B-6. The results of the plotting are tabulated in Table B-6.

For region C, where the dielectric is again nylon, the capacitance per unit depth is

$$C_{C\ pud} = \frac{.8318}{.1754} = 4.742\ \mu\mu f/inch$$

The corresponding total capacitance is

$$C_C = \pi\ (.4800)\ (4.742) = 7.151\ \mu\mu f$$

where .4800 inches is the mean diameter of the region.

Since the capacitances in regions C and D are parallel, an equivalent total for the two regions may be computed. Therefore,

$$C_{CD} = C_C \quad C = 7.151 + 2.047 = 9.198\ \mu\mu f \qquad (B\text{-}11)$$

where C_{CD} is the equivalent total capacitance for the two regions, C and D.

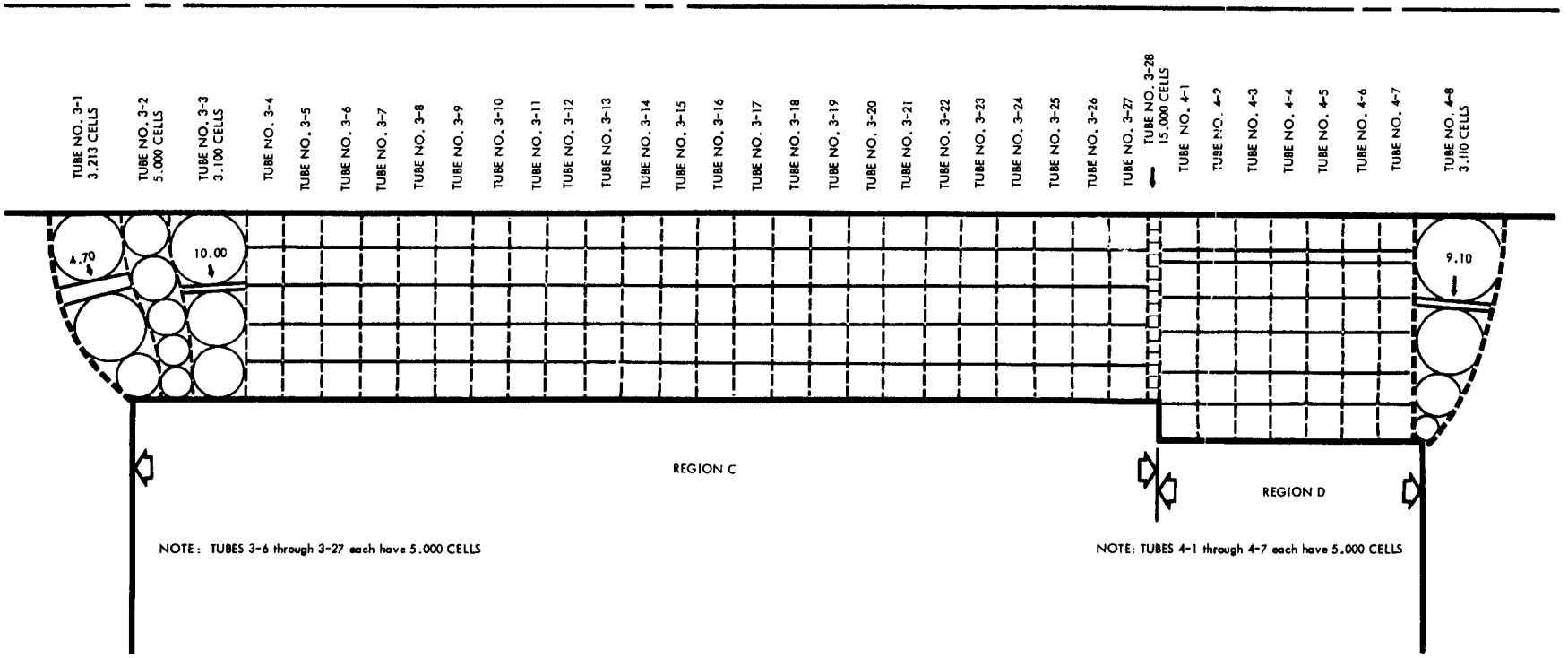

Figure B-6. Lower Cross Sections of Regions C and D Used to Determine Capacitance in Cryogenic Coil

REGION C

Tube No.	No. Cells	1/(No. Cells)
3-1	3.213	.3112
3-1	5.000	.2000
3-3	3.100	.3226
3-4	5.000	.2000
3-5	5.000	.2000
3-6	5.000	.2000
3-7	5.00	.2000
3-8	5.000	.2000
3-9	5.000	.2000
3-10	5.000	.2000
3-11	5.000	.2000
3-12	5.000	.2000
3-13	5.000	.2000
3-14	5.000	.2000
3-15	5.000	.2000
3-16	5.000	.2000
3-17	5.000	.2000
3-18	5.000	.2000
3-19	5.000	.2000
3-20	5.000	.2000
3-21	5.000	.2000
3-22	5.000	.2000
3-23	5.000	.2000
3-24	5.000	.2000
3-25	5.000	.2000
3-26	5.000	.2000
3-27	5.000	.2000
3-28	15.000	.0667
Total		5.7005
1/Total = R_{NT}		.1754

REGION D

Tube No.	No. Cells	1/(No.Cells)
4-1	6.263	.1604
4-2	6.263	.1604
4-3	6.263	.1604
4-4	6.263	.1604
4-5	6.263	.1604
4-6	6.263	.1604
4-7	6.263	.1604
4-8	3.110	.3215
Total		1.4443
1/Total = R_{NT}		.6924

Table B-6. Information Used in Determining Per-Unit Depth Capacitance in Regions C and D of Cryogenic Coil

Region E is also symmetrical. Thus, only the lower cross-section needs to be considered. The field map and required circle plots are shown in Figure B-7. The results of the capacitance determination are shown in Table B-7.

For region E, the capacitance per unit depth is

$$C_{E\ pud} = \frac{.8318}{.0842} = 9.879\ \mu\mu f/inch$$

The corresponding value of total capacitance is

$$C_E = \pi\ (.39675)\ (9.879) = 12.003\ \mu\mu f$$

where .38657 is the mean diameter of the region.

For the region F, it is useful to consider a subdivision into two subregions, F_1 and F_2 . If subregion F_1 is used to determine the capacitance existing in the region due to the electric field between the connector - base plate and the center bolt, while F_2 is used to determine capacitance due to the interaction of potentials between the coaxial feed lines and the center bolt; solution is simplified.

Capacitance in subregion F_1 may be determined in a manner similar to that used for regions A through E. The field mapping for subregion F_1 is shown in Figure B-8. The associated information appears in Table B-8. For this subregion the capacitance per unit depth is

$$C_{F_1 pud} = \frac{.8318}{.7008} = 1.1870\ \mu\mu f/inch.$$

Since the subregion as seen in Figure B-8 is not completely filled by the electric field, an effective mean must be found. The field distribution closely approaches a triangular area. Thus, if the centroid of this triangular area is used as the location of the effective mean radius, a solution for total subregion capacitance may be found. The distance from the center line of the center bolt to the centroid is

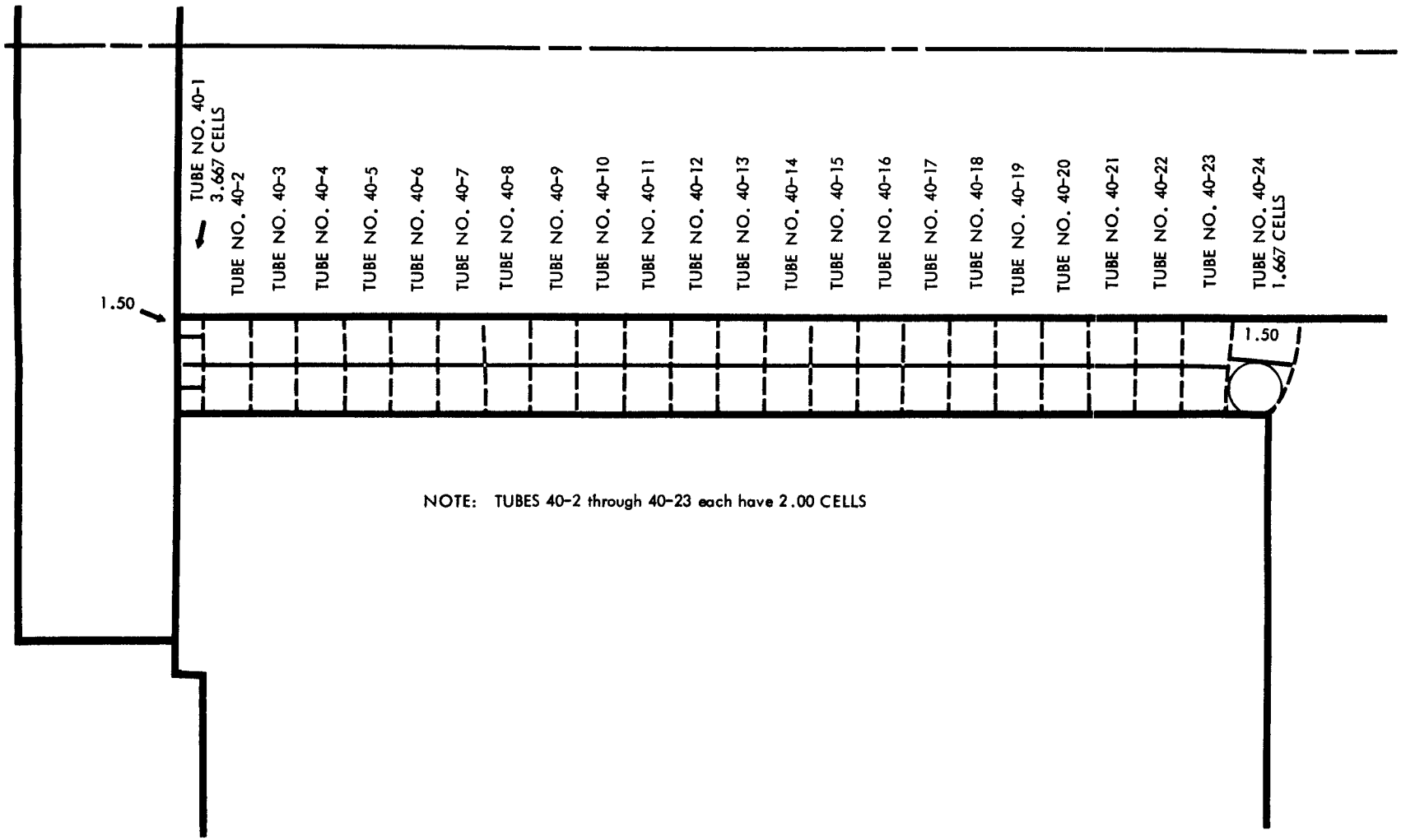

Figure B-7. Lower Cross Section of Region E Used to Determine Capacitance in Cryogenic Coil

REGION E		
TUBE NO.	NO. CELLS	1/(NO. CELLS)
40-1	3.667	.2727
40-2	2.000	.5000
40-3	2.000	.5000
40-4	2.000	.5000
40-5	2.000	.5000
40-6	2.000	.5000
40-7	2.000	.5000
40-8	2.000	.5000
40-9	2.000	.5000
40-10	2.000	.5000
40-11	2.000	.5000
40-12	2.000	.5000
40-13	2.000	.5000
40-14	2.000	.5000
40-15	2.000	.5000
40-16	2.000	.5000
40-17	2.000	.5000
40-18	2.000	.5000
40-19	2.000	.5000
40-20	2.000	.5000
40-21	2.000	.5000
40-22	2.000	.5000
40-23	2.000	.5000
40-24	1.667	.5999
TOTAL		11.8726
1/TOTAL R_{NT}		.0842

Table B-7. Information Used in Determining Per-Unit Depth Capacitance in Region E of Cryogenic Coil

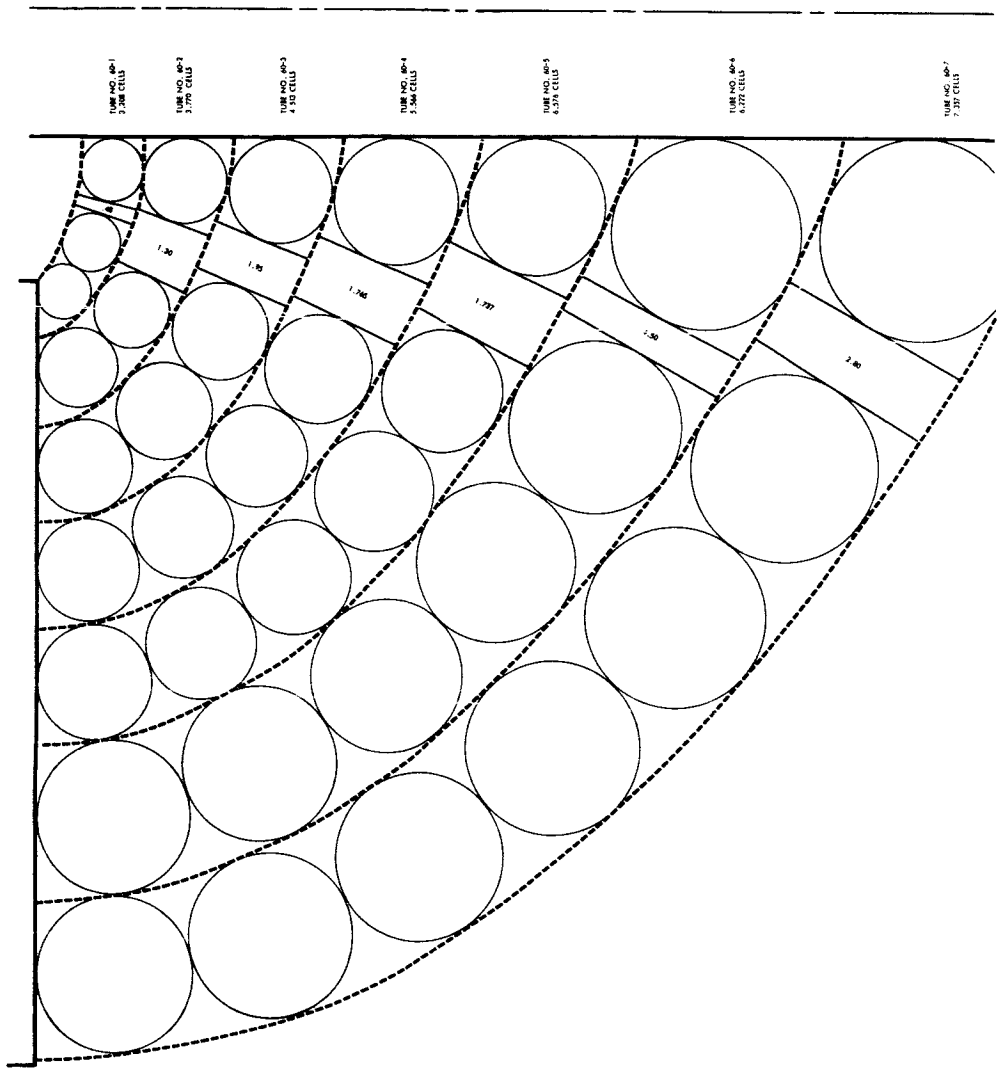

Figure B-8. Lower Cross Section of Subregion F_1 Used to Determine Capacitance in Cryogenic Coil

SUB-REGION F_1

TUBE NO.	NO. CELLS	1/(NO. CELLS)
60-1	3.208	.3117
60-2	3.770	.2653
60-3	4.513	.2216
60-4	5.566	.1797
60-5	6.576	.1521
60-6	6.222	.1607
60-7	7.357	.1359
TOTAL		1.4270
1/TOTAL = R_{NT}		.7008

Table B-8. Information Used in Determining Per-Unit Depth Capacitance in Sub-Region F_1 of Cryogenic Coil

$$D = 1/3h, \tag{B-12}$$

where h is the height of the triangular area. For the area in question, h = 1.3625 inches. Therefore,

$$D_{F_1} = \frac{1.3625}{3} = .4542 \text{ inches.}$$

Using D_{F_1} as the effective mean radius yields,

$$C_{F_1} = 2\pi (.4542)(1.187) = 3.387 \ \mu\mu f.$$

For subregion F_2, capacitance per individual coaxial feed line may be determined by

$$C = \frac{\varepsilon A_e}{.9(4\pi) D_s} \tag{B-13}$$

where ε is absolute permittivity for the nylon dielectric (.8318 μμf/inch), A_e is effective area and D_s is the effective distance of separation between the feed line and the center bolt. An end view of the area under consideration is shown in Figure B-9. Corresponding information concerning the figure is found in Table B-9.

Using information from Figure B-9 and Table B-9, Equation B-13 allows solution for capacitance. Thus,

$$C = \frac{(.8318)(.8068)}{.9(4\pi)(.9366)} = .0709 \ \mu\mu f/\text{feed line.}$$

The resulting capacitance for the six paralleled coaxial feed lines would be

$$C_{F_2} = (.709)(6) = .4254 \ \mu\mu F$$

Since both capacitances in region F are effectively paralleled, the total capacitance would be,

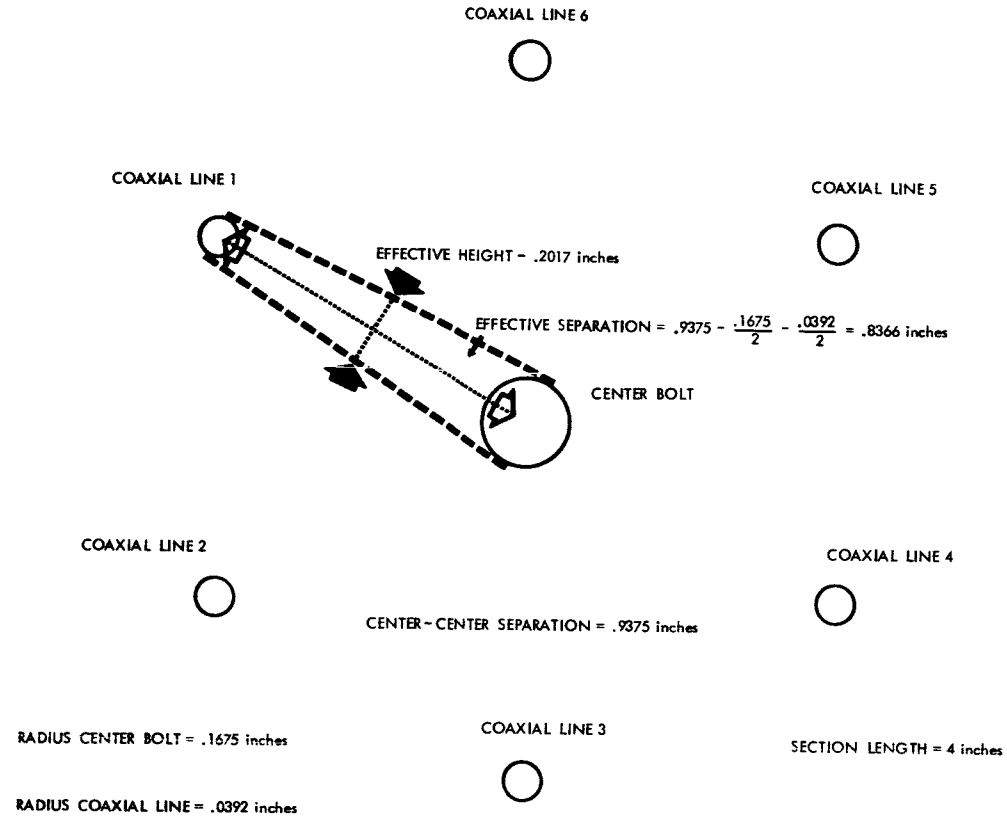

Figure B-9. End View Cross Section of Subregion F_2 Used to Determine Capacitance in Cryogenic Coil

LOCATION	EFFECTIVE SEPARATION	EFFECTIVE HEIGHT	LENGTH	EFFECTIVE AREA
CENTER BOLT - LINE 1.	.8366 inches	.2017 inches	4.0 inches	.8068 square inches
CENTER BOLT - LINE 2.	.8366 inches	.2017 inches	4.0 inches	.8068 square inches
CENTER BOLT - LINE 3.	.8366 inches	.2017 inches	4.0 inches	.8068 square inches
CENTER BOLT - LINE 4.	.8366 inches	.2017 inches	4.0 inches	.8068 square inches
CENTER BOLT - LINE 5.	.8366 inches	.2017 inches	4.0 inches	.8068 square inches
CENTER BOLT - LINE 6.	.8366 inches	.2017 inches	4.0 inches	.8068 square inches
TOTAL EQUIVALENT	.8366 inches	1.2102 inches	4.0 inches	4.8408 square inches

Table B-9. Parameters for Determining Capacitance in Subregion F_2 of Cryogenic Coil

$$C_{F_1F_2} = C_{F_1} + C_{F_2} = 3.3870 + .0709 = 3.458 \ \mu\mu f.$$

In summation, the capacitances associated with the cryogenic coil are:

C_A = 62.847 $\mu\mu$f/turn

C_B = 1.120 $\mu\mu$f/each section between turns

C_{CD} = 9.198 $\mu\mu$f

C_E = 12.003 $\mu\mu$f

$C_{F_1F_2}$ = 3.458 $\mu\mu$f.

DETERMINATION OF INDUCTANCE

Prior to obtaining the solution for inductances in the coil, it is necessary to begin by reviewing the coil under normal operation. Figure B-2 provides an understanding of how current flows through the coil. From Figure B-2 there appears to be two major sections where inductance will be an important factor. These are the coil turn section and the center bolt section. There are, to be sure, inductances associated with the other sections of the coil, but their effect will be small as compared to the inductances of the coil turn section and the center bolt section. This study will consider only the inductances associated with the coil turn section and the center bolt section.

The expression which allows solution for inductance associated with the individual turns in the coil turn section is

$$L = \Phi/I, \tag{B-14}$$

where Φ is the total flux in webers surrounding each turn which is carrying I amperes. For normalizing purposes, all inductances will be determined in webers.

Since flux, Φ, equals flux density, β, times area, a, and flux density further equals μH, the expression in Equation B-14 may be replaced by

$$L = \int_c^d \mu H \, da \text{ henrys} \tag{B-15}$$

If the value of H as a function of the perpendicular distance, y, from the center line of the center bolt to the center of each turn is found, inductance may be calculated.

Since all materials associated with the coil assembly are non-magnetic, μ has a constant value of 1.257×10^{-6} henrys per meter.[4] This is equivalent to

$$\mu = \frac{(1.257 \times 10^{-6})}{39.37} = .0319 \times 10^{-6} \text{ henrys/inch.} \qquad \text{(B-16)}$$

A review of the works of Rogers provides an excellent basis for studying the needed values of H, required in Equation B-15.[30] If each coil turn in the coil turn section were considered to be subdivided into an infinite number of differential current elements, the incremental vector magnetic potential found at a general point, p, as a result of one differential current element would be

$$dA = \frac{I\ dL}{4\ \pi\ R'} \qquad \text{(B-17)}$$

where dL is the length of the differential current element and R' is the distance from the general point, p, under study to the differential element in question.

If each of the remaining coil turns were likewise subdivided into an infinite number of differential elements and the total resultant vector magnetic potential were found at the point p, the value would be

$$A = 2 \int_0^{\pi} \frac{I\ dL}{4\ \pi\ R'} \qquad \text{(B-18a)}$$

Using spherical coordinates, Rogers defines R' as $(R^2 + b^2 - 2Rb \sin\theta \sin\phi)^{1/2}$ where R is the distance from the coordinate system origin to point p, and b is the distance in the x-y plane from the origin to each differential current element.[30] The differential element dL may be replaced by its spherical coordinate equivalent, $bd\phi$, while R' is replaced by its equivalent. Thus,

$$A = 2 \int_0^{\pi} \frac{I\ bd\phi}{4\ \pi\ (R^2 + b^2 - 2bR \sin\theta \sin\phi)^{1/2}} \qquad \text{(B-18b)}$$

An investigation, as performed by Rogers, of the x and y components of A, found by taking the respective dot products of A with the unit vectors i and j, shows that A_y equals 0.[30] Thus, the only non-zero component of A which exists

is A_x. Taking the dot product as indicated for A_x yields the elliptical integral

$$A_x = 2 \int_o^{\pi} \frac{-I\ b \sin \phi\ d\ \phi}{4\ \pi(R^2 + b^2 - 2bR \sin \theta \sin \phi)^{1/2}} \qquad \text{(B-19)}$$

Before actually solving Equation B-19, it is desirable to investigate the relationship between A_x and magnetic field intensity, H. By definition

$$H = \Delta \times A. \qquad \text{(B-20)}$$

The curl of A, with A_x the only non-zero component, produces two H vectors. They are

$$H_y = \frac{\partial A_x}{\partial z} \text{ and} \qquad \text{(B-21a)}$$

$$H_z = \frac{\partial A_x}{\partial y} . \qquad \text{(B-21b)}$$

Of the two H vectors, only the perpendicular component, H_y, is needed to determine ϕ. The normal vector, H_z, produces magnetic field intensity, and thus, flux, which is parallel to the plane of the area used for determining ϕ. Thus, it will contribute nothing to resulting answer for ϕ.

In the case where only H_y is considered,

$$H_y = \frac{\partial A_x}{\partial z} = \frac{dA_x}{dz} \qquad \text{(B-22)}$$

thereby reducing the partial differential equation to a differential equation.

With values of H_y, which will be a function of z, available, the expression for flux per ampere in Equation B-15 may be written as

$$\phi \text{ / ampere} = 2\ \mu \int_o^{\pi} \int_o^{r} H_y(z)\ R\ dZ\ d\theta. \qquad \text{(B-23a)}$$

However, since $H_y(z)$ equals dA_x/dz, the equation may be rewritten as

$$\phi \text{ / ampere} = 2\mu \int_o^{\pi} \int_o^{r} \frac{R\ dA_x\ dz\ d\theta}{dz} . \qquad \text{(B-23b)}$$

This may be further simplified to

$$\phi \text{ / ampere} = 2\mu \int_o^{\pi} \int_o^{r} R \, dA_x \, d\theta. \qquad \text{(B-23c)}$$

Since R now represents the distance from the z-axis to the point, p, where H is being determined in the y-z plane, it becomes a constant for each particular determination. Equation B-23c may therefore be still further simplified to

$$\phi \text{ / ampere} = 2\mu R \int_o^{\pi} \int_o^{r} dA_x \, d\theta \qquad \text{(B-23d)}$$

An investigation of the inter-integral of Equation B-23d,

$$\int_o^{r} dA_x,$$

produces some interesting conclusions. At the center of the coil turn section, A_x must equal zero since H_y has a maximum value at that point and A_x is the derivative of H_y. Further, at the center of each coil turn, H_y is zero and thus A_x must be maximum or equal to $A_{x\ max}$.

From the maximum value, at the center of each coil turn, A_x continually decreases, reaching zero at the center of the coil section. Therefore, evaluating the inter-integral must yield

$$\int_o^{r} dA_x = A_{x\ max}, \qquad \text{(B-24)}$$

where the limits of integration are from zero to r equal R.

Replacing the inter-integral with the results of Equation B-24 yields

$$\phi \text{ / ampere} = 2\mu R \int_o^{\pi} A_{x\ max} \, d\theta, \qquad \text{(B-25a)}$$

which when integrated leaves

$$\phi \text{ / ampere} = 2 \pi u R A_{x\ max}. \qquad \text{(B-25b)}$$

Equation B-25b, therefore, allows determination of flux per ampere and inductance without having to calculate and sum the values of H_y.

An IBM Fortran II program (see Appendix B-III) allows determination of

the A_x values ($A_{x\ max}$) at each coil turn's center by making use of Simpson's Rule.[24] The resulting values of $A_{x\ max}$, R, ϕ per ampere, and inductance, L, are summarized in Table B-10.

For the purposes of determining inductance for the center bolt section of the coil, it will be divided into five distinct areas as shown in Figure B-10. In area K, calculations for inductance will consider the bolt to be a long coaxial conductor with the ground plate forming the outer conductor. In area M, the calculations for inductance will again consider the bolt to be a long coaxial conductor. For this area, the inner surface of the coil turn section will be considered to form a solid outer conductor. In areas N and Q, the center bolt will also be considered as a long coaxial conductor with the connector-base plate as the outer conductor. Finally, the center bolt will be considered as a coaxial conductor for calculations of inductance in area T. The outer surface will be considered to be the coaxial feed lines.

In any region, the inductance as given by Skilling, per inch of a coaxial conductor is,

$$L_{pud} = \frac{1}{39.37} (.461 \log \frac{b}{a} + .050C_p) \ \mu h/inch \qquad (B-26)$$

where a is the radius of the outer surface of the inner conductor, b is the radius of the inner surface of the outer conductor, and C_p equals relative permeability times the ratio of ac inductance to dc inductance for the conductor.[16a] For dc considerations, C_p equals 1.

For area K, the dc inductance per inch is,

$$L_{Kpul} = \frac{1}{.3937} (.461 \log \frac{.21875}{.16750} + .05) = .00262 \ \mu h/inch \qquad (B-27a)$$

The length of the center bolt in area K is .59 inches. Thus,

$$L_K = .00154 \ \mu \text{ henrys} \qquad (B-27b)$$

Coil Turn No.	A_{max} In Amperes	R In Inches	L In μ henrys
1	1.07526	.99375	.214238
2	1.25835	.99375	.250717
3	1.36777	.99375	.2725186
4	1.41882	.99375	.282690
5	1.41882	.99375	.282690
6	1.36777	.99375	.2725186
7	1.25835	.99375	.250717
8	1.07256	.99375	.214238

Table B-10. Inductance and Other Parameters for Each Coil Turn of Cryogenic Coil.

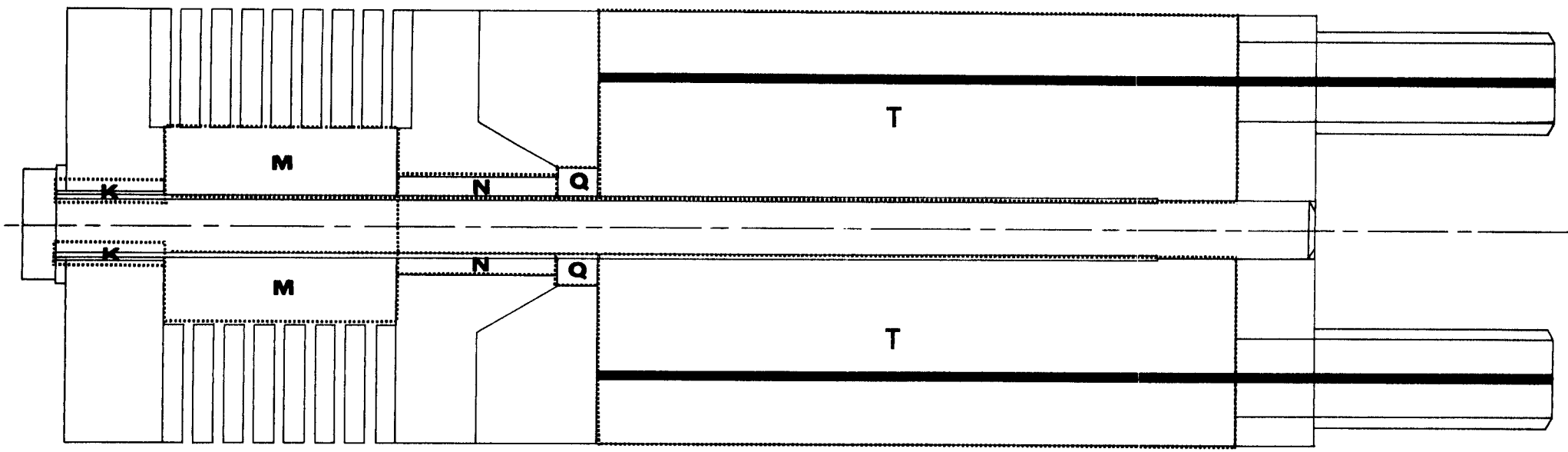

Figure B-10. Cryogenic Coil Assembly Cross Section Showing Areas of Inductance About Center Bolt

Applying Equation B-26 to area M under dc operation yields,

$$L_{Mpul} = \frac{1}{.3937}\left(.461 \log \frac{.6250}{.16750} + .05\right) = .00796\ \mu h/inch \qquad (B\text{-}28a)$$

The length of the center bolt in area M is 1.295 inches. Thus,

$$L_M = .01031\ \mu \text{ henrys} \qquad (B\text{-}28b)$$

In region N,

$$L_{N\ pul} = \frac{1}{.3937}\left(.461 \log \frac{.3125}{.1675} + .05\right) = .00444\ \mu h/inch \qquad (B\text{-}29a)$$

The length of the center bolt in region N is 1.00 inches. Thus,

$$L_N = .00444\ \mu \text{ henrys} \qquad (B29\text{-}b)$$

In region Q,

$$L_{Q\ pul} = \frac{1}{.3937}\left(.461 \log \frac{.375}{.1675} + .05\right) = .00536\ \mu h/inch \qquad (B\text{-}30a)$$

The length of region Q is .25 inches. Thus,

$$L_Q = .00134\ \mu \text{ henrys} \qquad (B\text{-}30b)$$

In region T,

$$L_{T\ pul} = \frac{1}{.3937}\left(.461 \log \frac{.9375}{.1675} + .05\right) = 1.00178\ \mu\ h/inch \qquad (B\text{-}31a)$$

The length of the center bolt in Region T is 4.00 inches. Thus,

$$L_T = 4.00712\ \mu \text{ henrys} \qquad (B\text{-}31b)$$

In conclusion, the inductances of the coil are summarized as

$$L_{turn\ 1} = 0.214238\ \mu \text{ henrys}$$

$$L_{turn\ 2} = 0.250717\ \mu \text{ henrys}$$

$$L_{turn\ 3} = 0.272518\ \mu \text{ henrys}$$

$L_{turn\ 4} = 0.282690\ \mu$ henrys

$L_{turn\ 5} = 0.282690\ \mu$ henrys

$L_{turn\ 6} = 0.272518\ \mu$ henrys

$L_{turn\ 7} = 0.250717\ \mu$ henrys

$L_{turn\ 8} = 0.214238\ \mu$ henrys

$L_K = 0.001540\ \mu$ henrys

$L_M = 0.103100\ \mu$ henrys

$L_N = 0.004440\ \mu$ henrys

$L_Q = 0.001340\ \mu$ henrys

$L_T = 4.007120\ \mu$ henrys

CONCLUSIONS - CRYOGENIC SEALING COIL

With respective values of resistance, capacitance, and inductance determined on a distributed parameter basis for the typical coil, an equivalent circuit based on the particular element locations is shown in Figure B-11. From Figure B-11 a second equivalent circuit, Figure B-12, with parameters grouped into seven basic impedance elements, is derived. In Figure B-11 and B-12 all elements have been included, although some contribute little to the over-all impedance.

The study of each of the seven impedance elements produces some interesting conclusions. For the coil turn section, a series inductance-resistance combination is in parallel with a capacitance for each turn. The shunting capacitance C_1, is a constant for each turn (62.487 μμf). The magnitude of its shunting impedance at 20,000 cps, the condition where it is minimum, and thus most apt to become important, is approximately 2×10^6 ohms. Relative impedance values for both resistance and inductance in the remaining parallel branch of the equivalent coil turn impedance are in the 10^{-6} ohm range. Thus, C_1 may be neglected in determining an equivalent impedance for the coil.

The C_3 element (12.003 μμf) has an approximate minimum impedance of 6.6×10^6 ohms at 20,000 cps. Element C_3 shunts the series R_3 and L_3 elements which has maximum impedance at 20,000 cps of approximately $(48 + j19.4) \times 10^{-6}$ ohms. The shunting effect is, therefore, neglibible.

Similarly, each C_4 element (1.120 μμf), the capacitance which shunts the coil turn section to the center bolt section, yields a minimum impedance at 20,000 cps of approximately 70×10^6 ohms. This value renders each of the C_4 elements insignificant in determination of the over-all coil impedance.

Finally, C_5 (9.198 μμf), whith an approximate minimim impedance of 8.7×10^6 ohms at 20,000 cps, contributes nothing of significance to the over-all coil impedance.

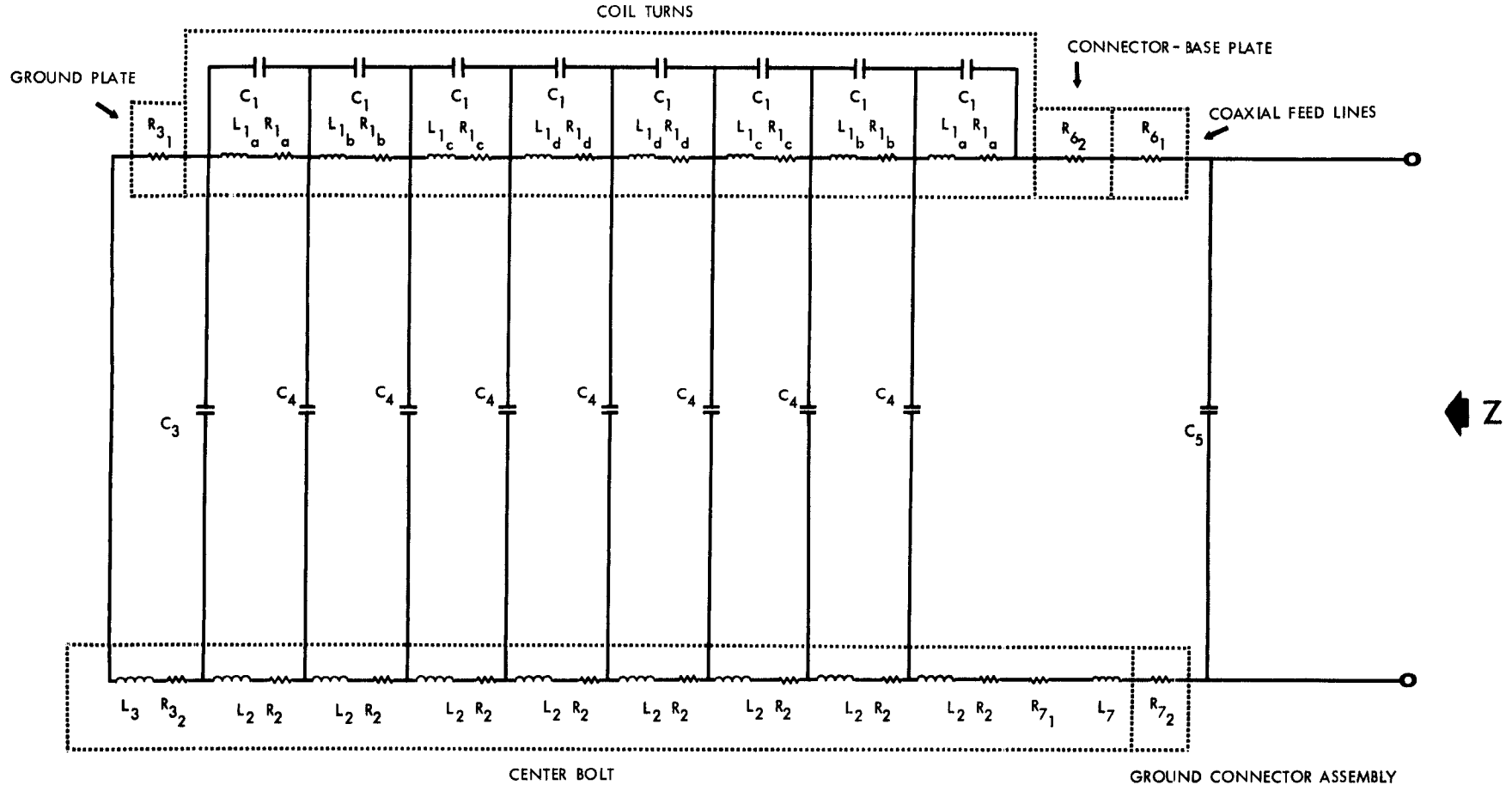

NOTE: $R_{3_1} + 8R_1 = R$ coil turn, $R_{3_2} + 8R_2 = R$ center bolt $\quad C_1 = C_A$, $C_3 = C_E$, $C_4 = C_B$, $C_5 = C_{CD}$ $\quad L_3 = L_K$, $L_2 = L_{M/8}$, $L_7 = L_N + L_Q + L_T$

Figure B-11. Equivalent Circuit of Cryogenic Coil Assembly Showing Respective Locations of Resistances, Capacitances, and Inductances

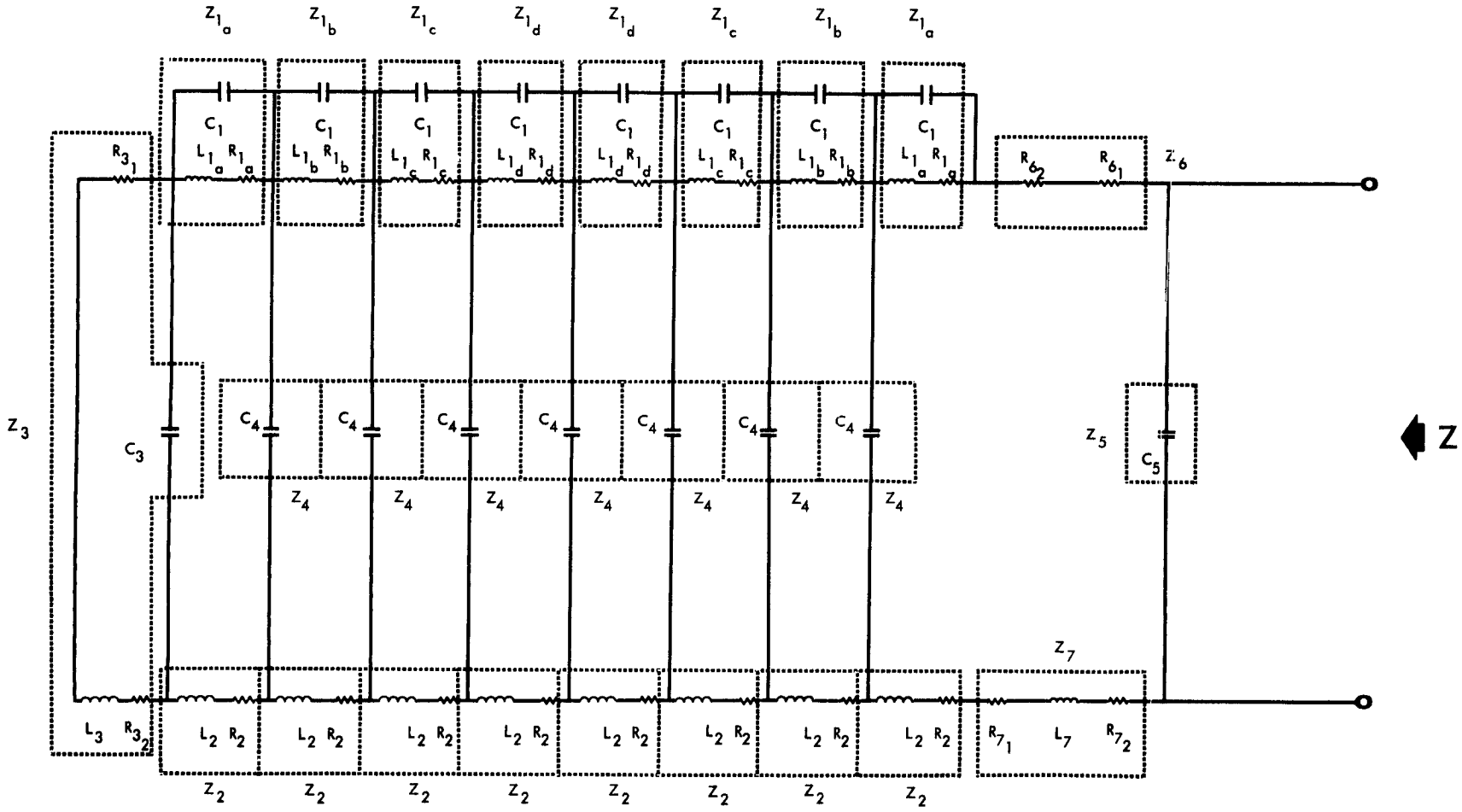

NOTE: $R_{3_1} + 8R_1 = R$ coil turn, $R_{3_2} + 8R_2 = R$ center bolt $\quad C_1 = C_A,\ C_3 = C_E,\ C_4 = C_B,\ C_5 = C_{CD} \quad L_3 = L_K,\ L_2 = L_{M/8},\ L_7 = L_N + L_Q + L_T$

Figure B-12. Equivalent Circuit of Cryogenic Coil Assembly Showing Grouped Impedance Elements Used to Derive Impedance Equation

After noting the negligible contributions of all capacitances, an expression, based on the remaining elements, may be derived for total impedance of the typical coil. It is

$$Z = (2R_{1a} + 2R_{1b} + 2R_{1c} + 2R_{1d} + 8R_2 + R_3 + R_6 + R_7) + j(2\omega L_{1a} + 2\omega L_{1b} + 2\omega L_{1c} + 2\omega L_{1d} + 8\omega L_2 + \omega L_3 + \omega L_7). \quad \text{(B-32a)}$$

Since values of R_{1a}, R_{1b}, R_{1c}, and R_{1d} are equal, the equation may be somewhat simplified to

$$Z = (8R_1 + 8R_2 + R_3 + R_6 + R_7) + j(2\omega L_{1d} + 2\omega L_{1b} + 2\omega L_{1c} + 2\omega L_{1d} + 8\omega L_2 + \omega L_3 + \omega L_7) \quad \text{(B-32b)}$$

The results of solving Equation B-32b to determine Z as a function of frequency are shown in Table B-11. Likewise, impedances associated with C_1, C_2, C_3, C_4, and C_5, are included. It should be noted that each of the elements R_1, R_2, R_3, and R_7 are functions of frequency as indicated in the section on resistances for the cryogenic coil. Information from Table B-11 is used to plot the frequency response as shown in Figure B-13. It graphically displays both magnitude and angle of impedance as a function of frequency.

In conclusion, the typical cryogenic coil may be said to be a simple series R-L circuit which becomes almost purely resistive at lower audio frequencies and almost purely inductive at the upper end of the spectrum. Should frequencies above the audio spectrum be considered, the shunting capacitance would eventually become important portions of the equivalent impedance function.

The scaled values of impedance elements may be studied in conjunction with Figures B-11 and B-12. Due to possible inclusion of skin effect considerations, the values of R_2, R_{3_2}, and R_{7_1}, the center bolt distributed resistances and the corresponding values of R_1, the coil turn distributed resistances, may be functions of frequency.

Symbol	f	R_1	ωL_{1a}	ωL_{1b}	ωL_{1c}	ωL_{1d}	$1/(\omega C_1)$	R_2	ωL_2	R	ωL_3	$1/(\omega C_3)$	$1/(\omega C_4)$	$1/(\omega C_5)$	R_6	R_7	ωL_7	Z Total Cartisian	Z Total Polar
Unit	cps	10^{-6} ohms	10^{-6} ohms	10^{-6} ohms	10^{-6} ohms	10^{-6} ohms	10^{-6} ohms	10^{-6} ohms	10^{-6} ohms	10^{-6} ohms	10^{-6} ohms	10^{-6} ohms	10^{-6} ohms	10^{-6} ohms	10^{-6} ohms	10^{-6} ohms	10^{-6} ohms	10^{-6} ohms	10^{-6} ohms
	20	208.8	2.7	3.2	3.4	3.6	1999.4	4.10	.16	19.66	.019	6630.0	71057.	8650.0	126.2	167.5	50.4	2016.6 + j 77.7	2016 ∠ 2.2°
	40	208.8	5.4	6.3	6.8	7.1	633.1	4.10	.32	19.77	.039	3320.0	35528.	4325.0	126.2	167.5	100.8	2016.6 + j 154.6	2016 ∠ 4.4°
	80	208.8	10.8	12.6	13.7	14.2	316.5	4.10	.65	19.66	.077	1660.0	17760.	2162.0	126.2	167.5	201.5	2016.6 + j 309.4	2039 ∠ 8.7°
	100	208.8	13.5	15.7	17.1	17.8	253.3	4.10	.81	19.66	.097	1330.0	14215.	1731.0	126.2	167.5	251.9	2016.6 + j 386.7	2048 ∠10.6°
	200	208.8	15.2	20.0	21.7	22.5	199.9	4.11	1.62	19.69	.184	663.0	7106.	865.0	126.2	167.7	503.8	2016.6 + j 675.7	2124 ∠18.5°
	400	208.8	53.8	63.0	68.5	71.0	63.3	4.12	3.24	19.74	.387	332.0	3553.	433.0	126.2	168.2	1007.6	2017.7 + j 1546.5	2539 ∠37.5°
	800	208.8	107.7	126.0	137.0	142.1	31.6	4.17	6.48	19.97	.774	166.0	1776.	216.0	126.2	170 2	2015.1	2020.2 + j 3093.4	3700 ∠56.8°
	1000	208.8	134.6	157.5	171.2	177.6	25.3	4.20	8.11	20.13	.968	133.0	1422	173.0	126.2	171 5	2518.9	2021.8 + j 3866.5	4370 ∠62.4°
	2000	209.4	152.5	199.5	216.9	225.0	20.0	4.47	16.21	21.41	1.935	66.3	711.	87.0	126.2	182.3	5037.7	2029.8 + j 6757.1	7060 ∠78.3°
	4000	211.9	538.5	630.1	684.9	710.5	6.3	5.38	32.42	25.77	3.871	33.2	355.	43.0	126.2	219.3	10075.8	2098.5 + j 15467.1	15600 ∠82.2°
	8000	214.9	1077.2	1260.5	1370.1	1421.3	3.2	7.09	64.84	33.99	7.741	16.6	178.	22.0	126.2	299.4	20151.2	2224.5 + j 30935.9	30940 ∠85.9°
	10,000	225.5	1345.8	1574.8	1711.8	1775.7	2.5	7.81	81.05	37.43	9.676	13.3	142.	17.0	126.2	318.0	25189.3	2337.1 + j 38663.6	38665 ∠86.5°
	20,000	285.2	1705.0	1995.1	2168.7	2249.7	2.0	10.02	162.10	47.99	19.352	6.6	71.	8.7	126.2	407.4	50377.1	2932.3 + j 67930.3	67930 ∠87.5°

Table B-11. Sectional and Total Impedances
For Typical Cryogenic Coil

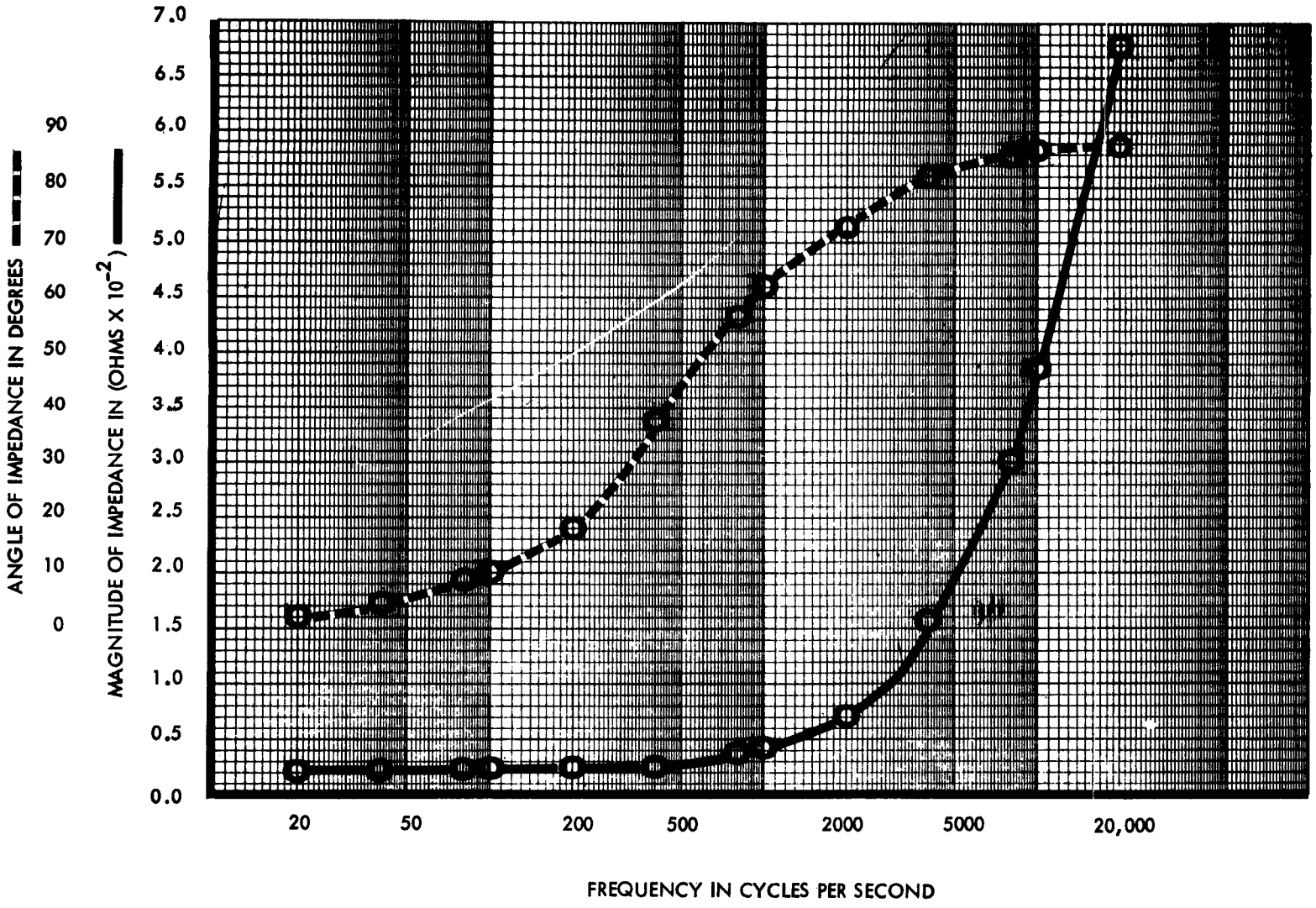

Figure B-13. Frequency Response of Typical Cryogenic Coil in Audio Spectrum

The net inductance for the coil assembly is found by summing the imaginary part of Equation B-32b. It is 6.172 μ henrys.

Since it is possible that the typical cryogenic coil may be scaled either upward or downward, a brief investigation of resulting changes in impedance should be noted. If the mean diameter of the typical coil turn section, 1.9875 inches, is chosen as the base for scaling, and a review of both the text and the appendixes of this section is made, results of the effects of the scaling may be determined. In each case D_m represents the new mean coil turn diameter.

The resistance of the coaxial feed lines (see Equation B-I-6) would become

$$r_{coax} = \frac{(6.78 \times 10^{-7})(5.5/1.9875)}{(6)\ (4.8 \times 10^{-3})} = 63.1 D_m \times 10^{-6} \text{ ohms} \qquad \text{(B-33)}$$

The resistance of the connector - base plate (see Equation B-I-7) would become

$$r_{\text{connector-base plate}} =$$

$$(3.08 \times 10^{-6})\ \{ \frac{(.250/1.9875)}{(1/1.9875)^2\ (\pi/4)\ [(2.725)^2 - (.75)^2]}$$

$$+ \frac{(1.00/1.9875)}{(1/1.9875)^2\ (\pi/4)[(2.725)^2 - (.625)^2]} \} = \frac{.497 \times 10^{-6}}{D_m} \text{ ohms} \qquad \text{(B-34)}$$

The resistance for the coil turn section (see Equation B-I-8) would become

$$r_{\text{coil turn/turn}} =$$

$$\frac{(3.081 \times 10^{-6})\ [(\pi)(1.9875/1.9875) + (.9984/1.9875)]^{1/2}}{(.7375/1.9875)(.1250/1.9875)} =$$

$$= \frac{415 \times 10^{-6}}{D_m} \text{ ohms/turn.} \qquad \text{(B-35)}$$

The resistance for the ground plate section (see Equation B-I-9) would become

$$r_{\text{ground plate}} = (3.09 \times 10^{-6}) \left\{ \frac{(.59/1.9875)}{(1/1.9875)^2\ (\pi/4)[(2.725)^2 - (4.375)^2} + \frac{(.06/1.9875)}{(1/1.9875)^2\ (\pi/4)\ [(.7500)^2 - (.4375)^2]} \right\} = \frac{1.9 \times 10^{-6}}{D_m} \text{ ohms.} \qquad \text{(B-36)}$$

The resistance of the center bolt section (see Equation B-I-10) would become

$$r_{\text{center bolt}} = (2.64 \times 10^{-6}) \left\{ \frac{(6.875/1.9875)}{(\pi/4)(.335/1.9875)^2} + \frac{(.5/1.9875)}{(\pi/4)(.375/1.9875)^2} \right\}$$

$$= \frac{433.3 \times 10^{-6}}{D_m} \text{ ohms} \qquad \text{(B-37)}$$

The resistance of the ground connector assembly (see Equation B-I-11) would become

$$r_{\text{ground connector assembly}}$$

$$= (2.6 \times 10\text{-}6) \left\{ \frac{(.50/1.9875)}{(1/1.9875)^2\ (\pi/4)\ [(2.725)^2 - (6)(.484)^2]} + \frac{(1.50/1.9875)}{(1/1.9875)^2(6\pi/4)\ [(6.25)^2 - (.484)^2]} \right\} = \frac{2.34 \times 10^{-6}}{D_m} \text{ ohms.} \qquad \text{(B-38)}$$

For the scaled resistances, it must be noted that the values for the coil turn section and the center bolt section are functions of frequency. This is a result of the skin effect associated with each of these two sections. The calculated values of Equations B-35 and B-37 are for dc conditions.

The exact values of ac scaled resistances for these two sections can not be given unless the scaling factor of the coil is known. Where exact scaling is known, a review of the works of Skilling[3] [28] would allow specific values of the two resistances, as a function of frequency, to be determined.

For capacitances, scaling would not effect determination of per unit depth values as determined in the capacitance section of the cryogenic coil study. However, the values of total capacitance would change due to changes in the equivalent mean diameters of the various sections.

For region A, the scaled capacitance would become

$$C_A = \frac{\pi}{8} \quad (1.9875/1.9875)80.523 = 31.62\ D_m \quad \mu\mu f/turn \qquad (B\text{-}39)$$

For region B the scaled capacitance is

$$C_B = \frac{\pi}{7}\ (.7975/1.9875)(3.150) = .564\ D_m\ \mu\mu f/turn \qquad (B\text{-}40)$$

For regions C and D, the scaled capacitance is

$$C_{CD} = \pi\ (.4800/1.9875)(.4742) + \pi\ (.5425/1.9875)(1.201) =$$

$$4.624\ D_m\ \mu\mu f. \qquad (B\text{-}41)$$

For region E, the scaled capacitance becomes

$$C_E = \pi\ (.38675/1.9875)(9.879) = 6.039\ D_m\ \mu\mu f. \qquad (B\text{-}42)$$

Finally, the capacitance in region F becomes

$$C_{F_1F_2} = 2\pi\ (.4542/1.9875)(1.1871) + \frac{6(.8318)(.8068)(1.9875)^2}{.9(4\pi)(.8366/1.9875)}$$

$$= (1.704\ D_m + \frac{.845}{D_m}\ )\ \mu\mu f. \qquad (B\text{-}43)$$

The scaled inductances associated with the coil turn section would vary directly as the mean diameter varies. Referring to Equation B-25b and Table B-10, numerical scaling yields

$$[\ L\ ]\ \text{Turns 1 \& 8} = 2\ \pi(.0319 \times 10^{-6})(.99375/1.9875)(1.07526)$$

$$= 1.0779\ D_m\ \mu\ \text{henrys} \qquad (B\text{-}44)$$

$$[\ L\ ]\ \text{Turns 2 \& 7} = 2\pi(.0319 \times 10^{-6})(.99375/1.9875)(1.25835)$$

$$= 1.2615\ D_m\ \mu\ \text{henrys} \qquad (B\text{-}45)$$

$$[L] \text{ Turns } 3 \text{ \& } 6 = 2\pi(.0319 \times 10^{-6})(.99375/1.9875)(1.36777)$$

$$= 1.3715\ D_m\ \mu \text{ henrys} \qquad \text{(B-46)}$$

$$[L] \text{ Turns } 4 \text{ \& } 5 = 2\pi\ (.0319 \times 10^{-6})(.99375/1.9875)(1.41882)$$

$$= 1.4223\ \mu \text{ henrys} \qquad \text{(B-47)}$$

Scaling for the five sections of the center bolt section produces values of inductances which are directly proportional to length. Specific values may be determined by modifying Equations B-27 through B-31. The respective results are

$$L_K = (.00262)(.59/19875) = .00077\ D_m\ \mu \text{ henrys} \qquad \text{(B-48)}$$

$$L_M = (.00796)(1.295/1.9875) = .00519\ D_m\ \mu \text{ henrys} \qquad \text{(B-49)}$$

$$L_N = (.00444)(1.00/1.9875) = .00223\ D_m\ \mu\text{henrys} \qquad \text{(B-50)}$$

$$L_Q = (.00536)(.25/1.9875) - .00067\ D_m\ \mu \text{ henrys} \qquad \text{(B-51)}$$

$$L_T = (1.00178)(4.00/1.9875) - 2.01616\ D_m\ \mu \text{ henrys} \qquad \text{(B-52)}$$

The scaled vaues of impedance elements may be studied in conjunction with Figures B-11 and B-12. Due to possible inclusion of skin effect considerations, the values of R_2, R_{3_2}, and R_{7_1}, the center bolt distributed resistances and the corresponding values of R_1, the coil turn distributed resistances, may be functions of frequency.

GENERAL CONCLUSIONS

The results of this investigation point out the fact that, in either of the coils in question, the capacitance is not a factor in the equivalent circuits. Both coils may be represented as having only inductance and resistance at audio frequencies.

In the general equation for the circuit parameters, it was assumed that all dimensions of the coil changed in the same ratio. Thus, the formulas are all based on the diameter of the coils. In this case, the capacitance and inductance would vary directly as the diameter of the coil. Since capacitance is negligible in the coils as presently constituted, it is felt that this might allow greater conductor area in the coil conductors without any appreciable capacitance being introduced.

In setting up the general equations based on the change in one dimension only, it was found that the current penetration depth or "skin effect" could not be made a function of this dimension. It was felt that this would have to be calculated individually for each coil size. For the actual coil sizes used, "skin effect" was found to be negligible for all audio frequencies of the hammer coil, but it was a factor in the upper audio frequencies of the cryogenic sealing coil.

This study was made assuming that both coils were in free space. Since the applications of both coils include some type of conducting material in the neighborhood of the coil, the magnetic field would be subject to considerable change. Also, the fields surrounding the coils depend on the conductivity and the magnetic properties of the conducting material. Further study should be made of these coils with a conducting material adjacent to the coils. This study should include both ferro-magnetic materials and others.

APPENDIX A

```
C       HAMMER COIL VECTOR MAGNETIC POTENTIAL DETERMINATION
        DIMENSION SSS(11)
        DO 11   1 = 1,11
        P = I - 1
   11 SSS(I) = SINF (3.14159/2.-P*3.14159/10.)
    2 READ 10, Y, Z
        PRINT 10, Y, Z
   10 FORMAT (2F10.4)
        A = .4792
        ZP = Z
        VMP = 0.
        COUNT = 0.
        DO 22  J = 1,45
        Q =J
        IF (COUNT-3.)  4,3,99
    3 COUNT = 1.
        A = A+.0594
        GO TO 9
    4 COUNT = COUNT+1.
        A = A+.0240
    9 DO 33  K = 1,10
        U = K
        Z = ZP+.0500* (U-1.)
        R = (Y*Y+Z)**.5
        THETA = 1.570796-ATANF(Z/Y)
        R2A2 = R*R+A*A
        TWORA = 2.*R*A*SINF(THETA)
        DO 44  L = 1,11
   44 W (L) = SSS(L)/((R2A2-TWORA*SSS(L) )**.5)
        WCOMP1 = 0.
        WCOMP2 = 0.
        WCOMP1 = W (2)+W(4)+W(6)+W(8)+W(10)
        WCOMP1 = 4.*WCOMP1
        WCOMP2 = W(3)+W(5)+W(7)+W(9)
        WCOMP2 = 2.*WCOMP2
        VMPI = (W(1)+W(11)+WCOMP1+WCOMP2)*A
        VMP = VMPI+VMP
   33 CONTINUE
   22 CONTINUE
        VMP = VMP*(1./1800.)
        PRINT  20,VMP
   20 FORMAT (E18.6)
        GO TO 2
   99 STOP
        END
```

```
C      HAMMER COIL VECTOR MAGNETIC POTENTIAL DETERMINATION
C      NEAR FIELD
       DIMENSION SSS(11), W(11)
       DIMENSION VMP(22,28)
       READ 50, IS
   50  FORMAT(I2)
       DO 11  I = 1,11
       P = I-1
   11  SSS(I) = SINF(3.14159/2.-P*3.14159/10.)
       DO 55  N = IS,28
       V = N
       FN=N/2
       NFN=FN*2.
       IF(NFN-N)12,13,99
   12  ZPP = .075
       GO TO 14
   13  ZPP = .025
   14  Y = 0.0976+.1074*(V-1.)
       DO 55  MM = 1,11
       M = MM
       WW = M
       Z = ZPP+.100*(WW-1.)
       IF(NFN-N)15,16,99
   15  M = 2*M
       GO TO 17
   16  M = (2*M)-1
   17  A = .4792
       PRINT 10, Y, Z
   10  FORMAT(2F10.4)
       ZP = Z
       VMPP = 0.
       COUNT = 0.
       DO 22  J = 1,45
       Q = J
       RF(CPUNT-3.) 4,3,99
    3  COUNT = 1.
       A = A+.0594
       GO TO 9
    4  COUNT = COUNT+1.
       A = A+.0240
    9  DO 33  K = 1,10
       U = K
       Z = ZP+.0500*(U-1.)
       R = (Y*Y+Z*Z)**.5
       THETA = 1.570796-ATANF(Z/Y)
       R2A2 = R*R+A*A
       TWORA = 2.*R*A*SINF(THETA)
       DO 44  L = 1,11
   44  W(L) = SSS(L)/((R2A2-TWORA*SSS(L))**.5)
```

```
      WCOMP1 = 0.
      WCOMP2 = 0.
      WCOMP1 = W(2)+W(4)+W(6)+W(8)+W(10)
      WCOMP1 = 4.*WCOMP1
      WCOMP2 = W(3)+W(5)+W(7)+W(9)
      WCOMP2 = 2.*WCOMP2
      VMPI = (W(1)+W(11)+WCOMP1+WCOMP2)*A
      VMPP = VMPP+VMPI
   33 CONTINUE
   22 CONTINUE
      VMP(M,N) = VMPP*(1./1800.)
      PRINT  20, VMP(M,N)
   20 FORMAT(E18.6)
   55 CONTINUE
      PRINT 40
   40 FORMAT(5X,1HY,9X,1HZ,12X,2HHY,12X,2HHZ,10X,5HHRSLT,6X,5HTHETA)
      ISS = IS+ 1
      DO 77 J = ISS,27
      E = J
      XFN = J/2
      NFX = XFN*2.
      IF(NFX-J)23,24,99
   23 ZPPP = .125
      GO TO 25
   24 ZPPP = .075
   25 Y = .2050+.1074*(E-2.)
      DO 77 KK = 1,10
      K = KK
      F = K
      Z = ZPPP+.100*(F-1.)
      IF(NFX-J)26,27,99
   26 K = (2*K)+1
      GO TO 28
   27 K = 2*K
   28 HY = (VMP(K-1,J)-VMP(K+1,J))*393.7
      HZ = (VMP(K,J+1)-VMP(K,J-1))*183.3
      HRSLT = (HY*HY+HZ*HZ)**.5
      THETA = ATANF(HZ/HY)
      THETA = THETA*(180./3.14159)
      PRINT 30, Y, Z, HY, HZ, HRSLT, THETA
   30 FORMAT(2F10.4,3E14.8,F10.4//)
   77 CONTINUE
   99 STOP
      END
```

```
C      HAMMER COIL VECTOR MAGNETIC POTENTIAL DETERMINATION
C      FAR FIELD
       DIMENSION SSS(11), W(11)
       DIMENSION VMP(22,28)
       READ 50, IS
   50  FORMAT(I2)
       DO 11  I = 1,11
       P = I-1
   11  SSS(I) = SINF(3.14159/2.-P*3.14159/10.)
       DO 55  N = IS,18
       V = N
       FN=N/2
       NFN=FN*2.
       IF(NFN-N)12,13,99
   12  ZPP = 1.000
       GO TO 14
   13  ZPP = .500
   14  Y = .500+.500*(V-1.)
       DO 55 MM = 1,18
       M = MM
       WW = M
       Z = ZPP+.500*(WW-1.)
       IF(NFN-N)15,16,99
   15  M = 2*M
       GO TO 17
   16  M = (2*M)-1
   17  A = .4792
       PRINT 10, Y, Z
   10  FORMAT(2F10.4)
       ZP = Z
       VMPP = 0.
       COUNT = 0.
       DO 22  J = 1,45
       Q = J
       IF(COUNT-3.) 4,3,99
    3  COUNT = 1.
       A = A+.0594
       GO TO 9
    4  COUNT = COUNT+1.
       A = A+.0240
    9  DO 33  K = 1,10
       U = K
       Z = ZP+.0500*(U-1.)
       R = (Y*Y+Z*Z)**.5
       THETA = 1.570796-ATANF(Z/Y)
       R2A2 = R*R+A*A
       TWORA = 2.*R*A*SINF(THETA)
       DO 44  L = 1,11
   44  W(L) = SSS(L)/((R2A2-TWORA*SSS(L))**.5)
```

```
      WCOMP1 = 0.
      WCOMP2 = 0.
      WCOMP1 = W(2)+W(4)+W(6)+W(8)+W(10)
      WCOMP1 = 4.*WCOMP1
      WCOMP2 = W(3)+W(5)+W(7)+W(9)
      WCOMP2 = 2.*WCOMP2
      VMPI = (W(1)+W(11)+WCOMP1+WCOMP2)*A
      VMPP = VMPP+VMPI
   33 CONTINUE
   22 CONTINUE
      VMP(M,N) = VMPP*(1./1800.)
      PRINT  20, VMP(M,N)
   20 FORMAT(E18.6)
   55 CONTINUE
      PRINT 40
   40 FORMAT(5X,1HY,9X,1HZ,12X,2HHY,12X,2HHZ,10X,5HHRSLT,6X,5HTHETA)
      ISS = IS+ 1
      DO 77 J = ISS,27
      E = J
      XFN = J/2
      NFX = XFN*2.
      IF(NFX-J)23,24,99
   23 ZPPP = 1.500
      GO TO 25
   24 ZPPP = 1.000
   25 Y = 1.000+.500*(E-2.)
      DO 77 KK = 1,10
      K = KK
      F = K
      Z = ZPPP+.500*(F-1.)
      IF(NFX-J)26,27,99
   26 K = (2*K)+1
      GO TO 28
   27 K = 2*K
   28 HY = (VMP(K-1,J)-VMP(K+1,J))*393.7
      HZ = (VMP(K,J+1)-VMP(K,J-1))*183.3
      HRSLT = (HY*HY+HZ*HZ)**.5
      THETA = ATANF(HZ/HY)
      PRINT 30, Y, Z, HY, HZ, HRSLT, THETA
   30 FORMAT(2F10.4,3E14.8,F10.4//)
   77 CONTINUE
   99 STOP
      END
```

```
C     HAMMER COIL IMPEDANCE CALCULATION
      DIMENSION R(16),XL(16), C(16)
      READ 10, (R(I),XL(I), C(I), I = 1,16)
   10 FORMAT (3F10.4)
      DO 22  I = 1,16
      R(I) = R(I)*.000001
      XL(I) = XL(I)*.000001
      C(I) = C(I)*.000001
   22 C(I) = C(I)*.000001
      READ 20,XLU,XLL, CU, CC, CL
      READ 20, RCOAX, RSH, RSU, RSL
   20 FORMAT (5E14.8)
    1 READ 30, FREQ
   30 FORMAT (F10.0)
      W = 2.*3.14159*FREQ
      ZTTX = 0.
      ZTTY = 0.
      DO 11  I = 1,16
      Z1 = (R(I)*R(I)+W*XL(I)*W*XL(I))**.5
      XXL = XL(I)
      ANGZ1 = ATANF(W*XXL /R(I))
      Z2 = 1./(W*C(I))
      Z3 = Z1*Z2
      ANGZ3 = ANGZ1-3.14159/2.
      Z4 = R(I)
      Z5 = W*XXL-1./(W*C(I))
      IF(Z5) 3,4,5
    3 ANGZ5 = -3.14159/2.
      GO TO 6
    4 ANGZ5 = 0.
      GO TO 6
    5 ANGZ5 = 3.14159/2.
    6 Z6 = (Z4*Z4+Z5*Z5)**.5
      ANGZ6 = ATANF(Z5/Z4)
      ZTT = Z3/Z6
      ANGZT = ANGZ3-ANGZ6
      ZTX = ZTT*COSF(ANGZT)
      ZTY = ZTT*SINF(ANGZT)
      ZTTX = ZTTX+ZTX
   11 ZTTY = ZTTY+ZTY
      ZT = (ZTTY*ZTTY+ZTTX*ZTTX)**.5
      ANGZ = ATANF(ZTTY/ZTTX)
    2 XC = 1./(W*CL)
      ZT = (ZT*XC)/((ZT*ZT+XC*XC)**.5)
      ANGZ = ANGZ-3.14159/2.-ATANF(-XC/ZT)
      ZTX = ZT*COSF(ANGZ)
      ZTY = ZT*SINF(ANGZ)
      ZTX = ZTX+RSH+RSL
      ZTY = ZTY+W*XLL
```

```
      ZT = (ZTX*ZTX+ZTY*ZTY)**.5
      ANGZ = ATANF(ZTY/ZTX)
      XC = 1./(W*CC)
      ZT = (ZT*XC)/((ZT*ZT+XC*XC)**.5)
      ANGZ = ANGZ-3.14159/2.-ATANF(-XC/ZT)
      ZTX = ZT*COSF(ANGZ)
      ZTY = ZT*SINF(ANGZ)
      ZTX = ZTX+RCOAX+RSU
      ZTY = ZTY+W*XLU
      ZT = (ZTX*ZTX+ZTY*ZTY)**.5
      ANGZ = ATANF(ZTY/ZTX)
      XC = 1./(W*CU)
      ZT = (ZT*XC)/((ZT*ZT+XC*XC)**.5)
      ANGZ = ANGZ-3.14159/2.-ATANF(-XC/ZT)
      ANGZ = ANGZ*180./3.14159
      ZT = ZT*1000000.
      PRINT 40, FREQ, ZT, ANGZ
      GO TO 1
   40 FORMAT(F12.2,F12.0,F10.2)
      END
```

APPENDIX B-I

Basic application of the equation

$$r = \rho \frac{L}{A}, \qquad \text{(B-I-1)}$$

where ρ is resistivity in ohm-inches, L is length of material in inches, and A is cross sectional area of the material; allows calculation for resistance.

Starting with ρ for standard annealed copper of 1.724×10^{-8} ohm-meters, the corresponding value for copper in ohm inches may be obtained.[6]

$$\rho_c \text{ ohm-inches} = (39.37)(\rho \text{ ohm-meters}) \qquad \text{(B-I-2a)}$$

$$\rho_c \text{ ohm-inches} = (39.37)(1.724 \times 10^{-8}) \qquad \text{(B-I-2b)}$$

$$\rho_c \text{ ohm-inches} = 6.78 \times 10^{-7} \text{ ohm-inches} \qquad \text{(B-I-2c)}$$

Relative conductivity may be expressed as relative resistivity by the equation

$$\rho_R = 100/\sigma_r \qquad \text{(B-I-3a)}$$

where ρ_R is relative resistivity and σ_r is relative conductivity of given material expressed in percentage of standard annealed copper. For Brylco-25 σ_r is given as 22 percent. Therefore,

$$\rho_R \text{ (Brylco-25)} = 100/22 = 4.55 \qquad \text{(B-I-3b)}$$

For brass, ρ_R is given as 3.9.[25]

With values of ρ_R obtained, the expression

$$\rho = (\rho_c).(\rho_R), \qquad \text{(B-I-4)}$$

where ρ_c is the resistivity of copper in ohm-inches and ρ_R is the relative resistivity of the material in question; computation of the absolute resistivity of the material in ohm-inches may be made.

Therefore,

$$\rho_{B-25} = (6.78 \times 10^{-7}).(4.55) = 3.081 \times 10^{-6} \text{ ohm-inches} \qquad \text{(B-I-5a)}$$

$$\rho_{Brass} = (6.78 \times 10^{-7}).(3.90) = 2.64 \times 10^{-6} \text{ ohm-inches} \qquad \text{(B-I-5b)}$$

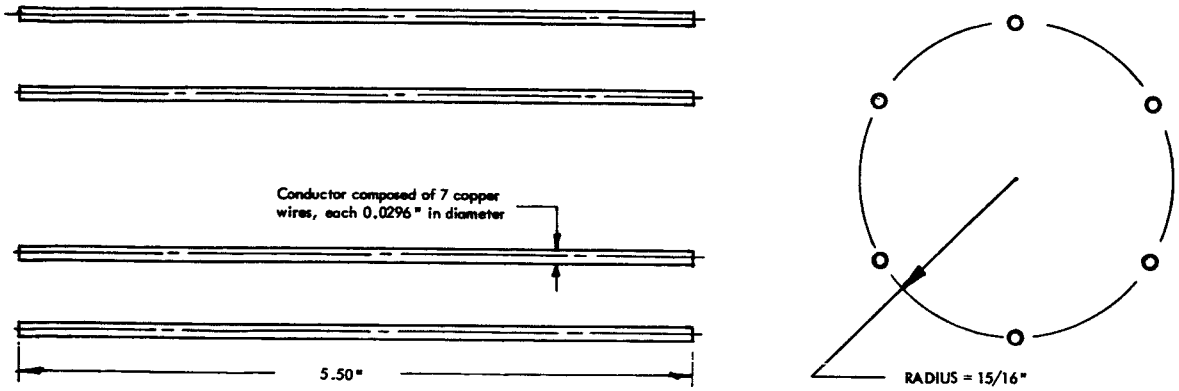

FIGURE B-I-1. COAXIAL FEED LINE SECTION

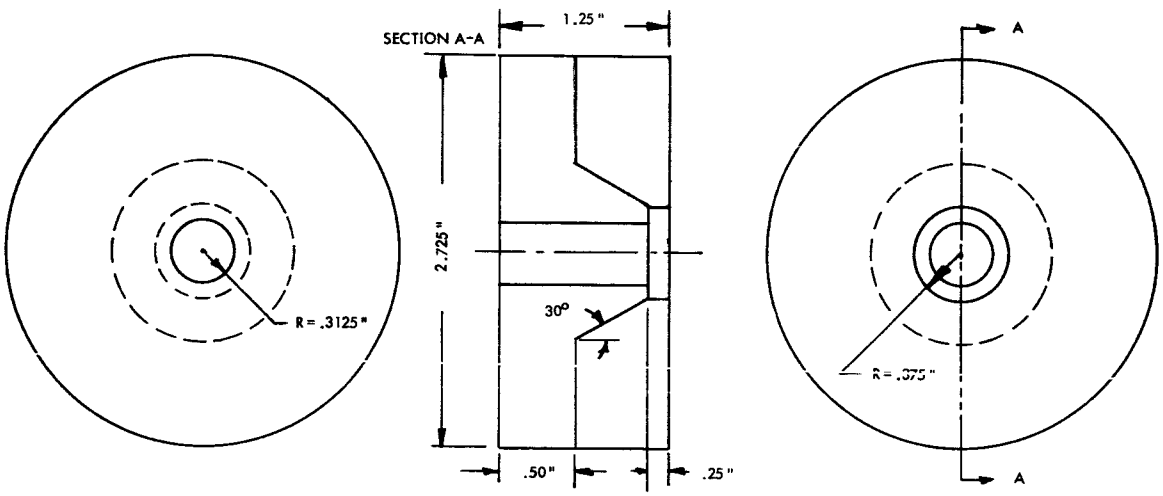

FIGURE B-I-2. CONNECTOR-BASE PLATE SECTION

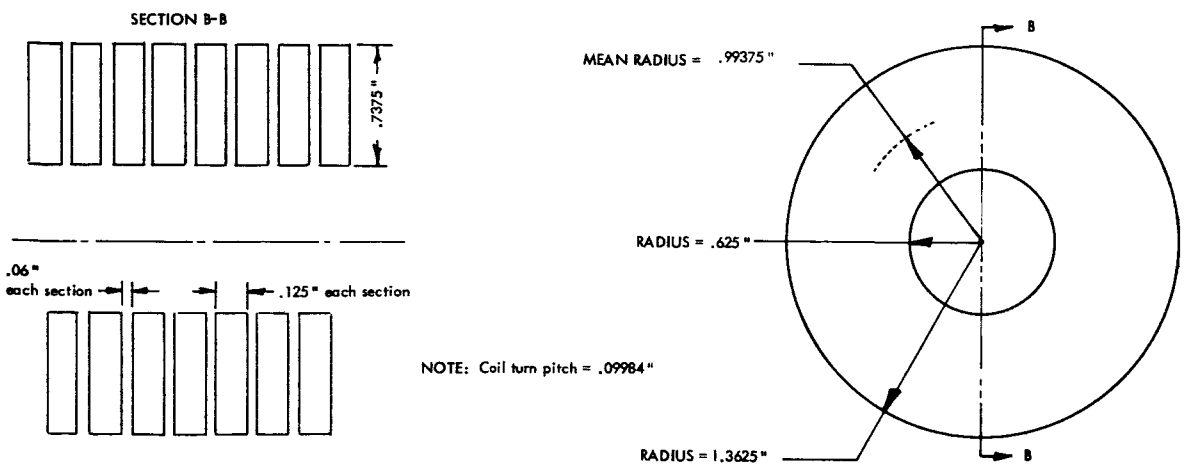

FIGURE B-I-3. COIL TURN SECTION

Having established absolute values of resistivity, Equation B-I-1 permits determination of the resistances of each coil section.

For the coaxial feed line section (see Figure B-I-1):

$$\rho = 6.78 \times 10^{-7} \text{ ohm-inches}$$

$$L = 5.5 \text{ inches}$$

$$A = \frac{\pi}{4} (7) (.0296)^2 = 4.81 \times 10^{-3} \text{ inches}$$

$$r_{coax} = 773 \times 10^{-6} \text{ ohms} \qquad \text{(B-I-6a)}$$

There are six paralleled coaxial feed lines, thus, the equivalent resistance for the section of the coil is 1/6 of the total, or

$$r_{coax} = \frac{773 \times 10^{-6}}{6} = 125.5 \times 10^{-6} \text{ ohms} \qquad \text{(B-I-6b)}$$

For the connector-base plate section (see Figure B-I-2):

$$\rho = 3.08 \times 10^{-6} \text{ ohm-inches}$$

$$\text{Equivalent } L/A = L_1/A_1 + L_2/A_2$$

where

$$L_1 = .250 \text{ inches}$$

$$A_1 = \frac{\pi}{4} [(2.725)^2 - (.75)^2] = 5.39 \text{ inches}^2$$

$$L_2 = 1.00 \text{ inches}$$

$$A_2 = \frac{\pi}{4} [(2.725)^2 - (.625)^2] = 5.52 \text{ inches}^2$$

$$r_{\text{connector-base plate}} = .702 \times 10^{-6} \text{ ohms} \qquad \text{(B-I-7)}$$

For the coil turn section (see Fibure B-I-3)

$$\rho = 3.081 \times 10^{-6} \text{ ohm-inches}$$

$$\text{Equivalent } L/A = \frac{\sqrt{(\pi 1.9875)^2 + (.09984)^2}}{(.7375)\ (.1250)} = 6.77/\text{inches}$$

$$r_{\text{coil turn/turn}} = 208.8 \times 10^{-6} \text{ ohms} \qquad \text{(-I-8a)}$$

Since there are eight turns in series, the equivalent total resistance of the coil turn section becomes eight times the per turn value, or

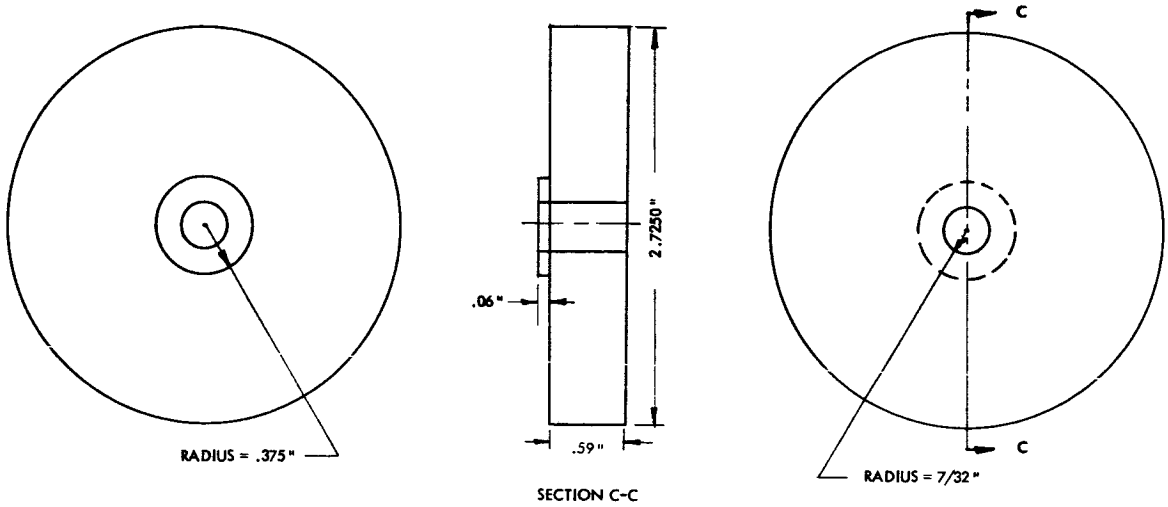

FIGURE B-I-4. GROUND PLATE SECTION

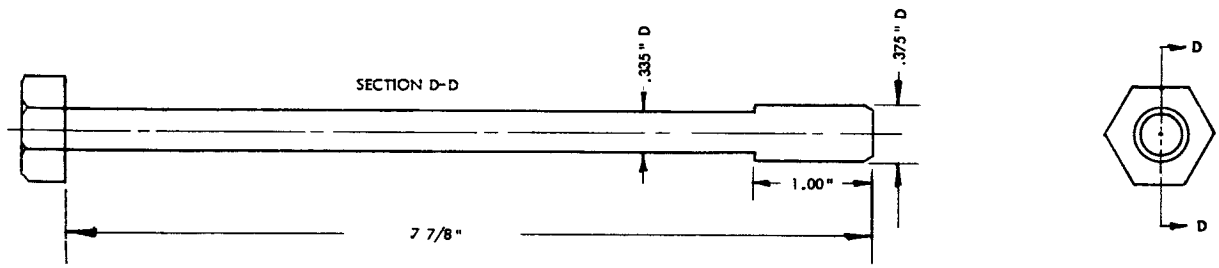

FIGURE B-I-5. CENTER BOLT SECTION

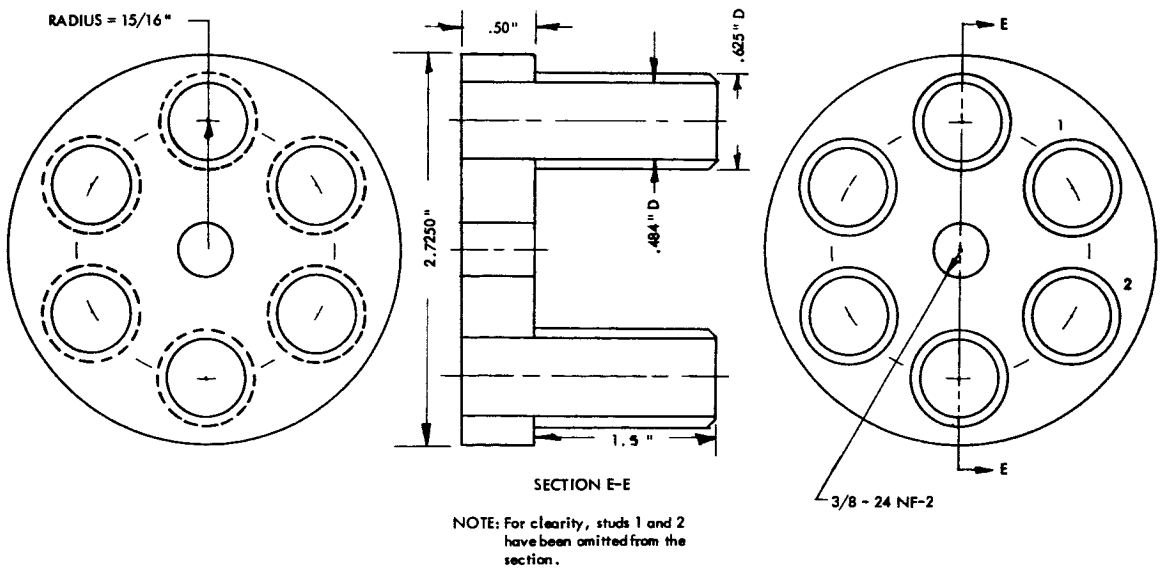

NOTE: For clearity, studs 1 and 2 have been omitted from the section.

FIGURE B-I-6. GROUND CONNECTOR ASSEMBLY SECTION

$$r_{\text{coil turn}} = (8).(208.8 \times 10^{-6}) = 1670.4 \times 10^{-6} \text{ ohms} \quad \text{(B-I-8b)}$$

For the ground plate section (see Figure B-I-4):

$$\rho = 3.081 \times 10^{-6} \text{ ohm-inches}$$

Equivalent $L/A = L_1/A_1 + L_2/A_2$

$$L_1 = .59 \text{ inches}$$

$$A_1 = \frac{\pi}{4}[(2.725)^2 - (.4375)^2] = 5.68 \text{ inches}^2$$

$$L_2 = .06 \text{ inches}$$

$$A_2 = \frac{\pi}{4}[(.7500)^2 - (.4375)^2] = .291 \text{ inches}^2$$

$$r_{\text{ground plate}} = .956 \times 10^{-6} \text{ohms} \quad \text{(B-I-9)}$$

For the center bolt section (see Figure B-I-5):

$$\rho = 2.64 \times 10^{-6} \text{ ohm-inches}$$

Effective $L/A = L_1/A_1 + L_2/A_2$

$$L_1 = 6.875 \text{ inches}$$

$$A_1 = \frac{\pi}{4}(.335)^2 = .0991 \text{ inches}^2$$

$$L_2 = .5 \text{ inches}$$

$$A_2 = \frac{\pi}{4}(.375)^2 = .1105 \text{ inches}^2$$

$$r_{\text{center bolt}} = 218.0 \times 10^{-6} \text{ ohms} \quad \text{(B-I-10)}$$

For the ground connector assembly section (see Figure B-I-6):

$$\rho = 2.64 \times 10^{-6} \text{ ohm-inches}$$

Effective $L/A = L_1/A_1 + L_2/A_2$

$$L_1 = .50 \text{ inches}$$

$$A_1 = \frac{\pi}{4}[(2.725)^2 - (6)\ (.484)^2] = 4.73 \text{ inches}^2$$

$$L_2 = 1.50 \text{ inches}$$

$$A_2 = \frac{3\pi}{2}\ [(.625)^2 - (.484)^2] = 2.944 \text{ inches}^2$$

$$r_{\text{ground connector assembly}} = 1.179 \times 10^{-6} \text{ ohms} \quad \text{(B-I-11)}$$

APPENDIX B-II

Calculations of penetration depth, δ, may be made for each material by expansion of the defining equation,

$$\delta = 39.37 \sqrt{\frac{2\rho}{\omega\mu}} \qquad \text{(B-II-1)}$$

For copper: $\rho = 1.724 \times 10^{-8}$ ohm-meters

$\mu = 1.257 \times 10^{-6}$ henries/meter

$\omega = 2\pi f$ radians/second

$$\delta \text{ copper} = 39.37 \sqrt{\frac{(2)\ (1.724 \times 10^{-8})}{(2)\ (f)\ (1.257 \times 10^{-6})}} = 2.605\sqrt{\frac{1}{f}} \qquad \text{(B-II-2a)}$$

where f is frequency expressed in cycles per second.

By similar calculation,

$$\delta \text{ B-25} = 5.55 \sqrt{\frac{1}{f}} \qquad \text{(B-II-2b)}$$

$$\delta \text{ brass} = 5.13 \sqrt{\frac{1}{f}} \qquad \text{(B-II-2c)}$$

Calculations of d for each material may be made at any particular frequency by solution of the respective forms of Equations B-2a through B-2c.

At 20,000 cps

$$\delta_{\text{copper}} = 2.605 \sqrt{\frac{1}{20{,}000}} = .0154 \text{ inches} \qquad \text{(B-II-3a)}$$

Similarly:

$$\delta_{\text{B-25}} = .0392 \text{ inches at } 20{,}000 \text{ cps} \qquad \text{(B-II-3b)}$$

$$\delta_{\text{brass}} = .0362 \text{ inches at } 20{,}000 \text{ cps} . \qquad \text{(B-II-3c)}$$

APPENDIX B-III

In Skilling's work a table is developed which relates the ac values of resistance in a solid round conductor to the dc value.[28] This is shown in Table B-III-1. From this table, interpolations can be made to arrive at ac resistance values for any solid round conductor in terms of its dc value.

To arrive at the results of skin effect on the coil turn section, which has a rectangular cross section rather than a circular cross section as required in Table B-III-1, changes equating the rectangular cross section to an equivalent circular cross section must be made.

To reduce the rectangular coil turn to an equivalent circular area, it is first necessary to establish a circular area which is equal to the given rectangular area.

Thus,

$$A_{circular} = A_{rect.} \qquad \text{(B-III-1)}$$

For this study,

$$A_{rect} = (.7375)(.1250) = .0921875 \text{ in.}^2 \qquad \text{(B-III-2)}$$

Therefore,

$$A_{circular} = .0921875 \text{ in.}^2$$

This corresponds to a circle with a radius

$$r = \left[\frac{A_{circular}}{\pi} \right]^{1/2} = \left[\frac{.921875}{\pi} \right]^{1/2} = .17125 \text{ in.} \qquad \text{(B-III-3)}$$

If equal values of penetration, δ, are assumed for both the circular and rectangular areas and the corresponding ratio of remaining areas are used in Table B-III-1, a reduction of the rectangular cross section to an equivalent circular cross section may be achieved. At the same time, the corresponding rc resistances, in terms of the dc resistance, for the rectangular cross section may be obtained.

$\sqrt{2}\ r/\delta$	$\frac{R_{ac}}{R_{dc}}$	$\sqrt{2}\ r/\delta$	$\frac{R_{ac}}{R_{dc}}$
0.00	1.000	3.00	1.318
0.20	1.000	3.20	1.385
0.40	1.000	3.40	1.456
0.60	1.001	3.60	1.529
0.80	1.002	3.80	1.603
1.00	1.005	4.00	1.678
1.20	1.011	5.00	2.043
1.40	1.020	6.00	2.394
1.60	1.033	7.00	2.743
1.80	1.052	8.00	3.094
2.00	1.078	10.00	3.799
2.20	1.111	20.00	7.328
2.40	1.152	30.00	10.861
2.60	1.201	40.00	14.395
2.80	1.256	50.00	17.930

Table B-III-1. Skilling's Table of Relative AC Resistances due to Skin Effect[28]

Symbolically, this may be represented as

$$\delta_{eff} = r - \{ [A_T - A_{rect}(f)]/\pi \}^{1/2} \qquad \text{(B-III-4)}$$

where δ_{eff} is the effective value of δ used to enter Table B-III-1, A is the dc area of the conductor and $A_{rect}(f)$ is the net area of the rectangular cross section remaining after the actual penetration area for δ at each frequency is subtracted.

For frequencies from 8,000 to 20,000 cycles per second, Equation B-III-4 yields usable values. However, for values from 1000 to 8,000 cycles per second, the penetration depth is so small that estimations of δ_{eff} must be made. Both calculated and estimated values are within desired accuracy. The results of calculations for δ_{eff} and the corresponding values of penetration ratio $\sqrt{2}\ r/\delta_{eff}$, are shown in Table B-III-2.

Frequency cps	A_T in.^{2}	r in.	A_{rect} in.^{2}	δ_{eff} in.	$\sqrt{2}\ r/\delta_{eff}$
1000	.0921875	.17125	*	.5930	.4000
1420	.0921875	.17125	*	.4050	.6000
2000	.0921875	.17125	*	.2790	.8700
4000	.0921875	.17175	*	.2620	.9250
8000	.092875	.17175	.091574	.1572	1.5400
10000	.0921875	.17125	.08405	.1204	2.0103
2000	.0921875	.17175	.07119	.0722	3.3640

*Values not calculable

Table B-III-2. Information Relating Rectangular Cross Section to an Equivalent Circuit Cross Section for Determination of Skin Effect

APPENDIX B-IV

```
C     CRYOGENIC COIL VECTOR MAGNETIC POTENTIAL DETERMINATION
      DIMENSION SSS(11), W(11)
      DO 11  I = 1,11
      P = I-1
   11 SSS(I) = SINF(3.14159/2.-P*3.14159/10.)
    2 READ 10, Y, ZX
      PRINT 10, Y, ZX
   10 FORMAT (2F10.5)
      AP= .63955
      Z = ZX-.04167
      VMPP = 0.
      COUNT = 0.
      DO 22  J = 1,24
      Q = J
      IF(COUNT-3.) 4,3,99
    3 COUNT = 1.
      Z = Z+.10166
      GO TO 9
    4 COUNT = COUNT+1.
      Z = Z+.04167
    9 DO 33  K = 1,18
      U = K
      A = AP+.04167*(U-1.)
      R = (Y*Y+Z*Z)**.5
      THETA = 1.570796-ATANF(Z/Y)
      R2A2 = R*R+A*A
      TWORA = 2.*R*A*SINF(THETA)
      DO 44  L = 1,11
   44 W(L) = SSS(L)/((R2A2-TWORA*SSS(L))**.5)
      WCOMP1 = 0.
      WCOMP2 = 0.
      WCOMP1 = W(2)+W(4)+W(6)+W(8)+W(10)
      WCOMP1 = 4.*WCOMP1
      WCOMP2 = W(3)+W(5)+W(7)+W(9)
      WCOMP2 = 2.*WCOMP2
      VMPI = (W(1)+W(11)+WCOMP1+WCOMP2)*A
      VMPP = VMPP+VMPI
   33 CONTINUE
   22 CONTINUE
      VMP = VMPP*(1./3240.)
      PRINT 20, VMP
   20 FORMAT(F18.6)
      GO TO 2
   99 STOP
      END
```

REFERENCES

1. Charles D. Hodgman, ed., Handbook of Chemistry and Physics. (Cleveland, 1961), p. 2627.

2. Ibid., p. 2634

3. Skillings, Hugh H., Electric Transmission Lines (New York, 1951), pp. 146 ff.

4. Hayt, William H., Jr., Engineering Electromagnetics (New York, 1958) p. 200.

5. Beryllium Corporation, Beryllium Copper Strip, Descriptive Bulletin No. S-1100 (Redding, Penn.), p. 5.

6. Hodgman, p. 2628.

7. International Telephone and Telegraph Company, Reference Data for Radio Engineers, 4th ed. (New York, 1956), p. 608.

8. Hodgman, p. 2628.

9. Moore, A. D., Fundamentals of Electrical Design (New York, 1927), pp. 38-62.

10. Hayt, pp. 133-152.

11. Moore, A. D., Mapping Techniques Applied to Fluid Mapper Patterns Electrical Engineering, Vol. 71, No. 5, p. 446.

12. Ramo, S. and J. R. Whinnery, Fields and Waves in Modern Radio, 2nd ed., (New York, 1953), pp. 123-124.

13. Kraus, J. D., Electromagnetics (New York, 1953), pp. 567-573.

14. Hayt, p. 28.

15. Ibid., p. 321.

16. Ibid.

16a. Skilling, inside front cover.

17. Hayt, p. 230.

18. Ibid., p. 234.

19. Skillings, p. 99.

20. Jordan, Edward C., Electromatic Waves and Radiating Systems (Englewood Cliffs, 1950), p. 89.

21. Byrd, Paul F. and Morris D. Friedman, Handbook of Elliptic Integrals for Engineers and Physicists (Berlin, 1954), passim.

22. Burington, Richard S., Handbook of Mathematical Tables and Formulas, 3rd ed. (Sandusky, Ohio, 1949).

23. Milne, William E., Numerical Calculus (Princeton, 1949), pp. 120-122.

24. Ibid.

25. Hayt, p. 233.

26. Skillings, inside front cover.

27. International Telephone and Telegraph Company, Reference Data for Radio Engineers, 4th ed. (New York, 1956), p. 45.

28. Skilling, pp. 147-157.

29. Hudson, R. G., The Engineer's Manual, 2nd ed. (New York, 1961), p. 80.

30. Rogers, W. E., Introduction to Electric Fields (New York, 1954) pp. 293-306.